JRC Scientific and Technical Reports

# NM-Series of Representative Manufactured Nanomaterials

# Zinc Oxide NM-110, NM-111, NM-112, NM-113 Characterisation and Test Item Preparation

C. Singh, S. Friedrichs, M. Levin, R. Birkedal, K.A. Jensen, G. Pojana, W. Wohlleben, S. Schulte, K. Wiench, T. Turney, O. Koulaeva, D. Marshall, K. Hund-Rinke, W. Kördel, E. Van Doren, P-J. De Temmerman, M. Abi Daoud Francisco, J. Mast, N. Gibson, R. Koeber, T. Linsinger, C.L. Klein

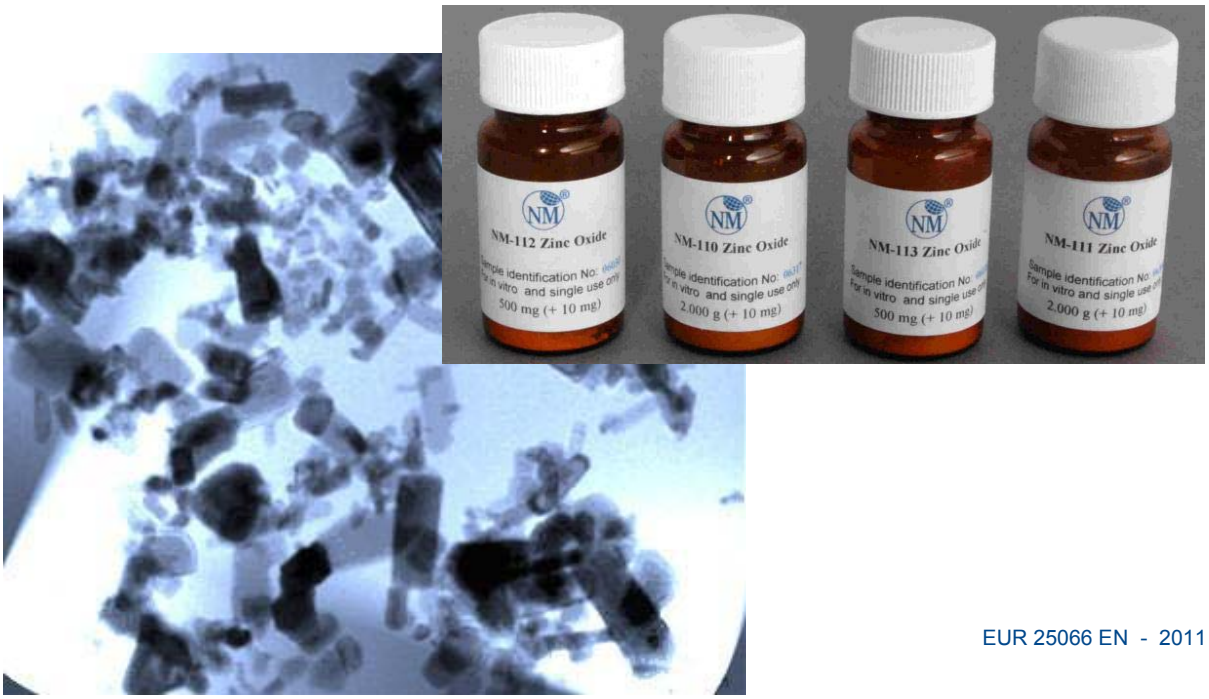


EUR 25066 EN - 2011

JRC EUROPEAN COMMISSION
Institute for Reference Materials and Measurements
Institute for Health and Consumer Protection
NIA Nanotechnology Industries Association

The mission of the JRC-IRMM is to promote a common and reliable European measurement system in support of EU policies.

European Commission
Joint Research Centre
Institute for Reference Materials and Measurements

**Contact information**
Address: Retieseweg 111, B-2440 Geel, Belgium
E-mail: christoph.klein@ec.europa.eu
Tel.: +32 (0)14 571308
Fax: +32 (0)14 584 273

http://irmm.jrc.ec.europa.eu/
http://www.jrc.ec.europa.eu/



JRC 64075

EUR 25066 EN
ISBN 978-92-79-22215-3
ISSN 1831-9424
doi:10.2787/55008

Luxembourg: Publications Office of the European Union



*Printed in Luxembourg*

# NM-Series of Representative Manufactured Nanomaterials

# Zinc Oxide
# NM-110, NM-111, NM-112, NM-113
# Characterisation and test item preparation

**C. Singh**
Nanotechnology Industries Association, United Kingdom

**S. Friedrichs**
Nanotechnology Industries Association, Belgium

**R. Birkedal, M. Levin, K. A. Jensen**
The National Research Centre for the Working Environment, Denmark

**G. Pojana**
University Ca' Foscari of Venice, Italy

**W. Wohlleben, S. Schulte, K. Wiench**
BASF SE, Ludwigshafen, Germany

**T. Turney, O. Koulaeva**
Micronisers Australasia Pty. Ltd., Australia

**D. Marshall**
LGC Standards, United Kingdom

**K. Hund-Rinke, W. Kördel**
Fraunhofer Institute for Molecular Biology and Applied Ecology, Germany

**E. Van Doren, P-J. De Temmerman, M. Abi Daoud Francisco, J. Mast**
Veterinary and Agrochemical Research Centre, Belgium

**N. Gibson**
European Commission Joint Research Centre, Institute for Health and Consumer Protection, Italy

**R. Koeber, T. Linsinger, C. L. Klein**
European Commission, Joint Research Centre,
Institute for Reference Materials and Measurements, Belgium

## Abstract

The European Commission's Joint Research Centre (JRC) provides scientific support to European Union policy also regarding nanotechnology. Over the last three years, the JRC, in collaboration with international public and private partners, focused part of its work on establishing and applying a priority list (NM-Series) of Representative Manufactured Nanomaterials (RMNs) in support of one of the most comprehensive nanomaterial research programmes that is currently being carried out: the Organisation for Economic Co-operation and Development's (OECD) Working Party on Manufactured Nanomaterials (WPMN) Sponsorship Programme. This collaborative programme enables the development and collection of data on characterisation, toxicological and eco-toxicological testing, as well as risk assessment and safety evaluation of nanomaterials (NMs). It is of utmost timely importance to make representative nanomaterials available to the international scientific community, in order to enable innovation and development of safe materials and products.

The present report describes the characterisation of NM-110, NM-111, NM-112, and NM-113, RMN Zinc Oxide substances, originating from defined batches of commercially manufactured material. The NM-Series materials were subsampled in collaboration with the Fraunhofer Institute for Molecular and Applied Ecology (Fh-IME), in order to be made available for measurement and testing for hazard identification, risk and exposure assessment studies. The results for more than 15 endpoints are addressed in the present report, including physical-chemical properties, such as size and size distribution, crystallite size and electron microscopy images. Sample and test item preparation procedures are addressed. The RMNs are studied by a number of international laboratories.

The properties of the Zinc Oxide RMNs NM-110, NM-111, NM-112, and NM-113 described in this report demonstrate their relevance for use in measurement and testing studies of nanomaterials. The studies were performed in close collaboration between the PROSPECT consortium partners, the JRC, the Fraunhofer Institute for Molecular and Applied Ecology (Fh-IME), BASF AG Ludwigshafen, LGC standards, the National Physical Laboratory (NPL), the

National Research Centre for the Working Environment, Denmark, CSIRO and the National Measurement Institute of Australia.

# Table of contents

# List of abbreviations

| | |
|---|---|
| AIM | Aerosol Instrument Management |
| APS | Aerodynamic Particle Sizer |
| a.u. | arbitrary unit |
| BET | Brunauer Emmett Teller |
| BJH | Barrett-Joyner-Halenda |
| BSA | Bovine Serum Albumin |
| CPC | Condensation Particle Counters |
| CRM | Certified Reference Material |
| CSIRO | Commonwealth Scientific and Industrial Research Organisation |
| DI | De-ionised |
| DLS | Dynamic Light Scattering |
| DMA | Differential Mobility Analyser |
| EtOH | ethanol |
| Fh-IME | the Fraunhofer Institute for Molecular and Applied Ecology |
| FBAG | Fluidised Bed Aerosol Generator |
| FMPS | Fast Mobility Particle Size |
| GLP | Good Laboratory Practice |
| ICP-AES | Inductively Coupled Plasma-Atomic Emission Spectroscopy |
| ICP-OES | Inductively Coupled Plasma-Optical Emission Spectroscopy |
| ISO | International Organisation for Standardisation, Geneva, Switzerland |
| IUPAC | International Union of Pure and Applied Chemistry, Triangle Park, USA |
| LOI | Loss On Ignition |
| MAD | Mutual Acceptance of Data |
| NIST | National Institute of Standards and Technology, USA |
| NM | Nanomaterial |

| | |
|---|---|
| NPL | National Physical Laboratory |
| NRCWE | National Research Centre for the Working Environment |
| OECD | Organisation for Economic Co-operation and Development, France |
| PDI | polydispersity index |
| PROSPECT | Ecotoxicology Test Protocols for Representative Nanomaterials in Support of the OECD Sponsorship Programme |
| REACH | Registration, Evaluation, Authorisation and Restriction of Chemicals regulation (EC) 1907/2006 |
| RM | Reference Material |
| RMN | Representative Manufactured Nanomaterial |
| ROS | Reactive Oxygen Species |
| RSD | Relative Standard Deviation |
| SD | Standard Deviation |
| SEM | Scanning Electron Microscopy |
| SMPS | Scanning Mobility Particle Sizer |
| SSA | specific surface area |
| SOP | Standard Operating Procedure |
| TEM | Transmission Electron Microscopy |
| TGA | Thermogravimetric Analysis |
| UV-VIS | Ultraviolet-visible Spectrophotometry |
| WPMN | Working Party on Manufactured Nanomaterials |
| XPS | X-ray Photoelectron Spectroscopy |
| XRD | X-Ray Diffraction |

# 1 Introduction – Zinc Oxide

Nanotechnologies have gained a great deal of public interest due to the needs and applications of nanomaterials (NM) in many areas of human endeavours such as industry, agriculture, business, medicine, public health amongst many others. Nanotechnologies include the integration of these nanoscale structures into larger material components and systems, providing the control and construction of new and improved materials at the nanoscale (Ju-Nam & Lead, 2008).

Nanoparticles can be naturally occurring or they can be manufactured; they can be classed into several categories, which include the following (Chandra Ray *et al.,* 2009):

1. Metal nanomaterials, such as gold and silver nanoparticles
2. Metal oxide nanomaterials, such as titanium dioxide and zinc oxide
3. Carbon nanomaterials such as fullerenes and nanotubes
4. Quantum dots such as cadmium telluride and cadmium selenide

One estimate for the production of engineered nanomaterials was 2000 tonnes in 2004 and increasing to 58,000 tonnes by 2011-2020 (Nowack & Buecheli, 2007).

The OECD's Working Party on Manufactured Nanomaterials (WPMN) launched the OECD WPMN Sponsorship Programme in November 2007, agreeing on a priority list of (initially 14, later reviewed to) 13 Manufactured Nanomaterials for testing (based on materials, which are in, or close to, commercial use). They also agreed a list of endpoints, for which the agreed commercially relevant nanomaterials should be tested. Much valuable information on the safety of NMs can be derived by testing a representative set for human health and environmental safety.

The following revised list of manufactured nanomaterials was adopted in July 2010:[*,†]

1. Fullerenes (C60)
2. Single-walled carbon nanotubes (SWCNTs)
3. Multi-walled carbon nanotubes (MWCNTs)
4. Silver nanoparticles
5. Iron nanoparticles
6. Titanium dioxide
7. Aluminium oxide
8. Cerium oxide
9. Zinc oxide
10. Silicon dioxide
11. Dendrimers
12. Nanoclays
13. Gold nanoparticles

PROSPECT[‡] is UK's contribution to the OECD Sponsorship Programme to examine the environmental safety of nanomaterials in accordance with the agreed OECD WPMN *'Guidance Manual for Sponsors of the OECD Sponsorship Programme for the Testing of Manufactured Nanomaterials*[§]. The PROSPECT project is a public-private-partnership dedicated to supporting the safe and responsible exploitation of nanomaterials, and developing a better understanding of their impact on humans and the environment; its objective is to *"provide crucial data to the OECD work, by addressing gaps in the current level of knowledge on the physical-chemical and ecotoxicological properties of these materials, followed by fundamental scientific research leading to establishing scientific test methodologies to study those endpoints that may not be assessed*

[*] The OECD WPMN list of representative nanomaterials initially contained 14 nanomaterial types, including (a) carbon black, and (b) polystyrene; in July 2010, during the 7th WPMN plenary, it was agreed to take those two nanomaterial types off the list, while nano-Gold was added. Follow this link to download the updated List of OECD WPMN representative NMs and List of Endpoints for Phase 1 of the Sponsorship Programme (Revision December 2010) (OECD WPMN Publication Series, No. 27).

[†] The order, in which the nanomaterials are listed, does not indicate a priority.

[‡] **PROSPECT: Ec**otoxicology **T**est **P**rotocols for **R**epresentative Nanomaterials in Support of the **O**ECD **S**ponsorship **P**rogramme'. For further information, please visit http://www.nanotechia-prospect.org/.

[§] Follow this link to download the *Guidance Manual for the Testing of Manufactured Nanomaterials: OECD's Sponsorship Programme (1st Revision: June 2010)* (OECD WPMN Publication Series, No. 25).

*through standard tests used for bulk chemicals."* Manufactured nanomaterials are characterised by specific properties which are "engineered" into the structure of the particle. NMs potentially offer many economic, environmental and technological advantages. However, there is concern that the properties engineered into NMs may represent risks to the environment, if released into the environment in an uncontrolled fashion. PROSPECT promises to specifically provide crucial data for the future development, manufacture and commercialisation of products containing nanoparticles of cerium dioxide and zinc oxide, but more generally help to support advancement and commercialisation of a broad group of nanomaterials. PROSPECT officially started on 1st January 2009 and is expected to complete by 31st December 2011.

This report focuses on zinc oxide (ZnO) NMs. In the majority of countries around the world, ZnO is approved as a sunscreen ingredient that enhances the sun protection properties. The European Commission, however, has for a number of years now been undecided whether to add ZnO to the list of approved sunscreen ingredients (SCCP, 2005), but some EU Member States have issued national exemption for the commercialisation of ZnO as a sunscreen additive. Other significant industrial uses of ZnO are in rubber, ceramics, optical glass, paint and plastics. Applications in cosmetics and pharmaceuticals include ointments, baby and skin creams, toothpaste, deodorants, sunscreens. ZnO is furthermore added to animal food and fertilisers as a source for the essential trace element Zn.

According to the Project on Emerging Nanotechnologies Inventory of nanotechnology-based Consumer Products[**], zinc oxide is present in at least 24 commercial products, primarily used in sunscreen formulations, due to its UV-absorbing properties. Sunscreens containing physical blockers of UV light (such as zinc oxide particles) have been shown to be highly effective in protecting cells against UV-induced DNA damage (Cayrol *et al.,* 1999). In normal pigment

[**] For further information on the Project on Emerging Nanotechnologies Inventory of nanotechnology-based Consumer Products, please visit http://www.nanotechproject.org/inventories/consumer/search

size ranges, these particles reflect and scatter light, making the sunscreens appear white. As the particle sizes decrease to smaller sub-micron (nano) dimensions, they absorb and scatter UV radiation, and largely absorb visible wavelengths (Wolf *et al.,* 2001), making the sunscreens appear transparent on skin and thus both more aesthetically pleasing and more acceptable as an ingredient in a wide range of cosmetics.

Nanoscale metal oxide particles in general offer greater UV protection compared to their micro sized counterparts, specifically in the UVA and UVB region (Popov *et al.,* 2005).

It has furthermore been reported that zinc oxide absorbs UV-radiation more effectively than titanium dioxide ($TiO_2$) over a broad range, and particularly in the UVA region (Pinnell *et al.,* 2000), and has consequently been used as the sole active ingredient in some broad-spectrum sunscreens.

Currently, metal oxide nanoparticles have not been comprehensively assessed in regard to potential effects on human health, from exposure (accidental or otherwise) in the workplace during nanoparticles production or exposure through use in commercial products, or for their effects on ecosystems if released into the environment. However, the risk of adverse impact on health from any material depends both on the biological toxicity associated with the properties of the material, and on the degree of exposure of an organism to it. The potential hazard posed may change during the lifecycle of the material from its time of manufacture through to its demise or transformation into other forms (Osmond *et al.,* 2010).

In order to reliably address the scientific questions of potential nano-ZnO induced effects, toxicity, ecotoxicity and fate, representative nanomaterials are required, which are relevant for industrial application and commercial use, and for which a critical mass of study results are generated or known. These Representative Manufactured Nanomaterials (RMNs) allow comparison of

testing results, the development of conclusive assessment of data, and pave the way for appropriate test method optimization, harmonisation and validation. The NM-110, NM-111, and NM-112 zinc oxide nanomaterial, as well as NM-113 as zinc oxide materials were introduced to fulfil this function.

The present report describes a number of relevant physical-chemical properties that have been measured for these NMs by international scientists related to and supporting the OECD WPMN Sponsorship Programme. The report also describes the sample and test item preparation, handling and dispersion protocols regarding both zinc oxide and surface modified zinc oxide NMs.

# 2 NM-Series of Representative Manufactured Nanomaterials and the OECD Sponsorship Programme

Nanotechnologies hold considerable promise in many technological areas and industrial sectors, and the application of nanosciences and nanomaterials to everyday products offers a range of benefits; their application in consumer products may make these lighter, stronger, cleaner, less expensive, more efficient, more precise, more functional, more durable, and also more aesthetically pleasing. Products with specific properties derived from nanotechnologies currently available on the market include textiles, cosmetics and beauty products, water filters, food, food-packaging materials, paints, glues and dental fillers.

Nanomaterials may also improve our quality of life via their use in applications leading to more efficacious pharmaceuticals, improved medical diagnostic tools and faster computers, to name but a few. This has been matched by growth in requests for characterised representative nanomaterials for the intended use as reference materials for measurement methods as well as reference matrices and reference items for testing, in order to reliably address health and safety concerns for humans and the environment related to nanomaterials and corresponding implementation of European policy and responsible nanotechnology decisions (Morris *et al.,* 2011).

## 2.1 OECD Working Party for Manufactured Nanomaterials

The Organisation for Economic Co-operation and Development's (OECD) Working Party on Manufactured Nanomaterials (WPMN) is carrying out one of the most comprehensive nanomaterial testing programmes: The OECD Guidance Manual ENV/JM/MONO(2009)20/REV describes the work programme as follows (OECD 2010): *"As a follow-up, the Joint Meeting decided to hold a Workshop on the Safety of Manufactured Nanomaterials in December 2005, in Washington, D.C. The main objective was to determine the "state of the art" for the safety assessment of manufactured nanomaterials with a*

*particular focus on identifying future needs for risk assessment within a regulatory context. Based on the conclusions and recommendations of the Workshop [ENV/JM/MONO(2006)19] it was recognised as essential to ensure the efficient assessment of manufactured nanomaterials so as to avoid adverse effects from the use of these materials in the short, medium and longer term. With this in mind, the OECD Council established the OECD Working Party on Manufactured Nanomaterials (WPMN) as a subsidiary body of the OECD Chemicals Committee."*

## 2.2 OECD WPMN: Testing a Priority Set of Representative Manufactured Nanomaterials

The OECD WPMN Sponsorship Programme concentrates on human health and environmental safety implications of manufactured nanomaterials (limited mainly to the chemicals sector), and aims *"to ensure that the approach to hazard, exposure and risk assessment is of a high, science-based, and internationally harmonised standard. This programme promotes international co-operation on the human health and environmental safety of manufactured nanomaterials, and involves the safety testing and risk assessment of manufactured nanomaterials."* As a first step, the WPMN agreed a list of (initially 14, later reviewed to) 13 types of representative manufactured nanomaterials with a number of selected materials within each "type". A priority set of Representative Manufactured Nanomaterials (RMNs) was agreed for inclusion in a set of reference nanomaterials for which development of data would support characterisation, measurement, toxicological and ecotoxicological testing, and risk assessment or safety evaluation of RMNs.

The OECD also agreed a list of endpoints including nanomaterial information/identification, physical-chemical properties and material characterisation, environmental fate, environmental toxicology, mammalian toxicology and material safety, which would be addressed for the hazard assessment of those nanomaterials.

In 2007, the WPMN launched the OECD WPMN Sponsorship Programme for the Testing of Manufactured Nanomaterials, in order to generate information on the safety of the specific manufactured nanomaterials through testing for human health and environmental safety endpoints.

It is worthwhile to mention that physical-chemical parameters are addressed by a variety of measurement techniques. Measurements are performed according to the requirements for regulatory testing and metrological principles. Test in the understanding of "predictive toxicological tests" and regarding toxicological endpoints and environmental fate are performed under conditions, such as for regulatory testing under Good Laboratory Practice (GLP). Several items of information and data required under the OECD WPMN Sponsorship Programme correspond to items, which are regularly generated and collected for (certified) reference materials.

The requested information and endpoints addressed within the OECD Sponsorship Programme are presented in Table 1.

**Table 1: Endpoints addressed for the NM-Series of Representative Manufactured Nanomaterials, as described in the OECD WPMN Manual (OECD 2010).**

| OECD endpoints according to the Guidance Manual for Sponsors (GMS) | GMS- data requirements |
|---|---|
| NM name | must be completed |
| CAS No | if available |
| structural formula/molecular structure | must be provided |
| composition of NM being tested including purity, known impurities or additives | must be provided |
| basic morphology | must be provided |
| description of surface chemistry | if feasible |
| major commercial uses | as completely as possible |
| known catalytic activity | should be described |
| method of production | must be described |
| **Identification, source, logistics of distribution** | |
| known aspects: manufacturer, facility location, lot number, other, see above | must be completed |
| records on distribution, shipment, storage | must be completed |
| quality of material: homogeneity within bottle/ between bottles | must be completed |
| quality of material: stability, short-term and long-term | must be completed |
| quality of material: stability, monitoring | must be completed |
| **Physical-chemical Properties and Material Characterization** | |
| Agglomeration/aggregation | must be addressed |
| Water Solubility/Dispersibility | must be completed |
| Crystalline phase | must be completed |
| Dustiness | must be addressed |
| Crystallite size | must be addressed |
| Representative Electron Microscopy (TEM) picture(s) | must be addressed |
| Particle size distribution – dry and in relevant media | must be completed |
| Specific surface area | must be completed |
| Zeta potential (surface charge) | must be completed |
| Surface chemistry | must be completed |
| Photocatalytic activity | must be addressed |
| Pour density | must be addressed |
| Porosity | must be addressed |
| Octanol-water partition coefficient | must be addressed |
| Redox potential | must be addressed |
| Radical formation potential | must be addressed |
| Other relevant Physical-Chemical Properties and Material Characterization information (where available) | must be addressed |
| **Environmental Fate** | |
| Dispersion stability in water | must be addressed |
| Biotic degradability | must be addressed |
| Identification of degradation product(s) | must be addressed |
| Further testing of degradation product(s) as required | must be addressed |
| Abiotic Degradability and Fate | must be addressed |
| Adsorption-Desorption | must be addressed |
| Adsorption to soil or sediment | must be addressed |
| Bioaccumulation potential | must be addressed |
| Other relevant environmental fate information (when available) | must be addressed |
| **Environmental Toxicology** | |
| Effects on pelagic species (short term/long term) | |
| Effects on sediment species (short term/long term) | |
| Effects on soil species (short term/long term) | must be addressed |
| Effects on terrestrial species | must be addressed |
| Effects on microorganisms | must be addressed |
| Effects on activated sludge at WWTP | |
| Other relevant information (when available) | if available |
| **Mammalian Toxicology** | |
| Pharmacokinetics/Toxicokinetics (ADME) | must be addressed |
| Acute toxicity | must be addressed |
| Repeated dose toxicity | must be addressed |
| Chronic toxicity | must describe any relevant existing study |
| Reproductive toxicity | must describe relevant reproductive toxicity test results |
| Developmental toxicity | |
| Genetic toxicity | must describe any relevant existing genetic toxicity test results |
| Experience with human exposure | must describe any relevant experience with human exposure |
| Other relevant test data | should be considered |
| Material Safety | |
| Flammability | if available |
| Explosivity | if available |
| Incompatibility | if available |

The range of RMNs used within the OECD WPMN Sponsorship Programme are sub-sampled in collaboration with the German Fraunhofer Institute for Molecular Biology and Applied Ecology (Fh-IME) under Good Laboratory Practice (GLP) conditions.

The NM-Series of RMNs currently include: Carbon nanotubes, silver, titanium dioxide, cerium oxide, barium sulphate, zinc oxide, bentonite, gold, and silicon dioxide. These representative nanomaterials provide researchers with characterised materials, for which a globally agreed number and quality of studies are performed for potentially regulatory relevant endpoints. The NM-Series RMNs may be used by scientists in their measurement and testing models, and utilised as test and reference items, performance standards and comparators. Table 2 provides an overview of the current list of NM-Series of RMNs (last updates: September 2011).

**Table 2: List of NM-Series of RMNs.**

| List of NM series representative nanomaterials currently available | | | | | | | | | |
|---|---|---|---|---|---|---|---|---|---|
| **NM code** | **Type of material** | **Label name** | **mean particle size [nm] by TEM and SEM** | **primary particle or crystal size [nm] by TEM and XRD or CPS**** | **specific surface area [m2/g] by BET** | **length [µm] by TEM,** applicable only to NM-40x series, CNT | **diameter [nm]** applicable only to NM-40x series, CNT by TEM | **other information** | **mass content per vial [mg]** |
| NM-100 | Titanium Dioxide | Titanium Dioxide, pigment | 299 | 42-90 | 10 | | | anatase | 500 |
| NM-101 | Titanium Dioxide | Titanium Dioxide | 38 | 6 | 320 | | | anatase | 2000 |
| NM-102 | Titanium Dioxide | Titanium Dioxide, anatase | 132 | 20 | 90 | | | anatase | 500 |
| NM-103 | Titanium Dioxide | Titanium Dioxide thermal, hydrophobic | 186 | 20 | 60 | | | rutile | 2000 |
| NM-104 | Titanium Dioxide | Titanium Dioxide thermal, hydrophilic | 67 | 20 | 60 | | | rutile | 500 |
| NM-105 | Titanium Dioxide | Titanium Dioxide rutile-anatase | 95 | 22 | 61 | | | rutile-anatase | 250 |
| | | | | | | | | | |
| NM-110 | Zinc oxide, uncoated | Zinc Oxide | 150 | 42 | 12 | | | | 2000 |
| NM-111 | Zinc oxide, coated | Zinc Oxide coated triethoxycaprylsilane | 140 | 34 | 15 | | | | 2000 |
| NM-112 | Zinc oxide, uncoated | Zinc Oxide | 119 | 24 | 27 | | | | 500 |
| NM-113 | Zinc oxide, uncoated | Zinc Oxide | 643 | 25 | 6 | | | | 500 |
| | | | | | | | | | |
| NM-200 | Silicon dioxide | Synthetic Amorphous Silica PR-A-02 | 47 | 20 | 230 | | | precipitated | 500 |
| NM-201 | Silicon dioxide | Synthetic Amorphous Silica PR-B-01 | 62 | 8-15 | 160 | | | precipitated | 500 |
| NM-202 | Silicon dioxide | Synthetic Amorphous Silica PY-AB-03 | 108 | 8-15 | 200 | | | thermal | 500 |
| NM-203 | Silicon dioxide | Synthetic Amorphous Silica PY-A-04 | 137 | 8-20 | 226 | | | thermal | 500 |
| NM-204 | Silicon dioxide | Synthetic Amorphous Silica PR-A-05 | 75 | 8-15 | 144 | | | precipitated | 500 |
| | | | | | | | | | |
| NM-211 | Cerium Dioxide | Cerium (IV) Oxide precipitated, uncoated, cubic | tbd | 10 | 66 | | | | 500 |
| NM-212 | Cerium Dioxide | Cerium (IV) Oxide precipitated, uncoated | 28 | 33 | 28 | | | | 500 |
| NM-213 | Cerium Dioxide | Cerium (IV) Oxide | 600 | 33 | 4 | | | | 500 |
| | | | | | | | | | |
| NM-220 | Barium Sulphate | Barium Sulphate | tbd | tbd | | | | | 500 |
| NM-221 | Barium Sulphate | Barium Sulphate, non-commercial grade control | tbd | tbd | | | | | 500 |
| | | | | | | | | | |
| NM-300 | Silver | Silver <20 nm | 15 | 15 | | | | | select NM-300K |
| NM-300K | Silver | Silver <20 nm | 15 | 15 | | | | | 2000 |
| NM-300 DIS | Silver Matrix/Media control | Ag - dispersant | NA | NA | | | | | select NM-300K DIS |
| NM-300K DIS | Silver Matrix/Media control | Ag - dispersant <20 nm | NA | NA | | | | | 1000 |
| *NM-301* | *Silver* | *Silver - 50-100 nm* | | | | | | | *no longer available* |
| NM-302 | Silver | Silver - elongated, rods | tbd | tbd | | | | | 2000 |
| NM-302 DIS | Silver Matrix/Media control | Ag - dispersant | NA | NA | | | | | 1000 |
| | | | | | | | | | |
| NM-330 | Gold | nano-Gold | 14 | 14 | | | | | 5000 |
| NM-330 DIS | Gold Matrix/Media control | Gold Matrix/Media control | NA | NA | | | | | 1000 |
| NM-332 | Gold | nano-Gold | tbd | tbd | | | | | 1000 |
| NM-332 DIS | Gold Matrix/Media control | Gold Matrix/Media control | NA | NA | | | | | 1000 |
| NM-333 | Gold | nano-Gold | tbd | tbd | | | | | tbd |
| | | | | | | | | | |
| NM-400 | MWCNT | Multi-walled carbon nanotubes | NA | NA | 280 | 1.5 | 11 | | 250 |
| NM-401 | MWCNT | Multi-walled carbon nanotubes | NA | NA | 300 | 4.5-15 | 67 | | 150 |
| NM-402 | MWCNT | Multi-walled carbon nanotubes | NA | NA | 250 | 1.5 | 11 | | 250 |
| NM-403 | MWCNT | Multi-walled carbon nanotubes | NA | NA | | >1 | 4-13 | | 150 |
| | | | | | | | | | |
| NM-410 | SWCNT | Single-walled carbon nanotubes | tbd | tbd | | | | | 150 |
| NM-411 | SWCNT | Single-walled carbon nanotubes | tbd | tbd | | | | | 150 |
| | | | | | | | | | |
| NM-600 | Nanoclay | Bentonite | 288 | D90=87* | 52 | | | | 500 |

# 3 Characterisation of Representative Nanomaterials

The issue of Reference Materials (RMs) for measurement and reference matrices and reference items for testing has been addressed in a variety of publications and reports from different scientific, regulatory or harmonisation-standardisation points of view. The present chapter addresses terminology of reference items, the use under Good Laboratory Practice and aspects related to characterisation needs.

Reference Material and as a sub-group of them Certified Reference Materials (CRMs) are the basis for reliable measurement results and are anchored in metrology. RMs (including CRMs) can be used for analytical method development, validation, calibration and means of quality control for specified material property. Because of the assured RM homogeneity regarding this material property, method variability, repeatability and intermediate precision can be addressed for the measurement system used. CRMs are accompanied by their certified value with its uncertainty and can be used among other purposes for assessment of the trueness of the analytical method within the frame of the intended use outlined in the certificate. The commutability of RMs needs to be addressed to ensure appropriateness of their use in corresponding measurement systems.

The so-called reference items under Good Laboratory Practice (GLP) are intended to be used in test studies, the outcome of which are used for regulatory purposes, such as a safety assessments or product approvals, *e.g.* for the registration, authorisation or restriction of chemical substances under Regulation (EC) No 1907/2006 (REACH), and for the approval of pharmaceuticals under Directive 2001/83/EC on the Community code relating to medicinal products for human use. Their characteristics are matching to a large extend those of RMs.

GLP is a quality system for a multitude of study types, from the straight-forward determination of a physical-chemical property to the most complex field,

toxicological or eco-toxicological studies. It is a legal requirement in many countries around the globe, including the USA, Japan and the EU Member States. For the data submitter, this provides the basis for mutual acceptance of the generated data (*i.e.* Mutual Acceptance of Data (MAD)) in the member countries of the OECD. Reference items are used in GLP studies to generate a predictive value for a defined (regulatory) endpoint. The "appropriate" identification of test and reference items under GLP is a requirement defined within GLP. It further comprises homogeneity and stability both under storage and test conditions.

Most evidently, representative materials for use as reference items under GLP are urgently required for implementation of policy and regulation. Representative materials, for which a high density of data has been generated, provide the best possible choice to serve as reference items. Representative materials, which are used as reference items in test studies may be qualified as RM or CRM, provided that the data are available, analysed and reported or certified for one or more specific property. The underlying definitions are cited in the subsequent sub-chapters.

## 3.1 Reference Items and Test Items in Good Laboratory Practice (GLP)

The OECD Good Laboratory Practice (OECD GLP, 1998) ENV/MC/CHEM(98)17 entitled *" OECD SERIES ON PRINCIPLES OF GOOD LABORATORY PRACTICE AND COMPLIANCE MONITORING, Number 1: OECD Principles on Good Laboratory Practice"* and the corresponding European Directive 2004/10/EC (EC GLP, 2004) describe the principles of Good Laboratory Practice (GLP). This understanding is of pivotal importance as "*the resources devoted to the tests should not be wasted by having to repeat tests owing to differences in laboratory practice from one Member State to another."* GLP therefore plays a decisive role regarding regulatory testing as firstly, it is mandatory to being applied for testing according to existing

legislation and secondly, leads to mutual acceptance of data results of the testing among the OECD member countries.

Regulation (EC) No 1907/2006 (REACH) in its article 13 paragraph 4 defines such mandatory requirement regarding the generation of information on properties of substances: *"Ecotoxicological and toxicological tests and analyses shall be carried out in compliance with the principles of good laboratory practice provided for in Directive 2004/10/EC or other international standards recognised as being equivalent by the Commission or the Agency…".* It should be noted, however, that the Commission and the European Chemicals Agency have not recognised any standards as being equivalent.

The mutual acceptance of data is re-addressed in the EC GLP original text saying: *"The Council of the Organisation for Economic Cooperation and Development (OECD) took a Decision on 12 May 1981 on the mutual acceptance of data for the evaluation of chemical products. It issued a recommendation on 26 July 1983 concerning the mutual recognition of compliance with GLP. The principles of GLP have been modified by OECD Council Decision (C(97) 186 (final)). (9) Animal protection requires that the number of experiments conducted on animals be restricted. Mutual recognition of the results of tests obtained using standard and recognised methods is an essential condition for reducing the number of experiments in this area."*

Given the obvious importance and cross-link to the testing and analyses area, the requirements regarding the test and reference items in GLP shall be taken into account as well for nanomaterials. Under *"6. Test and Reference Items"*, GLP thereby prescribes requirements for both receipt, handling and storage as well as regarding characterisation:

*6.1 Receipt, Handling, Sampling and Storage*

1. *Records including test item and reference item characterisation, date of receipt, expiry date, quantities received and used in studies should be maintained.*
2. *Handling, sampling, and storage procedures should be identified in order that the homogeneity and stability are assured to the degree possible and contamination or mix-up are precluded.*
3. *Storage container(s) should carry identification information, expiry date, and specific storage instructions.*

*6.2 Characterisation*

1. *Each test and reference item should be appropriately identified (e.g. code, Chemical Abstracts Service Registry Number [CAS number], name, biological parameters).*
2. *For each study, the identity, including batch number, purity, composition, concentrations, or other characteristics to appropriately define each batch of the test or reference items should be known.*
3. *In cases where the test item is supplied by the sponsor, there should be a mechanism, developed in co-operation between the sponsor and the test facility, to verify the identity of the test item subject to the study.*
4. *The stability of test and reference items under storage and test conditions should be known for all studies.*
5. *If the test item is administered or applied in a vehicle, the homogeneity, concentration and stability of the test item in that vehicle should be determined. For test items used in field studies (e.g. tank mixes), these may be determined through separate laboratory experiments.*
6. *A sample for analytical purposes from each batch of test item should be retained for all studies except short-term studies."*

In addition, a direct link to the requirements of GLP is also made in other documents, such as the OECD Guidance document on the validation of test methods for hazard assessment (OECD 2005) as well as the Guidance Manual ENV/JM/MONO(2009)20/REV (OECD 2010) regarding the testing of a representative set of representative manufactured nanomaterials, which are further described.

## 3.2 Reference Materials, Certified Reference Materials, and Commutability

According to ISO Guide 34 and the corrigendum of ISO Guide 30, the terms reference material, certified reference material and commutability are defined:

***Reference Material (RM)***

*Material, sufficiently homogeneous and stable with respect to one or more specified properties, which has been established to be fit for its intended use in a measurement process.*

*NOTE 1 RM is a generic term.*

*NOTE 2 Properties can be quantitative or qualitative (e.g. identity of substances or species).*

*NOTE 3 Uses may include the calibration of a measurement system, assessment of a measurement procedure, assigning values to other materials, and quality control.*

*NOTE 4 A single RM cannot be used for both calibration and validation of results in the same measurement procedure.*

*NOTE 5 VIM has an analogous definition (ISO/IEC Guide 99:2007, 5.13), but restricts the term "measurement" to apply to quantitative values and not to qualitative properties. However, Note 3 of ISO/IEC Guide 99:2007, 5.13, specifically includes the concept of qualitative attributes, called "nominal properties". [ISO Guide 30:1992/Amd.1:2008, definition 2.1]*

***Certified Reference Material (CRM)***

*Reference material characterized by a metrologically valid procedure for one or more specified properties, accompanied by a certificate that provides the value of the specified property, its associated uncertainty, and a statement of metrological traceability.*

*NOTE 1 The concept of value includes qualitative attributes such as identity or sequence. Uncertainties for such attributes may be expressed as probabilities.*

*NOTE 2 Metrologically valid procedures for the production and certification of reference materials are given in, among others, ISO Guides 34 and 35.*

*NOTE 3 ISO Guide 31 gives guidance on the contents of certificates.*

*NOTE 4 VIM has an analogous definition (ISO/IEC Guide 99:2007, 5.14).*

*[ISO Guide 30:1992/Amd.1:2008, definition 2.2]*

***Commutability of a Reference Material***

*Property of a reference material, demonstrated by the closeness of agreement between the relation among the measurement results for a stated quantity in this material, obtained according to two given measurement procedures, and the relation obtained among the measurement results for other specified materials.*

*NOTE 1 The reference material in question is normally a calibrator and the other specified materials are usually routine samples.*

*NOTE 2 The measurement procedures referred to in the definition are the one preceding and the one following the reference material (calibrator) in question in a calibration hierarchy.*

*NOTE 3 The stability of commutable reference materials is monitored regularly.*

*[ISO/IEC Guide 99:2007, definition 5.15]*

## 3.3 Scenarios for Characterisation of NM-Series RMNs

The OECD WPMN in its work in Steering Group 7 (SG7) on *The Role of Alternative Test Methods in Nanotoxicology* focuses to address the associated practical issues, in the close cooperation of an interdisciplinary approach with the Sponsorship Programme under SG3 (Steering Group 3 on *Safety Testing of a Representative Set of Manufactured Nanomaterials*) and SG4 (Steering Group 4 *on Manufactured Nanomaterials and Test Guideline*). In addition, ISO/TC 229 Working Group 3 (Health, Safety and Environmental Aspects of Nanotechnologies) is expected to launch a technical report, which addresses this item.

In practice, and in agreement with the requirements mentioned above, characterisation results should be gained and used in their appropriate context "as delivered" or "as prepared test item":

**Scenario 1 (*i.e.* "as delivered")** is the characterisation of the properties of a representative (reference) nanomaterial (NM) as delivered. A number of properties need to be determined for each NM. The physical state and preparation form of the material examined should thereby be representative for production and use, taking into account the chain of actors and life cycle. Typical preparation forms are dry or aqueous. Sample preparation steps corresponding to analytical sample preparation should be critically assessed with regard to being a determinant of the measurement result itself, such as particle size determinations dry, in aqueous solution or physiological media. A careful selection of parameters is used to assess stability and homogeneity of the NM-Series RMNs, such as particle size and size distribution, which is determined by the use of electron microscopy.

Matrix-Sample conditioning and processing:

Sample and test item preparation: Before entering the next stage of predictive toxicological testing, protocols are developed for test item preparation for use in test systems for toxicological evaluation or environmental fate analysis. This

comprises conditioning and choice of matrix components. The prepared test item should thereby correspond to the requirements of the test method and GLP, and typically be representative for the identified exposure, taking into account the chain of actors and life cycle. Test items are prepared for oral, dermal, (intravenous) and inhalation toxicity testing for human health and for application to environmental compartments soil, water and air, in the form which is envisaged to reach the biological entity in the test system. Representative nanomaterials can best be used and brought into a matrix under defined conditions, while applying defined procedures. The preparation protocols for test item and definition of corresponding matrices will guarantee a state-of-the-art standardisation of protocols, which were identified as a major source of uncertainties or methodological errors. Obviously, the issue is similarly addressed regarding sample preparation, in order to perform measurements. Resulting issues in terminology beyond the reflections in this Chapter are not further discussed in this report.

**Scenario 2 (*i.e.* "as prepared test item")** comprises the characterisation of matrix-dependent properties following the steps of test item preparation and corresponding to the prepared test item.

# 4 NM Characterisation: as delivered

The first part of this section describes the characteristics of the NM materials for ZnO as "delivered". For selected properties, vehicles or media need to be used for sample preparation to perform the measurement. The endpoints are selected and described in the Guidance Manual for Sponsors and take into account the document currently being developed by ISO TC 229 (ISO/AWI TR 13014). Where the measurement result depends on the matrix/media/vehicle selected, as well as the applied sample preparation procedure, results are addressed in Chapter 5 related to the respective protocols.

***SCENARIO 1: NM as delivered: OECD endpoint list including***

(1) Agglomeration/aggregation (SEM)
(2) Water Solubility/Dispersibility
(3) Crystalline phase
(4) Dustiness
(5) Crystallite size
(6) Representative Electron Microscopy (TEM) picture(s)
(7) Particle size distribution – dry (and in relevant media, see Chapter 5)
(8) Specific surface area
(10) Surface chemistry
(11) Photocatalytic activity (in relevant media, see Chapter 5)
(12) Pour density
(13) Porosity
(14) Octanol-water partition coefficient, if applicable
(15) Redox potential (in relevant media, see Chapter 5)
(16) Radical formation potential (in relevant media, see Chapter 5)
(17) Other relevant information

## 4.1 Handling Procedure for Weighing and Sample Introduction

A handling procedure has been established in cooperation with scientists at the different research institutions, which used the NM-Series for zinc oxide. The NM-Series vial contains the material under argon atmosphere. The vial should be kept upright and stored under appropriate conditions at room temperature and in the dark until use. Dedicated sample and test item preparation protocols need to be used depending on the specific requirements of the measurement procedure or the test method.

The suggested handling protocol for NM-110 (NM-111, NM-112 and NM-113) Zinc Oxide reads as follows:

*BE FAST, once the vial is open! If possible, work in a glove box under inert dry atmosphere. The vial containing the NM material is filled with argon. Keep the vial upright. Record the individual sample ID number as indicated on the NM label. If working outside glove box, please wear gloves.*

1. *record laboratory conditions including relative humidity of the laboratory air for QA*
2. *weigh NM material vial still closed with cap and with the funnel (to be used in step 5)*
3. *remove cap from vial*
4. *open sample dilution vessel*
5. *transfer immediately sample into the sample dilution vessel using a clean and dry plastic funnel*
6. *handle gently and avoid air dispersion and losing material*
7. *close sample dilution vessel*
8. *close vial with cap*
9. *immediately weigh the empty vial together with the cap and the plastic funnel*

10. c*alculate mass difference. The mass difference corresponds to the total mass of material, which you have transferred into the sample dilution vessel.*

***General remarks:***

*The NM material maybe hygroscopic therefore fast and correct operation is of paramount importance. This is especially valid for the weighing procedure; i.e. one has to avoid any kind of water uptake by the sample material.*

## 4.2 Agglomeration/aggregation

### 4.2.1 Scanning Electron Microscopy (SEM)

#### 4.2.1.1 SEM Method

SEM images were obtained using a Supra 40 field emission scanning electron microscope from Carl Zeiss (Welwyn Garden City, Hertfordshire, UK), in which the optimal spatial resolution of the microscope was a few nanometres. In-lens detector images were acquired at an accelerating voltage of 15 kV, a working distance of ≈ 3 mm, and a tilt angle 0°.

The SEM instrument was calibrated using a SIRA grid calibration set (SIRA, Chislehurst, Kent, UK). These are metal replicas of cross ruled gratings of area of 60 $mm^2$ with 19.7 lines/mm for low magnification and 2160 lines/mm for high magnification calibrations, accurate to 0.2 %.

For analysis of the “as delivered” NM powder, a sample of the powder was sprinkled over a SEM carbon adhesive disc; one side of the carbon disc was placed securely on a metal stub, whilst the other side was exposed to the NM powder. Excess powder was removed by gently tapping the stub on its side until a light coating of powder on the surface became apparent. For analysis of nanoparticles dispersed in liquid media, sample preparation requires to “fix” the nanoparticles on to a substrate surface. This involved the deposition of an appropriate liquid sample (1 ml) on to a poly-l-lysine coated microscope glass slide (purchased from Fisher Scientific, UK) and allowing it to incubate for a

period of 5 min at room temperature (≈ 20 °C) before dipping in a beaker of water in order to remove unbound nanoparticles. Slides were then allowed to dry under ambient conditions for ≈ 2 h before they were thinly sputtered with gold using an Edwards S150B sputter coater unit (BOC Edwards, UK). Sputtering was conducted under vacuum (≈ 7 mbar or 0.7 mPa), while passing pure, dry argon into the coating chamber. Typical plate voltage and current were 1200 V and 15 mA, respectively. The sputtering time was approximately 10 s, which resulted in an estimated gold thickness of not more than 2 nm being deposited on top of the substrate. An adequate magnification was chosen for image acquisition *e.g.* for the estimation of primary particle mean diameter. The shape and limits of the primary particles should become apparent.

#### 4.2.1.2 SEM Results

SEM images show that the “as delivered” NM powders were highly agglomerated and aggregated, as visible in the micrographs given below in Figure 1 to Figure 4.

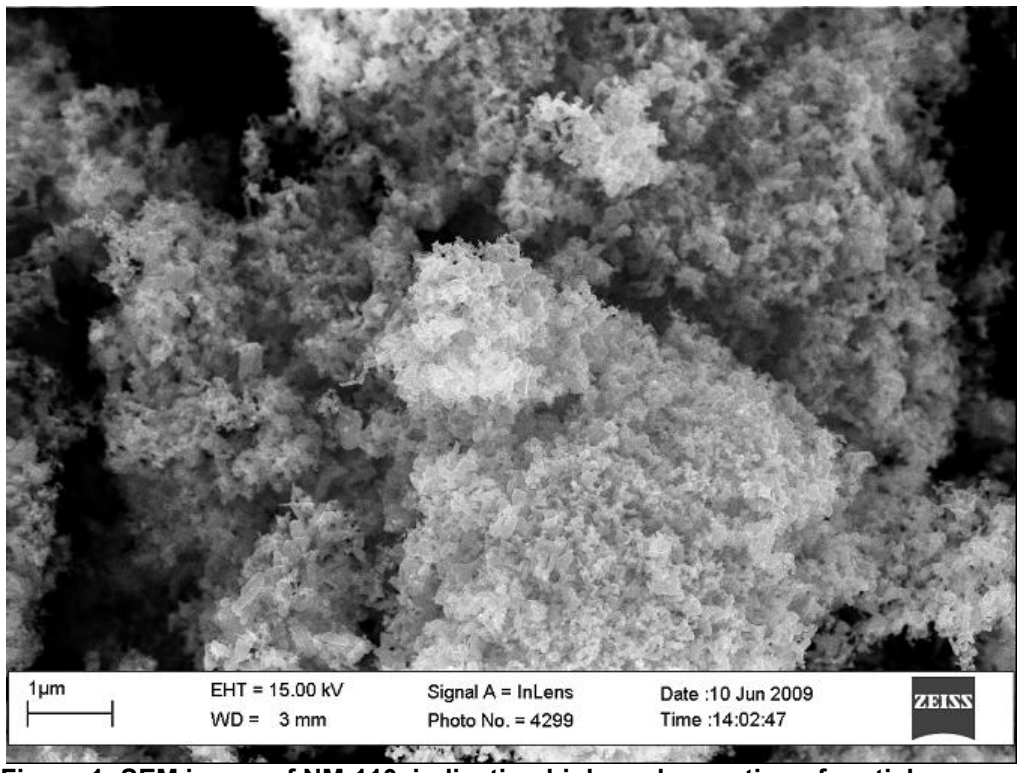


**Figure 1: SEM image of NM-110, indicating high agglomeration of particles.**

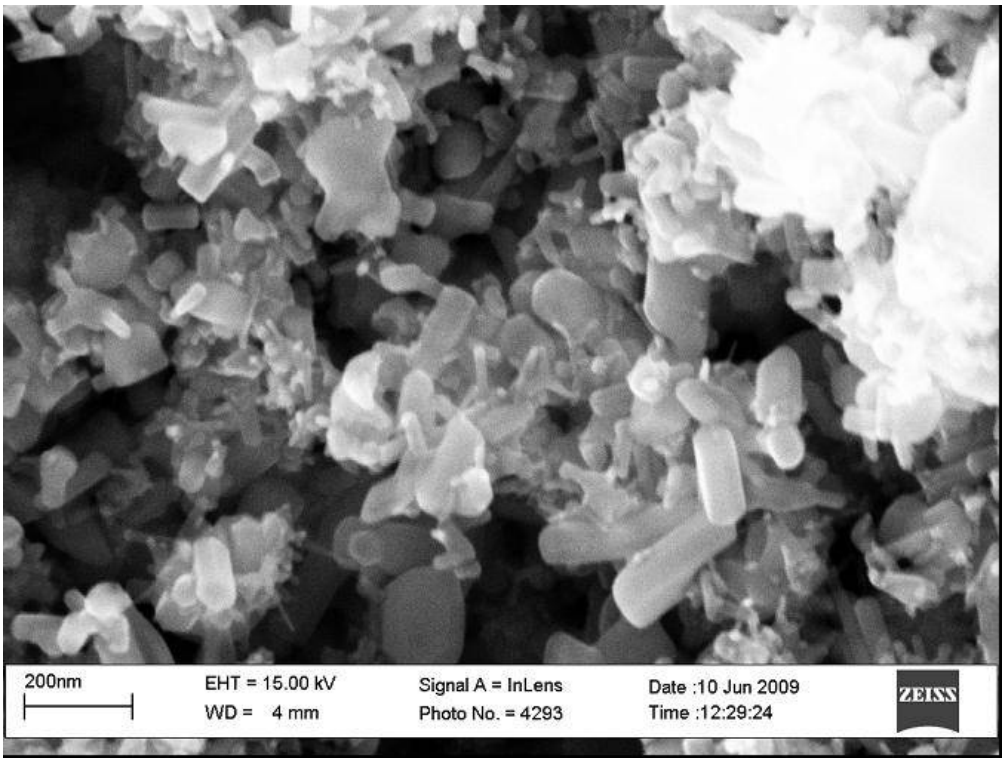


**Figure 2: High resolution SEM image of NM-111, indicating high agglomeration of particles.**

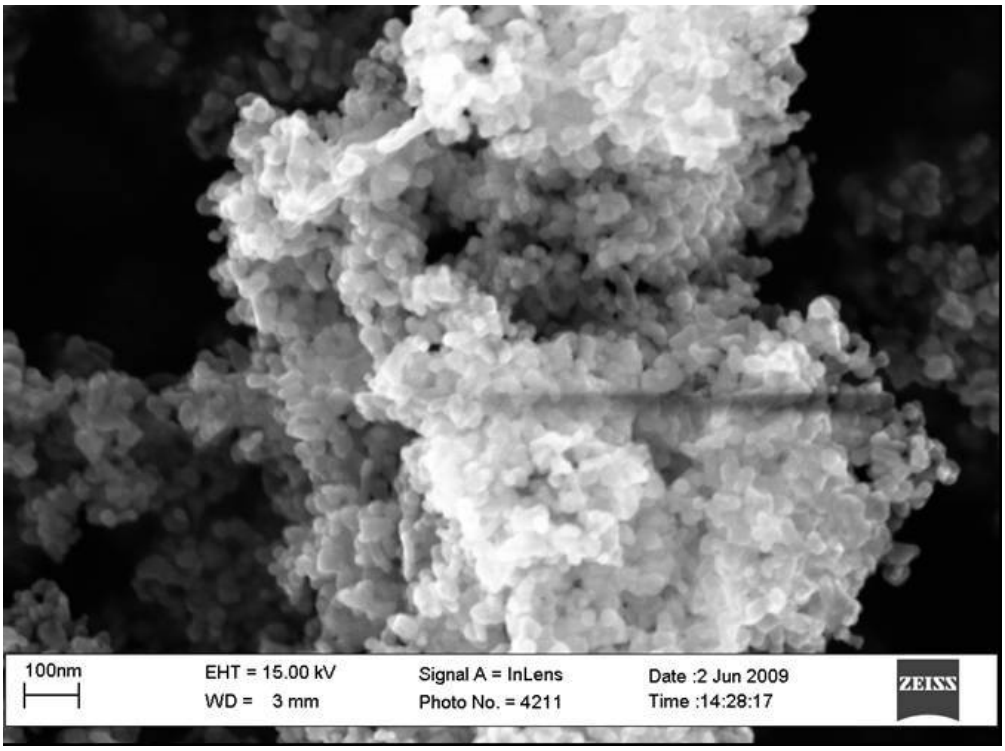


**Figure 3: High resolution SEM image of NM-112, indicating high agglomeration of particles.**

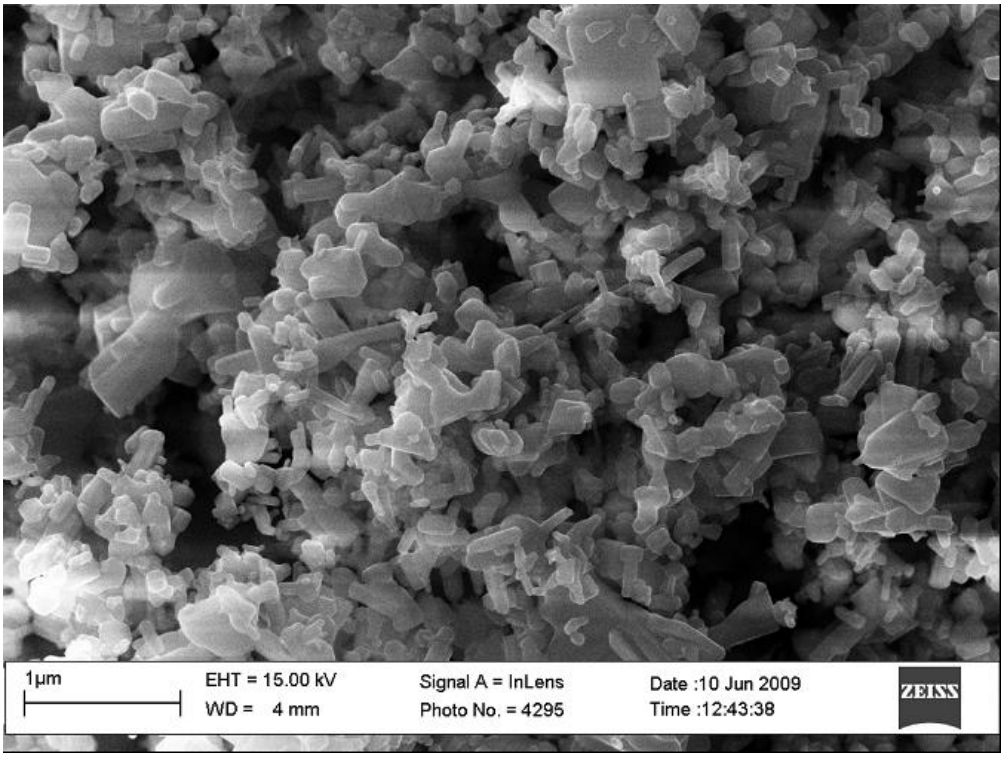


**Figure 4: SEM image of NM-113, indicating high agglomeration of particles.**

## 4.3 Water Solubility/Dispersability

### 4.3.1 Dispersability Method

Dispersion of NMs in an ecotoxicology relevant media (fish medium, daphnia medium and seawater) was carried out in accordance to a previously described protocol (refer Section 5.6 and 5.7). De-ionised (DI) water (and in some cases de-ionised water with 5 mM sodium chloride (Sigma Aldrich, UK); the NaCl here served as background electrolyte for the measurement of zeta-potential) was employed as the corresponding media control. DI water (resistivity of 18 MΩ) from Millipore, MilliQ system was used to prepare all aqueous solutions and suspensions. The chemical compositions used for making up the ecotoxicology media were obtained from the University of Exeter. Three types of ecotoxicology relevant media were prepared:

a) Seawater, in which 25 g per L of Tropic Marine Sea Salt (Tropical and Marine Limited), were made up resulting in pH ~ 8.8.
b) Daphnia freshwater media. This was prepared by firstly dissolving appropriate salts (196 mg $CaCl_2$•$2H_2O$, 82 mg $MgSO_4$•$7H_2O$, 65 mg $NaHCO_3$, 0.002 mg $Na_2SeO_3$ (as obtained by appropriate dilutions of a 2 mg/ml stock solution) in 1 L of DI water. Upon continued stirring, DI water was further added so that conductivity was between ~ 360 – 480 µS/cm. End volume ~ 1 – 1.5 L. Final pH ~ 7.9.
c) Fish freshwater media. This was prepared in three separate steps. First, salts (11.76 g $CaCl_2$•$2H_2O$, 4.93 g $MgSO_4$•$7H_2O$, 2.59 g $NaHCO_3$, 0.23 g KCl) were dissolved separately in 1L of DI water to make four separate stock solutions. Second, 25 mL of each salt stock solution was aliquot into a clean bottle and diluted in DI water (made up to 1 L volume). Third, 200 ml of the stock solution from Step 2 was aliquoted and further diluted with DI water (made up to 1L volume). Final pH ~ 7.3.

For long-term storage, the ecotoxicological solutions were autoclaved and kept refrigerated until needed.

### Colorimetric Measurements of $Zn^{2+}$

Zinc ions were measured using Cole-Palmer® Colorimetric Test Kits (Cole Palmer, UK); the kit consists of glass ampoules containing a dye that changes colour when in contact with zinc. The test measures $Zn^{2+}$ and so to get the dissolved zinc value, the supernatant was collected. To do this, particle removal was carried out using a three-step process. First is the extraction of aggregates/agglomerates using filtration through a Millipore Express PES membrane, 0.1 μm pore size filter (Fisher, UK) under vacuum. The second step involved centrifuging the resultant filtrant (Centrifuge 5430, Eppendorf, UK) at 7500 rpm for one hour. The third step involved the extraction of the clear supernatant using Peri-Star Pro peristaltic pump (World Precision Instruments, UK); this was done carefully (so as to not disturb the pellet). Only half of the supernatant was collected; supernatant was collected on Day 2 after making dispersions. The ampoules were used in accordance to the manufacturer's instructions in which 8 ml of the supernatant was allowed to sufficiently mix with the powdered dye in the ampoules and was left to equilibrate for at least 15 minutes prior to determining the zinc concentrations with the aid of a colour chart (included with the kit).

### 4.3.2 Dispersability Results

Figure 5 shows the results of the colorimetric zinc ion tests; the aim here was to evaluate the dissolution events, for 21 days, of the NM powders in the various media. The dispersions were stored in a refrigerator after day 2 in order to prevent degradation of the sample, *e.g.* minimising bacterial growth.

a)

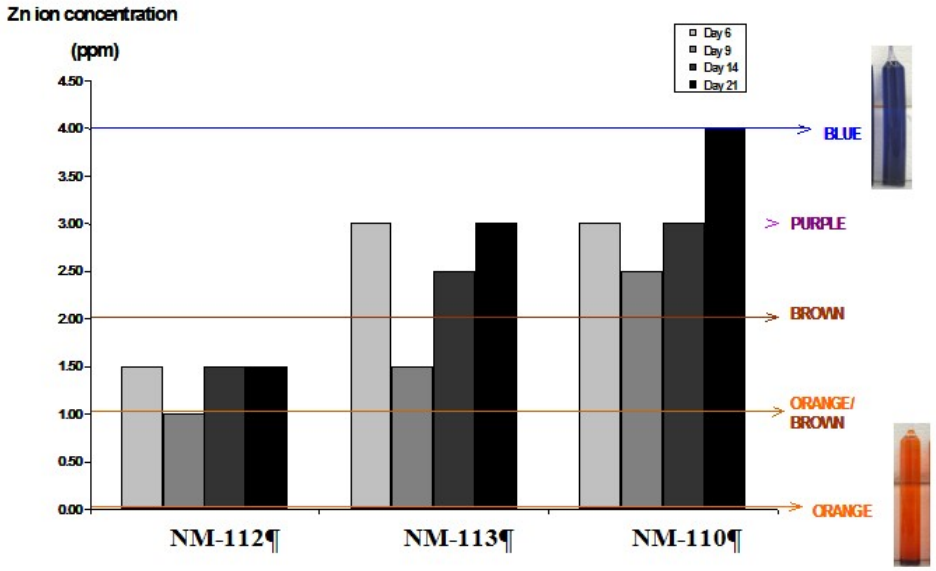


b)

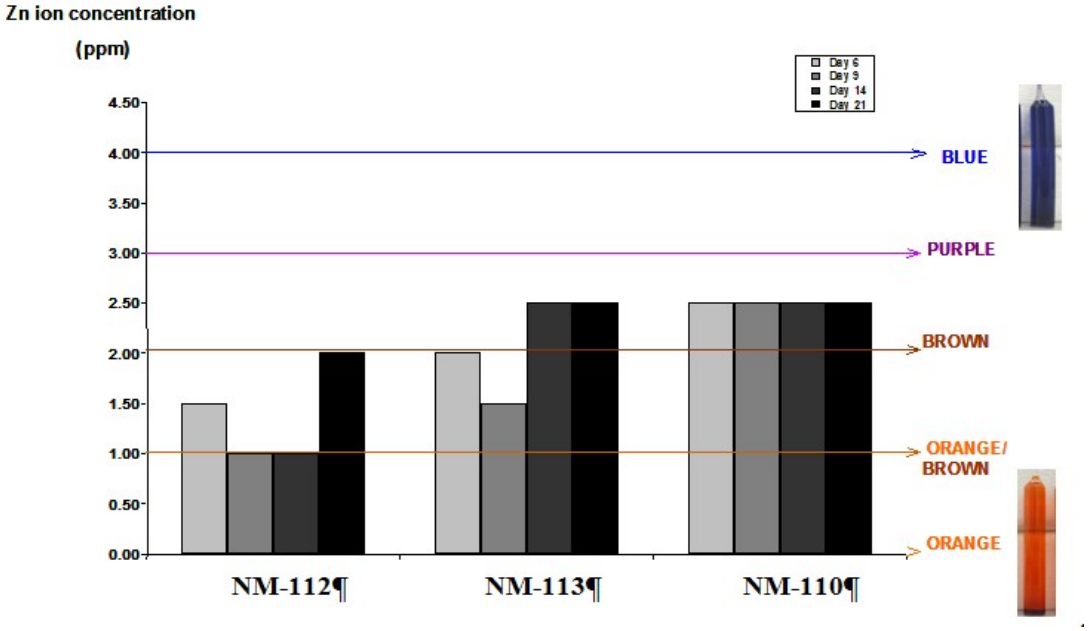


c)

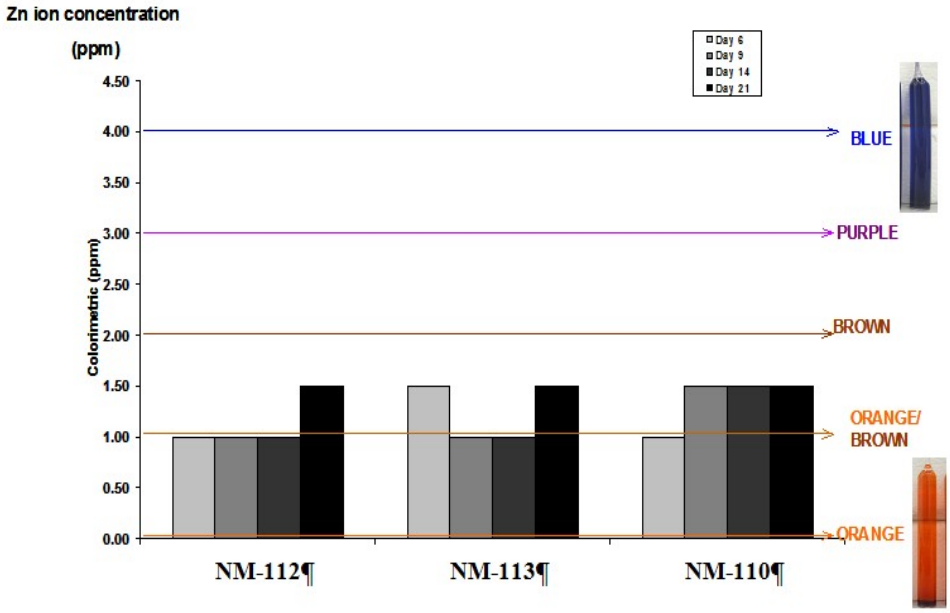


d)

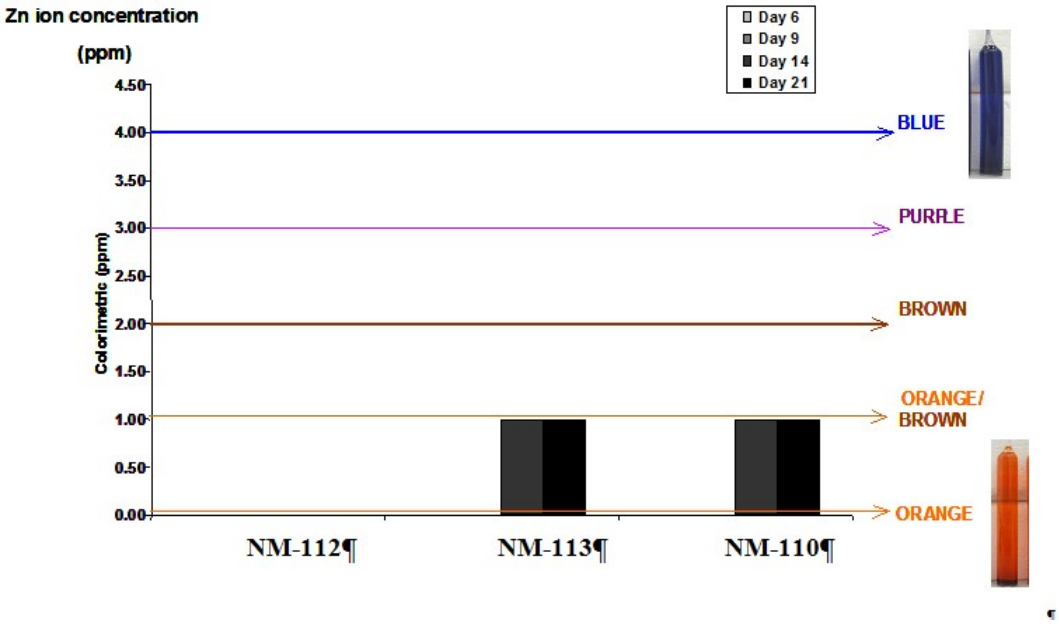


**Figure 5: Bar graphs showing colorimetric test results for zinc. The colorimetric measurement was used to evaluate NMs when dispersed (in four different media: a) DI water b) fish medium c) daphnia medium d) seawater) over time; the extracted supernatant from the dispersions were obtained prior to performing the colorimetric tests.**

Results show the following trends:

- Dissolution rates were fastest when the NMs were dispersed in DI water, with NM-110 dissolving the fastest and NM-112 dissolving the slowest. DI water yielded the most stable dispersions and this increase in stability will mean less aggregation/agglomeration (and subsequent sedimentation) in the dispersion. Hence, the total surface area is greater when the particles are dispersed in DI if compared to corresponding ecotoxicology media; an increase in surface area means that the ion dissolution rate will also increase.
- Of particular interest is the result in Figure 5a, in which we see an apparent decrease in zinc concentrations from Day 6 to Day 9, for all zinc oxide NMs. This effect may be indicative of the dissolution-precipitation process occurring during this time.
- Out of all the ecotoxicology media, fish medium had the largest dissolution rate followed by daphnia and then seawater. Dispersing NMs in such ecotoxicology media would mean less stable dispersion and this subsequently equates to the reduced surface area concentrations and thus a lower dissolution rate. In addition, the much larger ionic concentration in seawater may indirectly affect the dissolution rates, possibly through the ability to influence “inner–sphere adsorption”, which have been known to be important in mineral dissolution (Johnson *et al.,* 2004).

## 4.4 Crystalline Phase

### 4.4.1 X-Ray Diffraction (XRD) Measurement and Analysis Method

XRD analysis of nanomaterial is performed on a dedicated glancing angle X-ray diffractometer developed at the JRC in Ispra. The instrument consists of a fixed X-ray (copper anode) source, a sample ($\theta$) goniometer, and a detector ($2\theta$) goniometer. A Soller slit is mounted in front of the detector, which is a liquid nitrogen cooled HPGe detector with a low background count rate that allows the Cu-K$\alpha$ diffracted X-rays to be energy-resolved, with no interference from Cu-K$\beta$ or (generally) sample X-ray fluorescence. A variable precision slit system is used to set the incident beam at the required opening (usually 150$\mu$m), while a

precise laser alignment system is used to set the incident angle. Unless the sample requires different parameters, this is set at 1° for most measurements. NPs are drop-deposited on, or fixed to (*e.g.* using PMMA/anisole) a silicon wafer over an area of several $mm^2$. Due to the glancing angle geometry and resulting low penetration depth of X-rays into the sample, only a very small amount of NP powder is required for analysis. The resolution of the system depends on the slit opening and the Soller slit geometry. At 150μ the resolution is approximately 0.15°. X-ray patterns are compared to JCPDS reference values for phase analysis. Peak shifts from reference values give information about crystallite distortion, for example due to impurities, or macrostrains (in the case of thin films). Analysis of the diffraction peak shapes consists in separation of the Gaussian and Lorentzian (or Cauchy) components and application of standard equations (*e.g.* Scherrer) for deduction of the crystallite size and microstrain.

### 4.4.2 XRD Measurement and Analysis Results

XRD analysis of zinc oxide NM allows the identification of the crystalline phase and, in theory, to deduce the average primary particle size of the crystallite structures in the sample. In practice primary particle size can only be determined for nanoparticles below a certain average dimension, because instrumental resolution and statistical noise in the collected data causes uncertainties to increase for larger average particle sizes, for which the XRD peaks are narrower. While the glancing angle geometry allows the analysis of very small quantities of nanoparticle powder, it achieves this at the expense of poorer instrumental resolution and counting statistics with respect to conventional diffractometers. In the case of the zinc oxide examined in this study, it was decided that primary particle size could not be determined with a suitable degree of certainty.

The XRD patterns for the two samples, NM-110 and NM-111, examined by GAXRD indicate clearly the hexagonal zincite structure. Figure 6 shows the patterns for both NM-110 and NM-111, together with the ZnO reference pattern.

As discussed above, a reasonably accurate determination of average primary particle size could not be made for these two materials. However, it can be stated with reasonable certainty that the value of this parameter was greater than 20 nm in both cases.

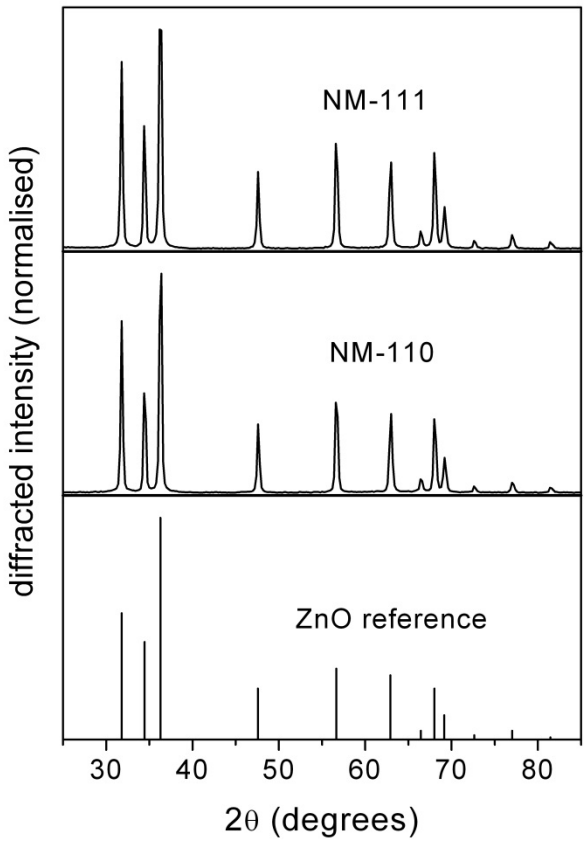


**Figure 6: XRD patterns of NM-110 and NM-111, together with the ZnO hexagonal zincite structure reference lines.**

Crystallite phases for NM-112 and NM-113 were determined by using a Bruker ASX-D8 X-Ray Diffractometer using Cu Kα radiation over a 2θ range of 5° to 85° with a step size of 0.02°. Figure 7 displays the XRD patterns for NM-112 and NM-113; he only detectable crystallite phase in these samples was hexagonal zincite.

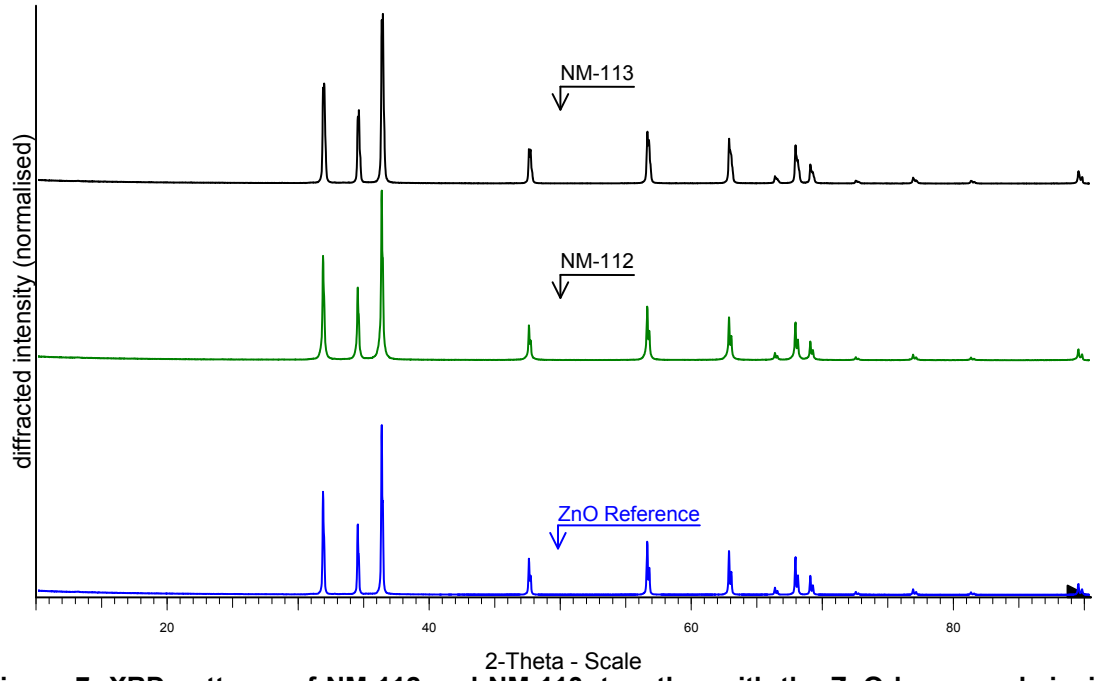


**Figure 7: XRD patterns of NM-112 and NM-113, together with the ZnO hexagonal zincite structure reference lines.**

## 4.5 Dustiness

### 4.5.1 Dustiness Method

The NM powders were tested “as delivered” for their propensity to generate dust in standardised agitation. The method applied is a downscaled version of the EN15051 rotating drum dustiness test (Schneider and Jensen, 2008). In summary the dustiness index is conducted by measuring the filter-collected mass release of respirable and inhalable dust (in mg/kg powder) during 33 repeated agitations for 1 minute and 2 minutes of subsequent collection of the airborne residual dust. The collection efficiency of the inhalable dust fraction practically follows the efficiency curve for inhalability in calm air and hence underestimates the index as compared to conventional inhalability. On-line monitoring of particle size distributions are made by a Fast Mobility Particle Size (FMPS) Model 3091 (5.6 to 560 nm) and an Aerodynamic Particle Sizer (APS) Model 3022 (0.7 to 20 µm) (both from TSI Inc.). APS size data for particles smaller than 0.7 µm were not used due to poor counting efficiency.

Six gram of material was tested in each quantitative run in a 50% RH HEPA-filtered test atmosphere at ambient temperature. Each material was tested in triplicates after an initial saturation run, which prevent underestimations of emission potential by wall- and tube loss. The average flow through the 5.9 L drum was 11 L/min. The mass of collected dust was determined in a conditioned weighing room (20°C; 50% RH) using a Sartorius microbalance.

Particle size distributions are plotted using unit density, which strongly deviate from the true density of NM-110 and NM-111. The density effect will be most pronounced for aerodynamic sizes.

### 4.5.2 Dustiness Results

#### 4.5.2.1 Gravimetric Dustiness

Test results of the dustiness studies showed a significant difference in the inhalable dustiness levels of NM-110 and NM-111 (Table 3). The respirable

dustiness index, however, was quite comparable and possibly influenced by larger variation than the inhalable dust fraction.

**Table 3: Dustiness indices for NM-110 and NM-111.**

| Dust size fraction | NM-110 | σ | NM-111 | Σ |
|---|---|---|---|---|
| Respirable Dust | 85.2 | 18.8 | 70.6 | 40.3 |
| Inhalable Dust | 855 | 96 | 1,546 | 112 |

The inhalable dustiness index is classified to be at the high end of "Low" dustiness (NM-110) to just "Moderate" (NM-111). As shown in Figure 8, this compares approximately to the levels of nanoparticle powders of goethite, organoclay and talc compared to dustiness data on other test nanomaterials published by Schneider and Jensen, and Jensen *et al.,* (Schneider and Jensen, 2008, Jensen *et al.,* 2009). For respirable dust both samples are in the lower "Moderate" dustiness range (range: 50 to 250 mg/kg).

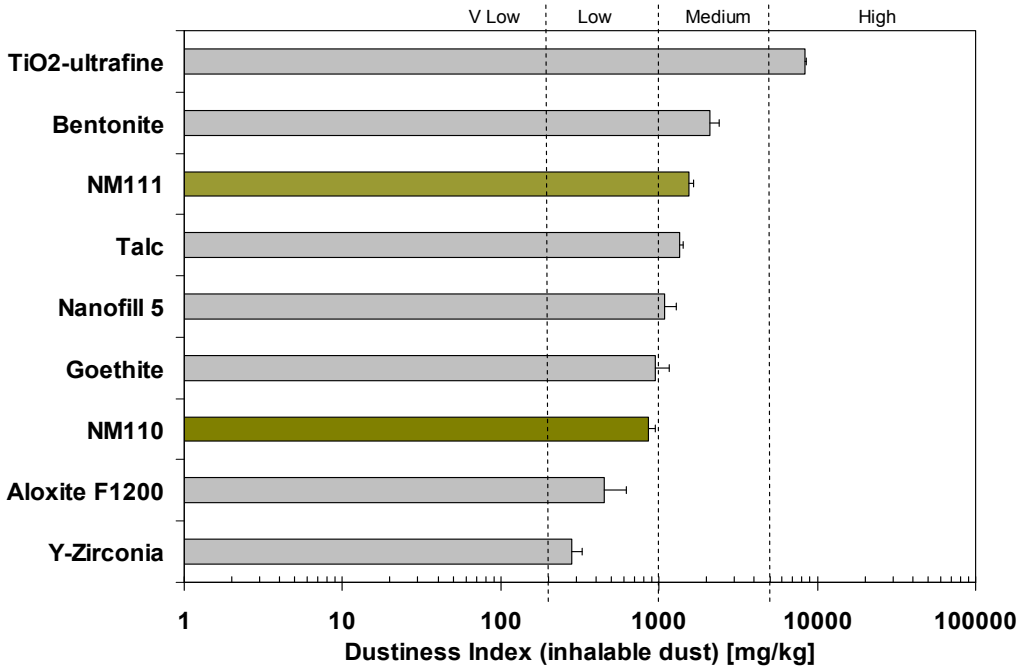


**Figure 8: Inhalable dustiness index for NM-110 and NM-111 compared to data for other common powder materials. (Schneider and Jensen, 2008; Jensen *et al.,* 2009)**

#### 4.5.2.2 Size-Distribution Data

Figure 9 shows the size distribution spectra of the two NM test materials. Both powders are characterised by liberating a relatively high number of small-size particles with a peak-mode around 30 - 40 nm and another major broad size mode ca. 200 nm. The dust in the µm-range is either almost merged broad bimodal or clearly bi- or tri-modal. Interestingly, it is the surface-coated NM-111, which emits more distinct size modes in the coarse fraction. Comparing the dustiness size distributions indicates that the 30-40 nm size-mode may be primary singlet particles or small size aggregates.

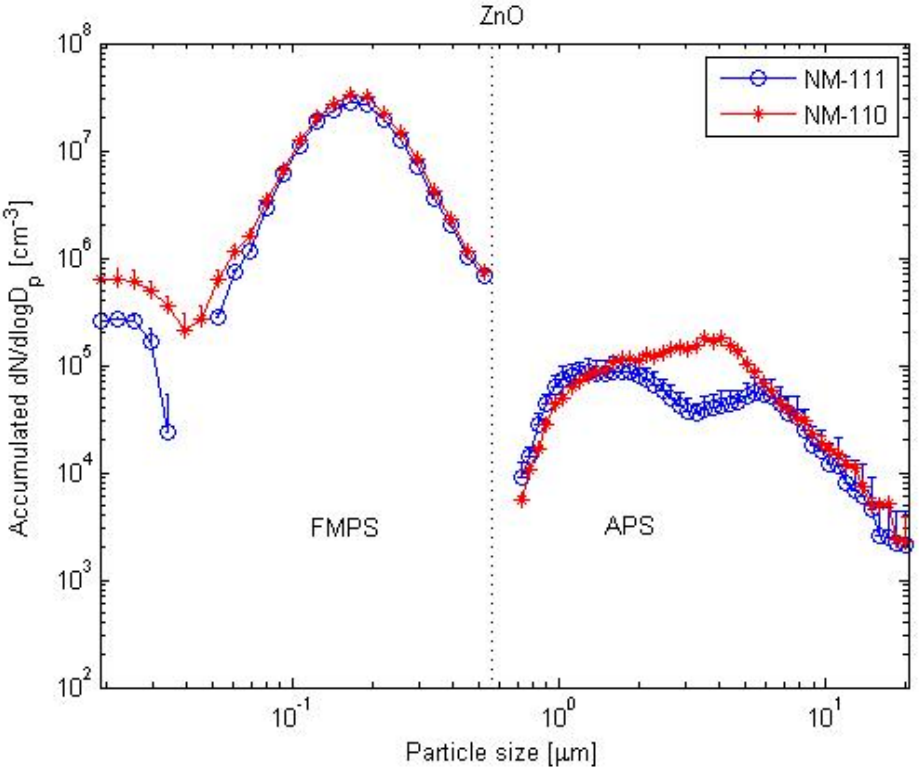


**Figure 9: Particle number-concentration size spectra of NM-110 and NM-111. The dip in particle number concentration in the APS data below 1 µm is probably caused by a rapid drop in counting efficiency for sub-µm powders.**

## 4.6 Crystallite Size

### 4.6.1 XRD Method

X-ray diffraction traces were obtained using a Siemens D5000 diffractometer. This consisted of a theta-theta goniometer and an NPL specimen stage. The X-ray source used for these measurements was the Cu- K$\alpha$ X-ray (40 kV, 30 mA) filtered using a Ni filter that removed the Cu- K$\beta$ component of the X-ray. The X-ray optics consisted of a 0.6mm anti scatter slit, a 1mm collimation slit and a 1mm detector slit. The diffraction measurement was conducted using coupled theta-theta drives in standard Bragg-Brentano geometry. The data was collected over a 2-theta range of 5 to 150° using a step size of 0.010° and a count time of 1.5 s/step. The diffracted data was electronically collected and stored on the laboratory PC. Prior to the measurement the X-ray beam was aligned by placing the X-ray source and the detector in line and passing the X-ray beam through a glass slit, the direct beam was attenuated using copper foil placed in front of the detector. Having aligned the two drives and the stage height a standard reference material (corundum) was used to check the alignment over a range of 2-theta values. Having collected the full diffraction trace the Scherrer equation was used to evaluate the crystallite size.

### 4.6.2 XRD Results

Table 4 shows that crystallite sizes for the powders were in the range of 24 nm to 42 nm. Both NM-110 and NM-113 have the same crystallite size of ~ 42 nm. The average crystallite size determined by Rietveld refinement taking the structure and morphology into consideration yield larger crystallite sizes of NM-110 (> 85.5 nm) and NM-111 (75.5 nm). (ENPRA, 2010)

**Table 4: XRD crystallite sizes determined using Scherrer's equation.**

| Sample Name | Crystallite Diameter from XRD/nm |
|---|---|
| NM-110 | 41.5 |
| NM-111 | 33.8 |
| NM-112 | 24.1 |
| NM-113 | 41.5 |

It is interesting to compare results of the crystallite size as obtained by X-ray diffraction (XRD) to those of particle size as obtained by SEM imaging. Overall, results show that particle size (as reported from SEM image analysis) is much larger than the corresponding reported crystallite size. This is not surprising as a particle (or grain) may be made up of several different crystallites.

## 4.7 Representative TEM Picture(s)

### 4.7.1 TEM Measurement and Analysis Method

Transmission electron microscopy (TEM) was completed using a JEOL (Tokyo, Japan) 3010 transmission electron microscope operating at 300 kV.

#### 4.7.1.1 Sample Preparation

Samples were prepared by dispersing particles on carbon-coated TEM Cu-grids after dispersion in approximately 15 mL of ethanol (EtOH). Particle dispersions in EtOH were deposited onto the inner meshed surface of the TEM grid. After a few seconds, the excess of the dispersion was removed with a filter paper and the grids were dried overnight in the dark at 25 °C.

For samples NM-112 and NM-113, carbon-coated grids (copper, 300 mesh) were glow discharged in nitrogen for 30 seconds to render them hydrophilic. Samples were dispersed by briefly sonicating a few mg of the material in approximately 20ul ethanol to form a milky dispersion. 5ul of dispersion was applied to the freshly glow discharged grids. After 2 minutes adsorption time, excess dispersion was wicked off using filter paper (Whatman 541) and the grids were air-dried for 15 minutes. Grids were examined using a Tecnai 12 TEM (FEI, Eindhoven, Netherlands) operating at 120 kV, and micrographs were recorded using an Olympus Megaview III CCD camera (Tokyo, Japan) running AnalySiS imaging software (Olympus) at a variety of magnifications chosen to highlight both the aggregation state of the samples (lower magnifications *e.g.* 6000x) as well as higher magnifications adequate for showing particle morphology (100 000x - 360 000x).

#### 4.7.1.2 Quantitative Analysis of the Particles

The particle size distribution was determined from the analysis of approx. 500-1000 particles, randomly examined from collected pictures.

### 4.7.2 TEM Results

#### 4.7.2.1 NM-110

Using TEM, the primary ZnO crystals were observed to be polyhedral with quite variable morphology. Two main types of morphology could be distinguished:-

1. particles with aspect ratio close to 1 (typically 20 – 250 nm size and very few particles of approx. 400 nm size) and hexagonal morphology
2. particles with aspect ratio 2 to 7.5 (50 – 350 nm) with cubic, tetragonal and orthorhombic morphologies.

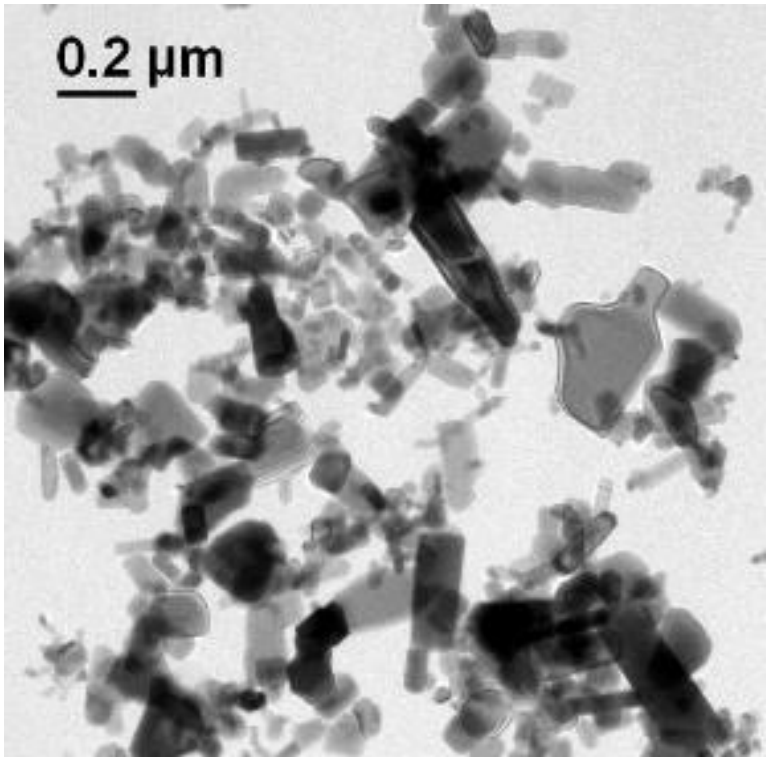


**Figure 10: TEM image of NM-110, showing the coarse particle size variation and their agglomerated/aggregate structure.**

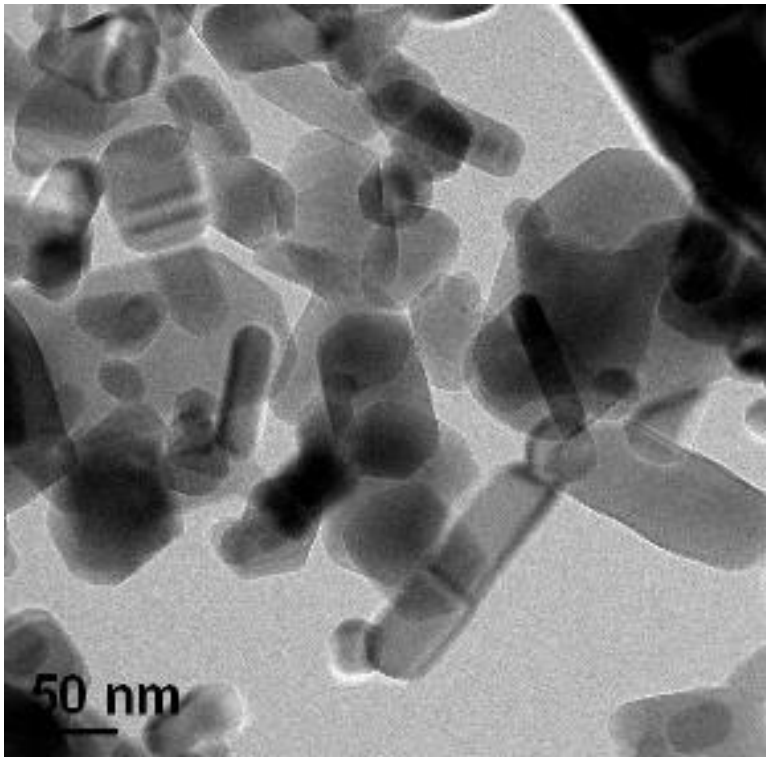


**Figure 11: High-magnification TEM image of NM-110, showing the size-range and morphological variation of small ZnO crystallites.**

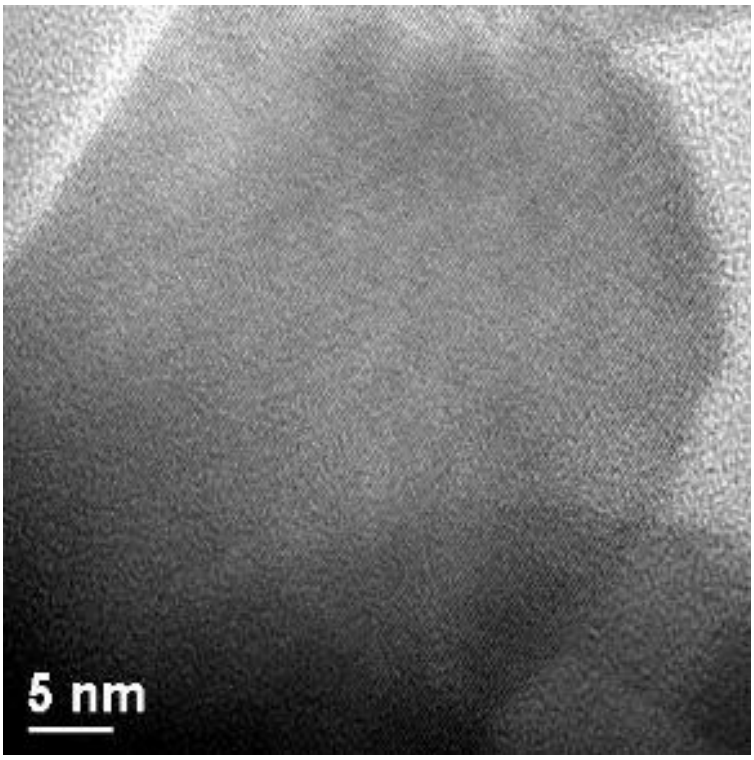


**Figure 12: High-resolution image of NM-110, showing the perfect structure of zincite crystallites.**

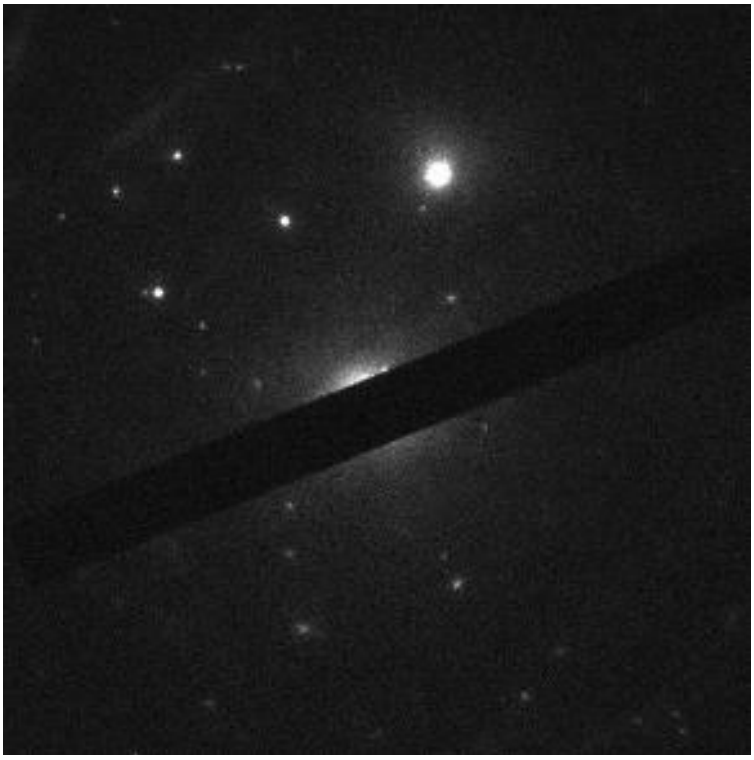

**Figure 13: Electron diffraction pattern of NM-110, showing the presence of large (bright single spots) crystallites in the sample.**

#### 4.7.2.2 NM-111

TEM analysis indicates that the primary particles appeared polyhedral and with variable morphology as observed in NM-110, but with different size distributions. Once again, two main morphological types could be distinguished:-

1. particles with aspect ratio close to 1 (~90% in the 20 – 200 nm range)
2. particles with aspect ratio 2 to 8.5 (~90% in the 10 – 450 nm range).

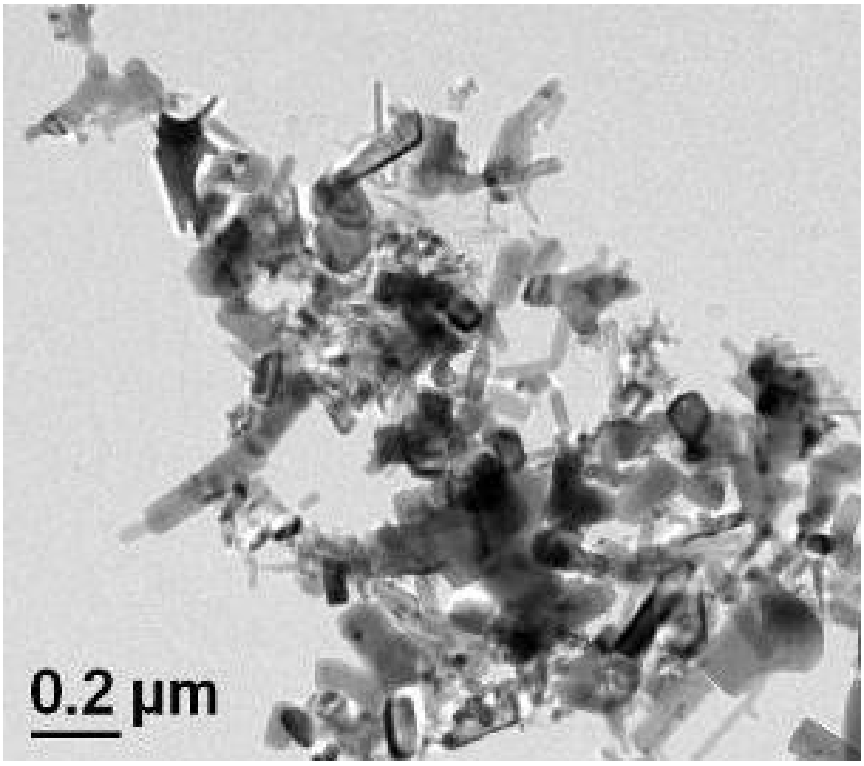


**Figure 14: TEM image of NM-111, showing the agglomerated aggregate structure of particles.**

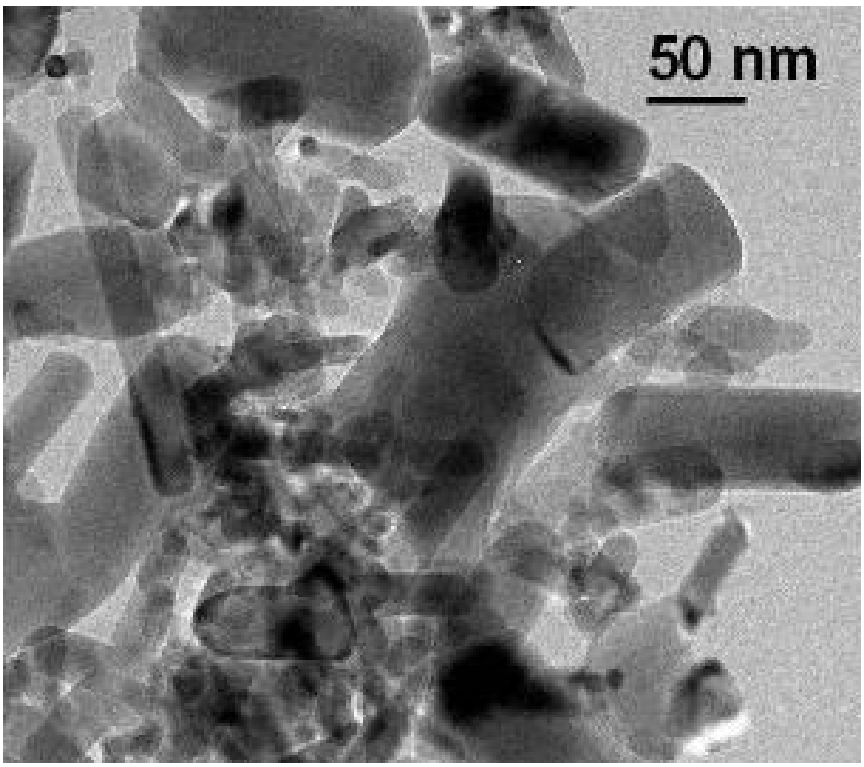


**Figure 15: High magnification TEM-image of NM-111, showing the large size-range of ZnO crystallites.**

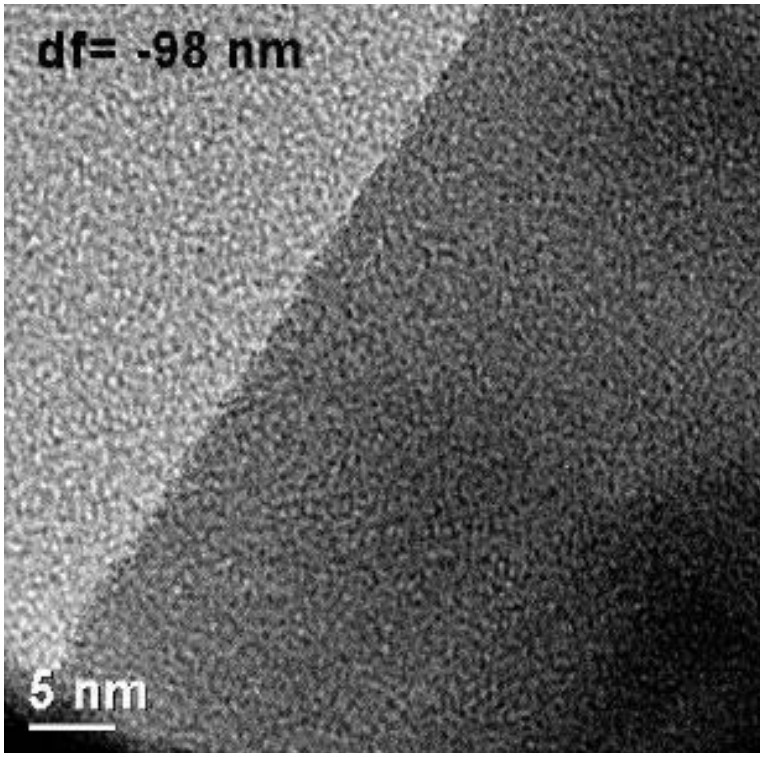


**Figure 16: High-resolution image of NM-111, showing partially amorphous crystallite (possibly due to beam-damage).**

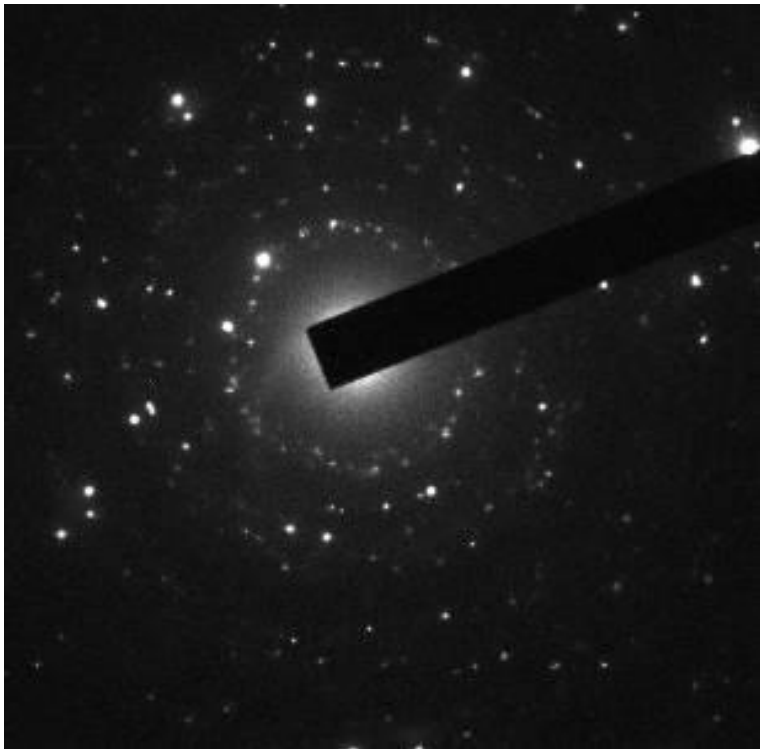

**Figure 17: Electron diffraction pattern of NM-111, showing the presence of both large (bright single spots) and small (ring pattern) crystallites in the sample.**

#### 4.7.2.3 NM-112

Qualitative TEM analysis indicates that primary particles appeared to be near spherical rather than polyhedral with regular morphology and a relatively homogenous size distribution. Generally, particles have an aspect ratio close to 1 and with sizes between 20 – 50 nm and appear distinctly different to all the other samples (NM-110, NM-111 and NM-113).

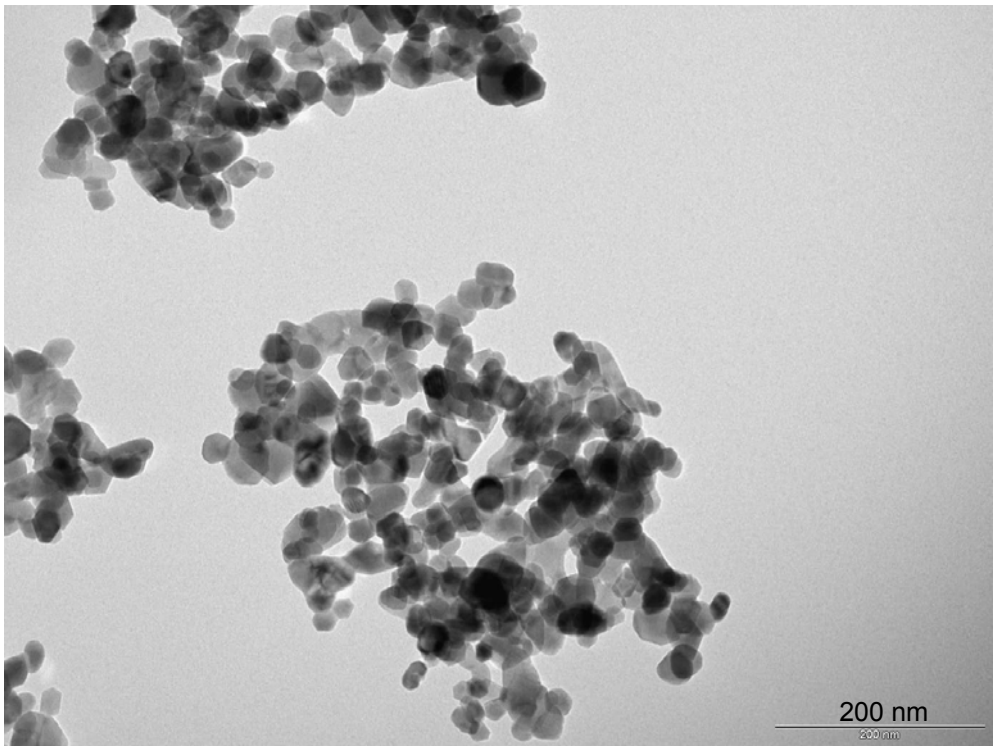


**Figure 18: TEM image of NM-112, showing the relatively regular particle sizes and shapes in agglomerated/aggregated structures.**

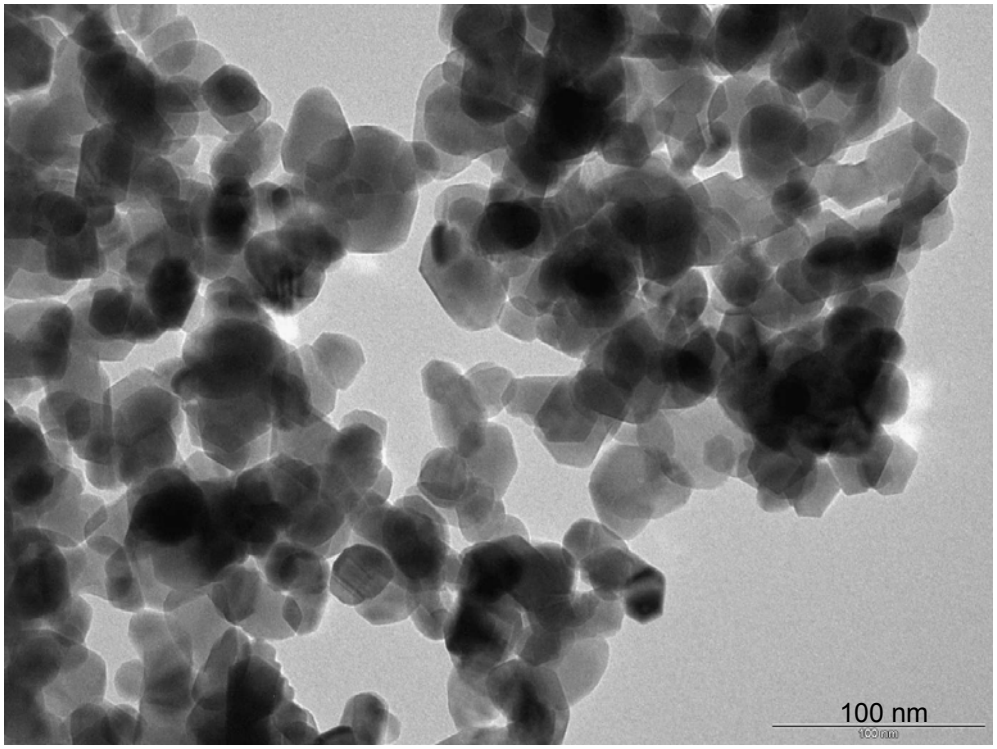


**Figure 19: TEM image of NM-112, showing relatively regular and homogeneous particle sizes and shapes.**

#### 4.7.2.4 NM-113

TEM analysis indicates that the primary particles appeared polyhedral and with variable morphology as observed for NM-110 and NM-111 (but not NM-112) with different size distributions. Qualitatively, two main morphological types appear distinguishable:

1. particles with aspect ratio near 1 (typically in the 80 – 100 nm range)
2. particles with aspect ratio > 2 (typically in the 180 – > 200 nm range)

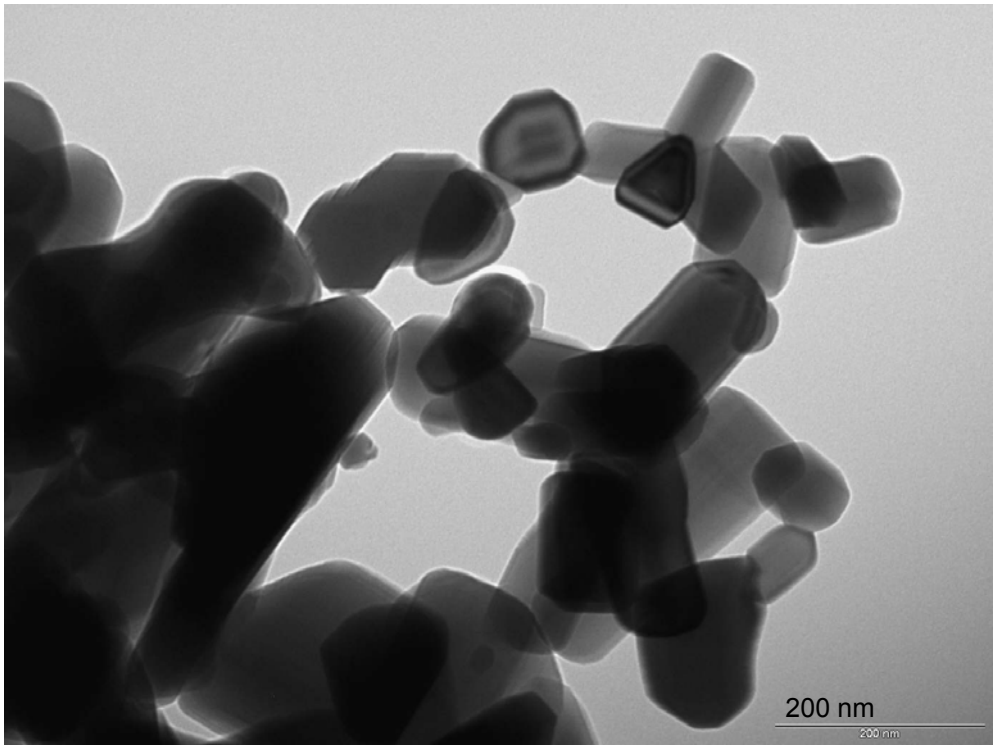


**Figure 20: TEM image of NM-113, showing irregular and non-homogeneous particle sizes and shapes.**

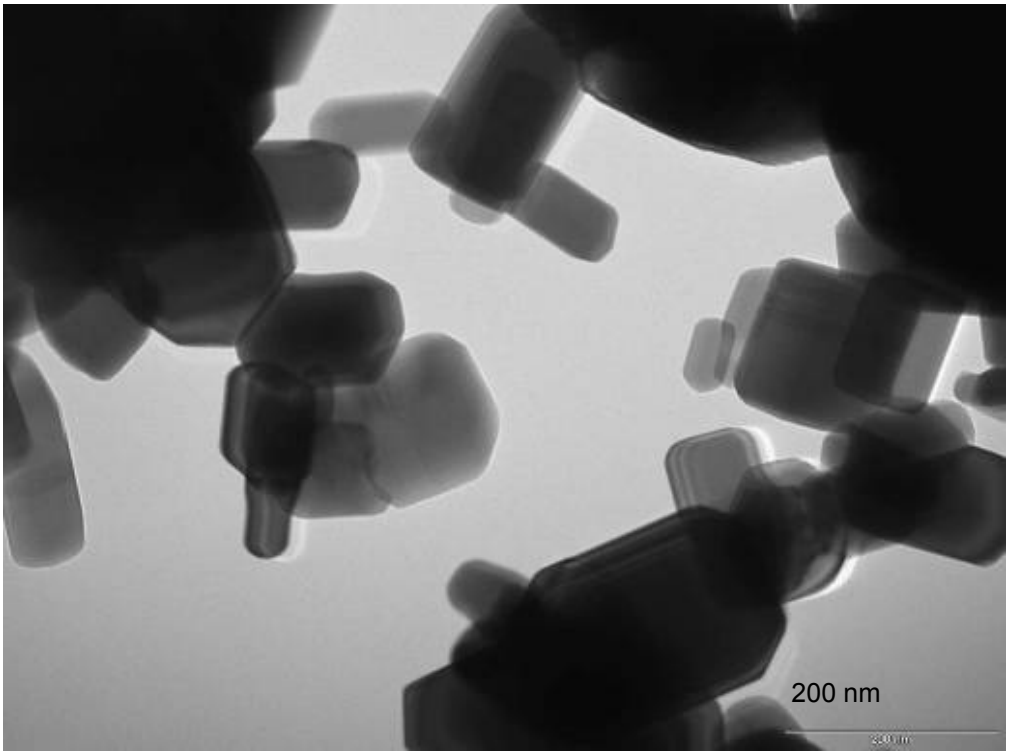


**Figure 21: TEM image of NM-113, showing irregular and non-homogeneous particle sizes and shapes.**

## 4.8 Qualitative and Quantitative Analyses using TEM

### 4.8.1 Introduction

The aim of these analyses is to characterise these NM qualitatively and quantitatively.

Qualitative analyses describe the characteristics of the ZnO NM that are related to their toxicity[††] and which are accessible by TEM. They include the visualization of particles in representative and selected micrographs. These analyses also evaluate whether the particles are homogeneously distributed on the EM-grid. This is, in addition to the stability of suspension, a condition that determines whether a quantitative EM-analysis is feasible.

In the quantitative analyses, the particles were distinguished from the background based on their grey value corresponding with their inherent electron density. Relevant parameters are measured on a per-particle level, for a representative fraction of the sample.

### 4.8.2 TEM Materials and Methods

#### 4.8.2.1 Materials

The ZnO samples NM-110, NM-111, NM-112 and NM-113 are provided as powders by Mercator GmbH, Berlin, Germany. These samples were individually labelled with a sample ID number and prepared under Good Laboratory Practice (GLP) for use in test studies.

#### 4.8.2.2 Sample Preparation:

In a preliminary experiment, the effects of different media on the dispersion of NM-110 and NM-111 were examined by qualitative TEM analysis. The tested sample preparation conditions are summarised in Table 6.

[††] Scientific Committee on Emerging and Newly Identified Health Risks (SCENIHR) (2009) Risk Assessment of Products of Nanotechnologies http://ec.europa.eu/health/ph_risk/committees/04_scenihr/docs/scenihr_o_023.pdf.

To obtain more stable suspensions for the qualitative analyses of NM-112 and NM-113, and for the quantitative analyses of all examined ZnO NMs, the protocol optimised for dispersion of NM-11X zinc oxide was applied. This protocol is described in detail in paragraph 5.8. Essentially, the protocol consists of pre-wetting the ZnO NM with a small amount of EtOH followed by their suspension in double distilled water, containing 0.05 % BSA, to obtain a concentration of 2.56 mg/ml, followed by a sonication step.

In CODA-CERVA, the samples were sonicated for 16 minutes using a Vibracell™ 75041 ultrasonifier (750 W, 20 kHZ, Fisher Bioblock Scientific, Aalst, Belgium) equipped with a 13 mm horn (CV33) at 20 % amplitude. This gave an average horn power of about 8 W, which resulted in a sample specific energy of approximately 8 kJ/m³. During sonication the samples were cooled in icy water to prevent excessive heating.

Suspensions were brought on pioloform- and carbon- coated 400 mesh copper grids (Agar Scientific, Essex, England). The effects of grid pretreatement with 1 % Alcian blue (Fluka, Buchs, Switzerland) to increase hydrophilicity as described by Mast and Demeestere were examined for samples NM-110 and NM-111 (Mast and Demeestere, 2009). For NM-112 and NM-113, Alcian blue pre-treatment was applied systematically.

**Table 5: Conditions applied for sample preparation: Material, vehicle and sample conditioning.**

| Condition | Pre-wetting | Medium | TEM grid treatment | Remarks |
|---|---|---|---|---|
| 1 | no | Water | Alcian blue | 12.8 mg of ZnO powder was suspended in 5 ml of water |
| 2 | Ethanol | Water | Alcian blue | 12.8 mg ZnO powder was pre-wetted with 25 µl of EtOH and mixed thoroughly during 1 min and suspended in 5 ml of water. |
| 3 | no | Water | Standard grid | 12.8 mg of ZnO powder was suspended in 5 ml of water |
| 4 | Ethanol | Water | Standard grid | 12.8 mg ZnO powder was pre-wetted with 25 µl of EtOH and mixed thoroughly during 1 min and suspended in 5 ml of water. |
| 5 | no | Water | Alcian blue | 12.8 mg of ZnO powder was suspended in 5 ml of water and sonicated for 16 min (9 kJ). |
| 6 | Ethanol | Water | Alcian blue | 12.8 mg ZnO powder was pre-wetted with 25 µl of EtOH and mixed thoroughly during 1 min, suspended in 5 ml of water and sonicated for 16 min (9 kJ). |
| 7 | no | Water | Standard grid | 12.8 mg of ZnO powder was suspended in 5 ml of water and sonicated for 16 min (9 kJ). |
| 8 | Ethanol | Water | Standard grid | 12.8 mg ZnO powder was pre-wetted with 25 µl of EtOH and mixed thoroughly during 1 min, suspended in 5 ml of water and sonicated for 16 min (9 kJ). |
| 9 | No | Hexane | Alcian blue | 4 mg of ZnO powder suspended in 0,5 ml hexane |
| 10 | No | Hexane | Standard grid | 4 mg of ZnO powder suspended in 0,5 ml hexane |

The grid-on-drop method that conventionally is used for aqueous suspensions of particles could not be applied for NM suspended in hexane because of its low surface tension. In the latter case, the drop-on-grid method was applied instead. In order to minimise possible artifacts due to long term grid storage, micrographs were recorded as soon as possible after grid preparation.

#### 4.8.2.3 Imaging

The samples were imaged in bright field mode using a Tecnai Spirit TEM (FEI, Eindhoven, The Netherlands) with BioTWIN lens configuration operating at 120 kV at spot size 1 or 3. The condenser lens current was chosen such that the

beam was parallel and images were taken approximately 500 nm below minimal contrast conditions.

#### 4.8.2.4 Qualitative TEM analysis

Based on representative and selected electron micrographs; the size, agglomeration and aggregation state, the general morphology as described by Krumbein and Sloss, the surface morphology and topography, the general structure based on morphology and diffraction contrast and the presence of visible impurities are described (Krumbein and Sloss, 1963). This analysis allows evaluating whether a quantitative EM-analysis is feasible.

#### 4.8.2.5 Quantitative TEM based on image analysis

The micrographs were taken by systematic random sampling of ten predefined positions on the grid. When the field of view was obscured by a grid bar or an artifact, the stage was moved sideways to the nearest suitable field of view. Ten transmission electron micrographs per sample were made with a 4*4 K Eagle CCD-camera (FEI), at a magnification of 18,500 times, corresponding pixel size of 0.6 nm and micrograph size of 2,450 nm. The images were stored in a dedicated database integrated in iTEM (Olympus, Münster, Germany) together with the imaging conditions, added directly to the micrograph by the TiaTag module developed at the CODA-CERVA and the sample references.
The ‘Detection module’ of iTEM was used for threshold-based image analysis. Briefly: contrast and brightness of the micrographs were optimised, the involved particles were enclosed in a pre-defined frame or region of interest and thresholds were set to separate particles from the background based on their electron density and size. For each particle, 24 relevant parameters were selected for particle characterization. These are described in detail in ISO9276-6:2008 and in the iTEM help-files (ISO, 2008). A table of descriptions for these parameters is provided in Table 6.

**Table 6: Description of the parameters measured by quantitative TEM.**

| Measured parameter | Description |
|---|---|
| Area | The area of a measured object is (the number of pixels of the measured object) times (calibration factors in X- and Y-direction). |
| Convex Area | The area of the convex cover of the measured object. |
| Hole Area | The total area of the holes of the measured object. |
| Rectangle Max | The area of the biggest rectangle whose sides consist of tangents to the measured object borders. |
| Rectangle Mean | The area of the mean rectangle whose sides consist of tangents to the measured object borders. |
| Rectangle Min | The area of the smallest rectangle whose sides consist of tangents to the measured object borders. |
| ECD (Equivalent Circle Diameter) | The equivalence refers to the area of the measured object. The ECD is the diameter of a circle that has an area equal to the area of the measured object. |
| Feret Max | The maximum distance of parallel tangents at opposing measured object borders. |
| Feret Mean | The mean distance of parallel tangents at opposing measured object borders. |
| Feret Min | The minimum distance of parallel tangents at opposing measured object borders. |
| Next Neighbor Distance | Gives the distance to the closest measured object. |
| New Radius of Inner Circle | Radius of the maximal circle inside the measured object. |
| Central Distance Max | The maximum distance between the center and the border of a measured object. |
| Central Distance Mean | The mean distance between the center and the border of a measured object. |
| Central Distance Min | The minimum distance between the center and the border of a measured object. |
| Diameter Max | The maximum diameter of a measured object (for angles in the range 0° through 179° with step width 1°). |
| Diameter Mean | The mean diameter of a measured object (for angles in the range 0° through 179° with step width 1°). |
| Diameter Min | The minimum diameter of a measured object (for angles in the range 0° through 179° with step width 1°). |
| Hole Count | The number of holes in a measured object. |
| Convex Perimeter | The perimeter of the convex cover of the measured object. |
| Perimeter | The sum of the pixel distances along the closed boundary. |

| | |
|---|---|
| Aspect Ratio | The maximum ratio of width and height of a bounding rectangle for the measured object. |
| Convexity | The fraction of the measured object's area and the area of its convex hull. |
| Elongation | The elongation of the measured object can be considered as lack of roundness. It results from the sphericity. |
| Shape Factor | The shape factor provides information about the "roundness" of the measured object. For a spherical measured object the shape factor is 1; for all other measured objects it is smaller than 1. |
| Sphericity | Describes the sphericity or 'roundness' of the measured object by using central moments. |

Each particle in the micrograph received a unique number, written in the overlay of the image, corresponding to the qualitative measurements of the particle. This allowed the extraction of data for specific particles and post-analysis deleting of non-conform particles.

The results obtained for each micrograph of a sample were combined in an excel data sheet and descriptive statistics and number-based histograms were generated using the Sigmaplot® software (Systat Software Inc, USA).

In addition to the number of non-missing observations (Size), the smallest (Min) and largest observation (Max), the average value (mean), the standard error of mean (Std. Error) and the standard deviation (Std. Dev.) are presented. However, because for all measured parameters of all examined NM, the Kolmogorov-Smirnov and the Shapiro-Wilk probabilities were <0.001 (not shown), none of these parameters can be assumed to be normally distributed. Hence, non-parametric estimates of these parameters describe the sample better. These include the median and the 25 and 75 percentiles.

### 4.8.3 TEM Results

#### 4.8.3.1 Stability of suspensions of NM-110 and NM-111 in different media

Different combinations of ethanol pre-wetting with different suspension media and sonication (Table 5) were evaluated with respect of the distribution of NM-110 and NM-111 on EM-grids. Representative micrographs are presented in Figure **22** and Figure 23. Stable suspensions (for at least 10 minutes) were only obtained when NM-110 and NM-111 were pre-wetted with ethanol, suspended in water and sonicated.

Although some individual particles and smaller agglomerates were observed, most NM were present in large agglomerates which were not homogeneously distributed on the EM-grid. Increasing the hydrophilicity of the grids by Alcian blue pre-treatment augmented the number of particles on the grid surface, but it did improve the homogeneity of the distribution of the NM. Since large agglomerates tend to detach from the EM-grid relatively easily, it is unlikely that the particles that remain attached to the grid are representative for the sample. Hence, it is assumed that the fraction of the attached NM does not suitably represent the particles in the suspension. In conclusion, the examined preparation conditions are not suitable for a quantitative analysis.

It is assumed that the sonication breaks up agglomerates into smaller sizes which results in their temporary suspension. Once sonication is stopped, however, the smaller agglomerates tend to re-agglomerate into larger ones. To overcome this problem, the protocol optimised for dispersion of NM-11X zinc oxide (paragraph 5.8) is applied for the qualitative characterisations of NM-112 and NM-113 and for all quantitative characterisations. Addition of 0.05 % BSA coats and hence stabilises the smaller aggregates obtained by sonication. This coating does not interfere with the detection of the NM because BSA is much less electron-dense than ZnO. It remains an interesting scientific question to what degree the size and shape of the agglomerates depends on (the charge density of) the coating agent, in this case BSA.

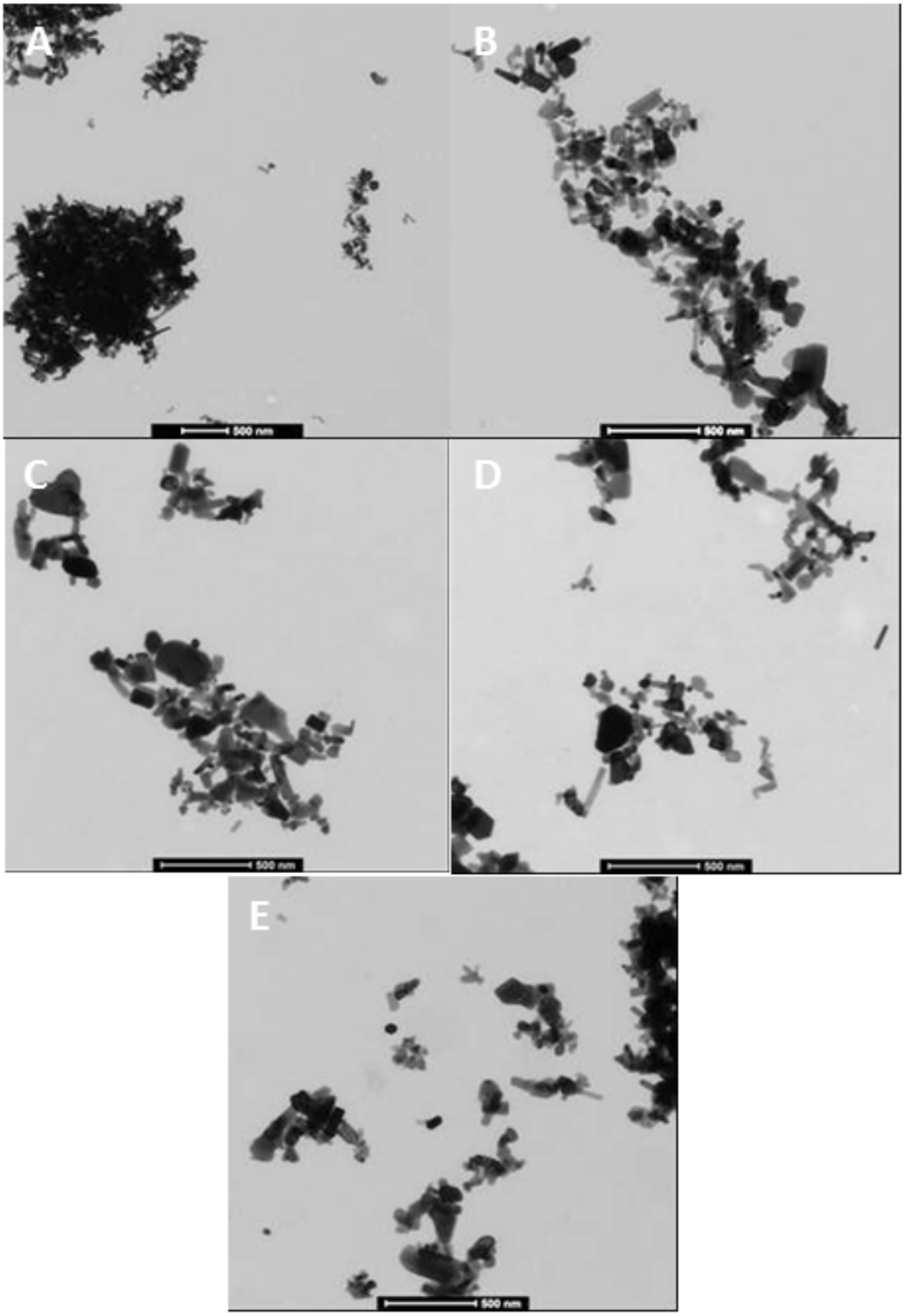


**Figure 22: Representative micrographs illustrating the effects of pre-wetting and of the suspension media on the distribution of ZnO NM-110 on Alcian blue-coated EM-grids. A, B, C, D and E correspond with conditions 1, 2, 5, 6 and 9 in Table 6, respectively.**

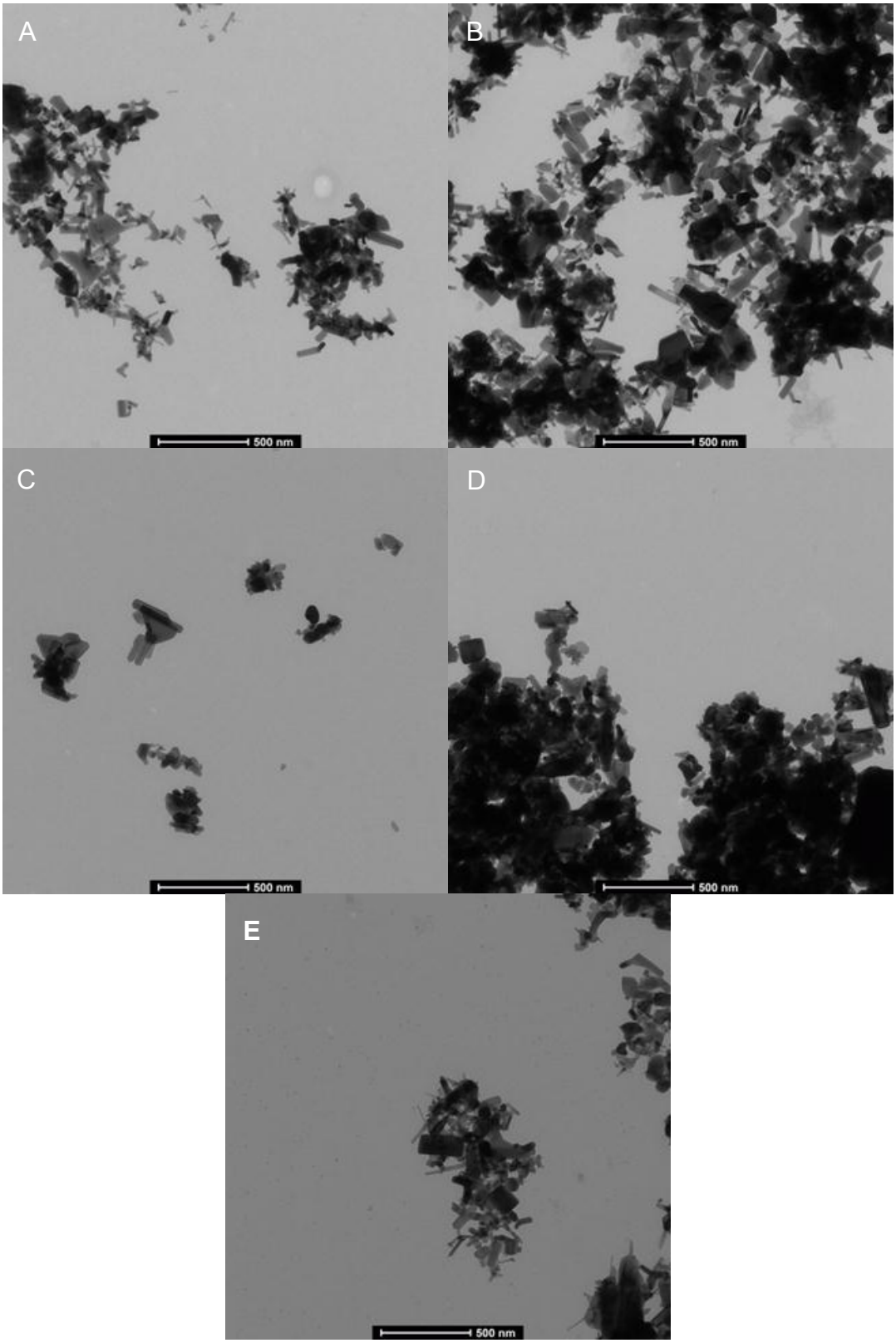


**Figure 23: Representative micrographs illustrating the effects of pre-wetting and of the suspension media on the distribution of ZnO NM-111 on Alcian blue-coated EM-grids. A, B, C, D and E correspond with conditions 1, 2, 5, 6 and 9 in Table 6, respectively.**

#### 4.8.3.2 Qualitative TEM analysis of NM-110

In the absence of a stabilising agent, like BSA, the primary particles of NM-110 tend to form very large agglomerates (Figure 22), such that under these conditions only qualitative TEM analysis of the primary particles remains possible. As expected, no coating of the particles was observed when these were suspended in double distilled water.

Figure 24 illustrates the large heterogeneity in size and shape of the primary subunits of NM-110. No predominant type was detected: amongst others; bottle-like, rod-shaped, rectangular particles of different sizes (for example: 215 nm x 66 nm and 115 nm x 40 nm), sticks (180 nm x 23 nm) and angular NP were observed.

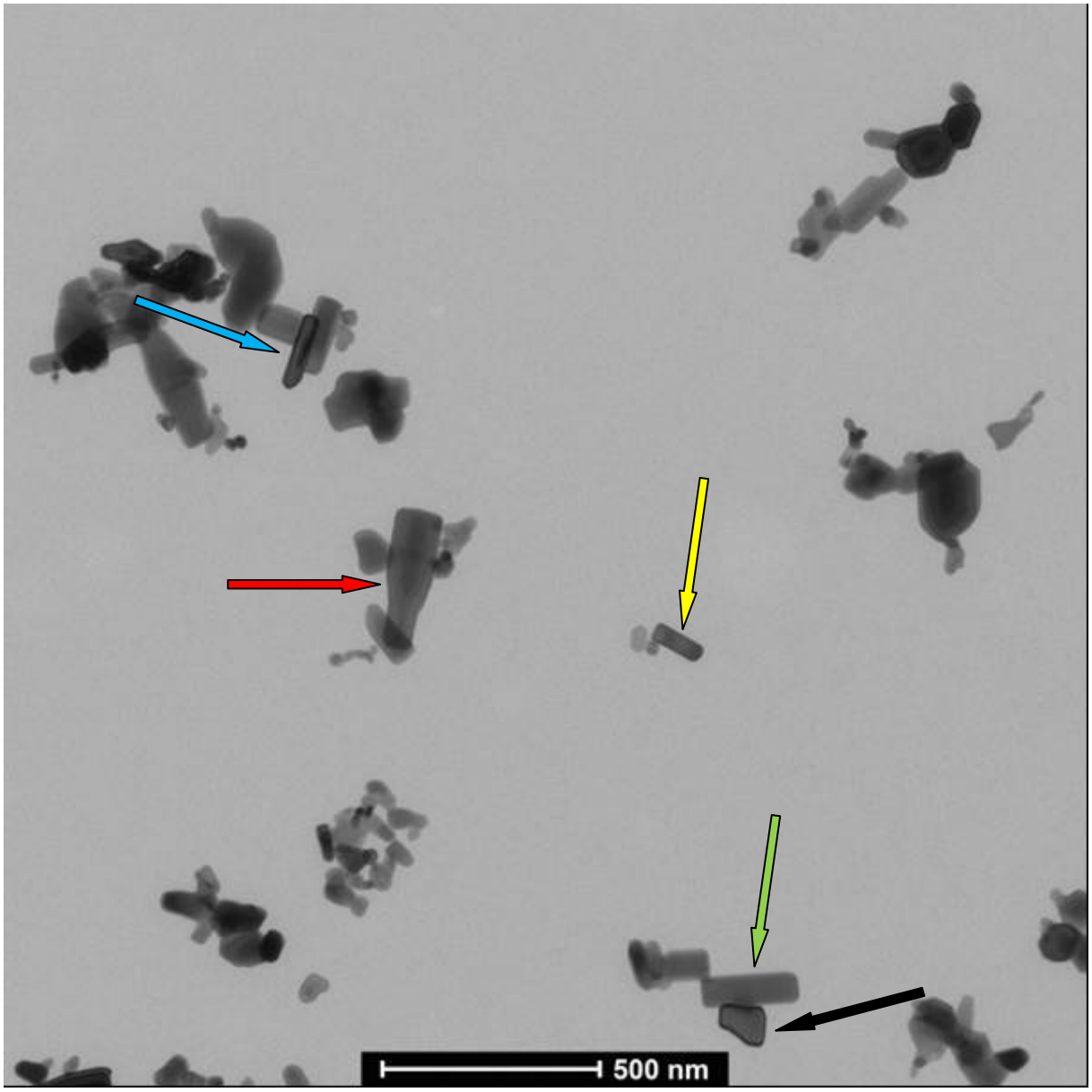


**Figure 24:. Selected micrograph illustrating the heterogeneity of the size and shape of the primary particles of the ZnO NM-110. Bottle-like (red arrow), rod-shaped (yellow arrow), larger (green arrow) and smaller (blue arrow) rectangular NP and angular NP (black arrow) were observed amongst other shapes.**

#### 4.8.3.3 Quantitative TEM analysis of NM-110

It was relatively easy to detect and measure NM-110 ZnO NM semi-automatically due to the very high electron density of the particles (Figure 25). One hundred and twenty seven (non-Alcian blue coated grid) and 195 (Alcian blue coated grid) particles were analysed. Because the results of analyses of

Alcian blue- and non-treated grids were similar, only results of Alcian blue treated grids are presented in this report.

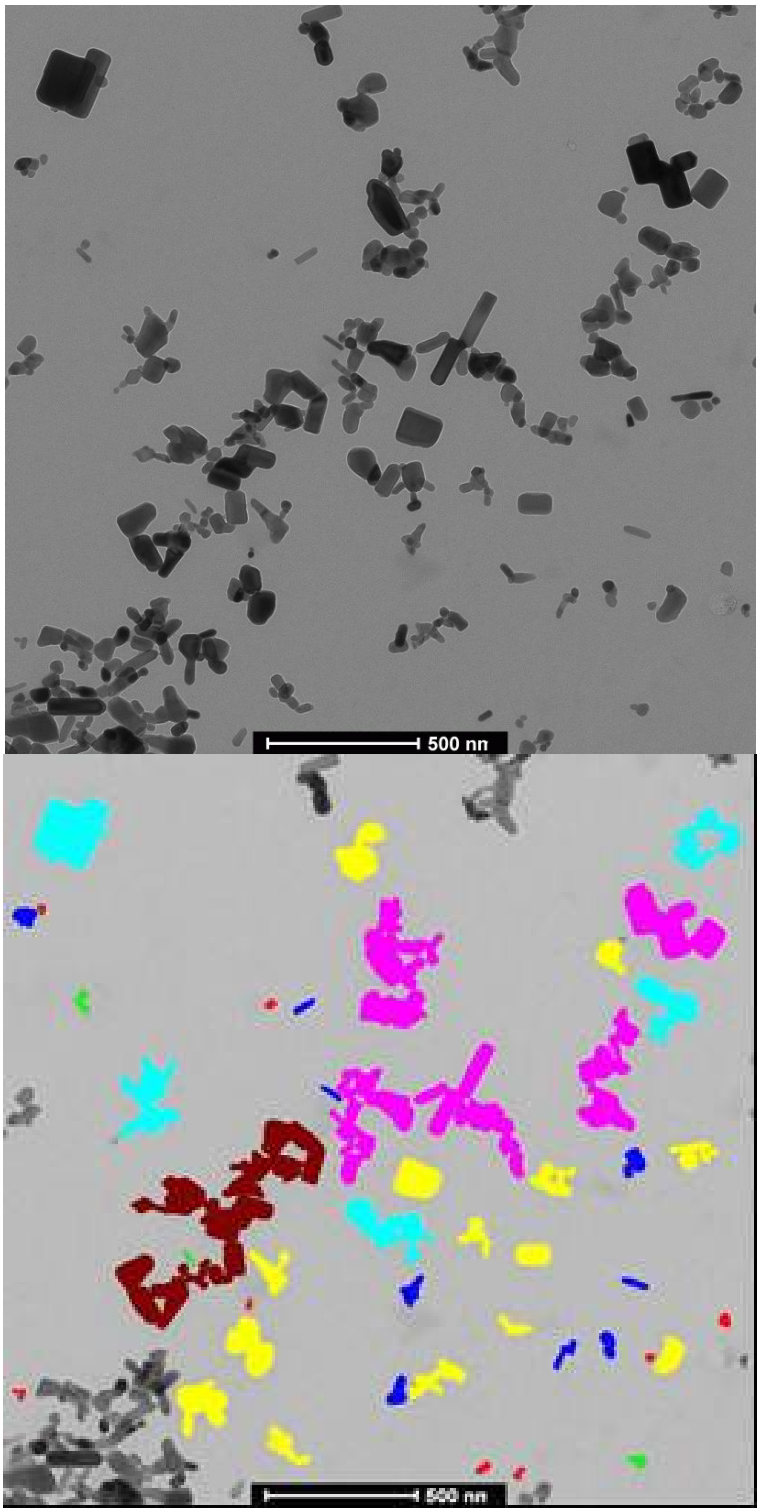


**Figure 25: Illustration of the detection of ZnO NM-110 based on electron density using iTEM. The annotated bottom panel shows the particles in color that are detected in the original micrograph (top panel). Particles at the borders of detection region are colored in grey and excluded from analysis.**

The descriptive statistics of 26 parameters of ZnO NM-110, measured by quantitative TEM analysis are given in Table 7.

**Table 7. Descriptive statistics of the quantitative TEM analysis of ZnO NM-110.**

| Column | Size | Mean | Std Dev | Std. Error | Max | Min | Median | 25% | 75% |
|---|---|---|---|---|---|---|---|---|---|
| Area | 195 | 17606 | 66817 | 4785 | 908838 | 266 | 6953 | 3127 | 16333 |
| Convex Area | 195 | 27891 | 135955 | 9736 | 1864210 | 315 | 7653 | 3628 | 21164 |
| Hole Area | 195 | 471 | 4378 | 314 | 60574 | 0 | 0 | 0 | 0 |
| Rectangle Max | 195 | 47450 | 229090 | 16405 | 3130013 | 496 | 13890 | 6373 | 34829 |
| Rectangle Mean | 195 | 42599 | 205048 | 14684 | 2802913 | 464 | 11805 | 5713 | 32219 |
| Rectangle Min | 195 | 36471 | 176391 | 12632 | 2411183 | 411 | 9840 | 4467 | 26726 |
| ECD | 195 | 114 | 97 | 7 | 1076 | 18 | 94 | 63 | 144 |
| Feret Max | 195 | 178 | 175 | 13 | 1912 | 26 | 135 | 93 | 214 |
| Feret Mean | 195 | 147 | 149 | 11 | 1684 | 22 | 111 | 76 | 180 |
| Feret Min | 195 | 106 | 111 | 8 | 1289 | 15 | 79 | 50 | 133 |
| Next Neighbor Distance | 195 | 292 | 149 | 11 | 974 | 59 | 276 | 188 | 351 |
| New Radius of Inner Circle | 195 | 32 | 18 | 1 | 138 | 6 | 29 | 19 | 40 |
| Central Distance Max | 195 | 96 | 100 | 7 | 1110 | 13 | 73 | 48 | 116 |
| Central Distance Mean | 195 | 60 | 54 | 4 | 610 | 10 | 48 | 34 | 74 |
| Central Distance Min | 195 | 21 | 17 | 1 | 145 | 0 | 17 | 11 | 27 |
| Diameter Max | 195 | 178 | 175 | 13 | 1911 | 26 | 135 | 93 | 214 |
| Diameter Mean | 195 | 158 | 158 | 11 | 1761 | 23 | 120 | 84 | 189 |
| Diameter Min | 195 | 111 | 116 | 8 | 1346 | 15 | 84 | 51 | 140 |
| Hole Count | 195 | 1 | 5 | 0 | 70 | 0 | 0 | 0 | 0 |
| Convex Perimeter | 195 | 484 | 490 | 35 | 5548 | 70 | 365 | 249 | 592 |
| Perimeter | 195 | 676 | 1495 | 107 | 19659 | 76 | 385 | 251 | 663 |
| Aspect Ratio | 195 | 1,7 | 0,6 | 0,0 | 4,5 | 1,1 | 1,6 | 1,4 | 1,9 |
| Convexity | 195 | 0,8 | 0,1 | 0,0 | 1,0 | 0,5 | 0,8 | 0,7 | 0,9 |
| Elongation | 195 | 1,9 | 0,7 | 0,0 | 5,1 | 1,1 | 1,8 | 1,4 | 2,1 |
| Shape Factor | 195 | 0,5 | 0,2 | 0,0 | 1,0 | 0,0 | 0,5 | 0,4 | 0,7 |
| Sphericity | 195 | 0,4 | 0,2 | 0,0 | 0,9 | 0,0 | 0,3 | 0,2 | 0,5 |

The raw data of Table 7 selected parameters are presented as number-based histograms in Figure 26.

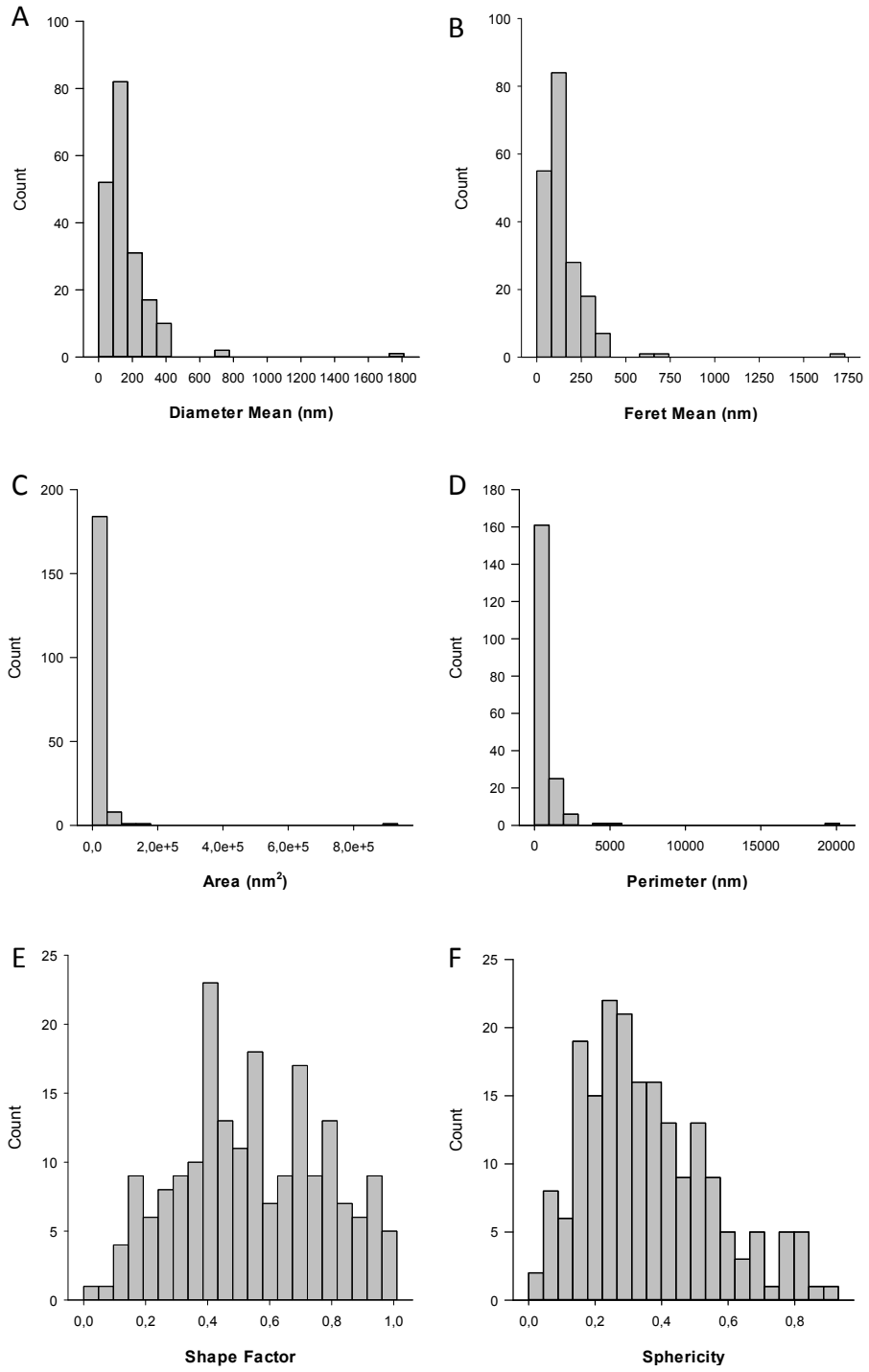


**Figure 26: Histograms showing the number-based distributions of 6 selected parameters of ZnO NM-110. The mean diameter (A) and the ferret mean (B) describe the size of the particle. The area (C) and perimeter (D) are estimates of the volume and surface area, respectively. The shape factor (E) and the sphericity (F) describe the morphology of the particles.**

#### 4.8.3.4 Qualitative TEM analysis of NM-111

In the absence of a stabilising agent, like BSA, the primary particles of NM-111 tend to form very large agglomerates (Figure 23), such that under these conditions only qualitative TEM analysis of the primary particles remains possible.

When the NM-111 particles were suspended in double distilled water, a coating was suspected. Its presence was confirmed by negative staining (not shown): an irregularly shaped coating (thickness ranging from a few nm up to 10 nm) was detected. For some particles, the coating seemed absent or very thin (< 1 nm).

Figure 27 illustrates the large heterogeneity in size and shape of the primary subunits of NM-111. Particle projections appeared very heterogeneously in size and shape. No predominant type was detected. Amongst others, tetrapods, needle-like structures, rectangular NP and angular NP were detected.

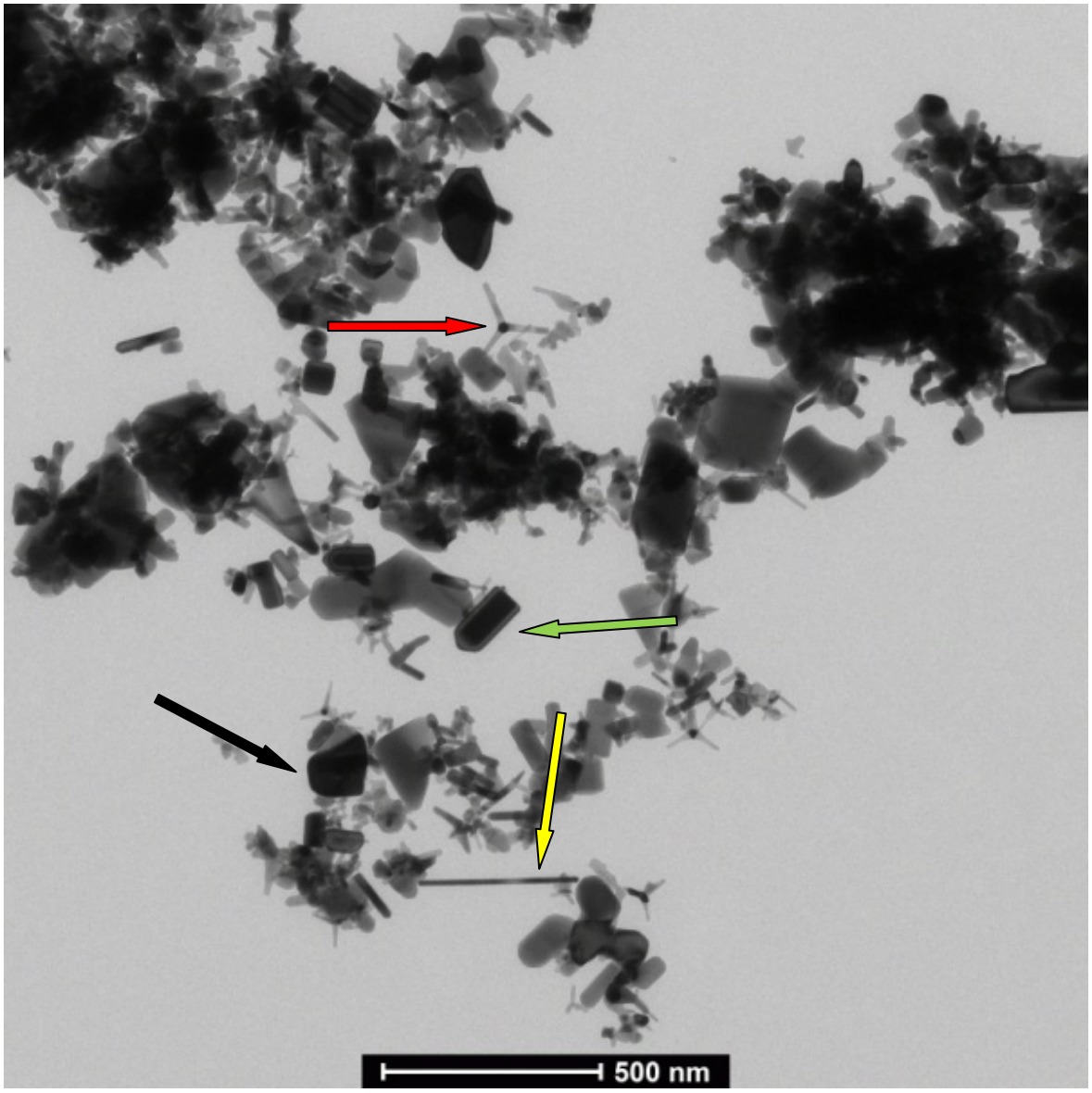


**Figure 27: Selected micrograph illustrating the heterogeneity of the size and shape of the primary particles of the ZnO NM-111. Amongst other shapes, tetrapods (red arrow), needle-like structures (yellow arrow), rectangular NP (green arrow) and angular NP (black arrow) are shown.**

#### 4.8.3.5 Quantitative TEM analysis of NM-111

It was relatively easy to detect and measure NM-111 ZnO NM semi-automatically due to the very high electron density of the particles (Figure 28). One hundred and fifty three (non-Alcian blue coated) and 226 (Alcian blue coated) particles were analysed. Because the results of analyses of Alcian blue- and non-treated grids were similar, only results of Alcian blue treated grids are presented in this report.

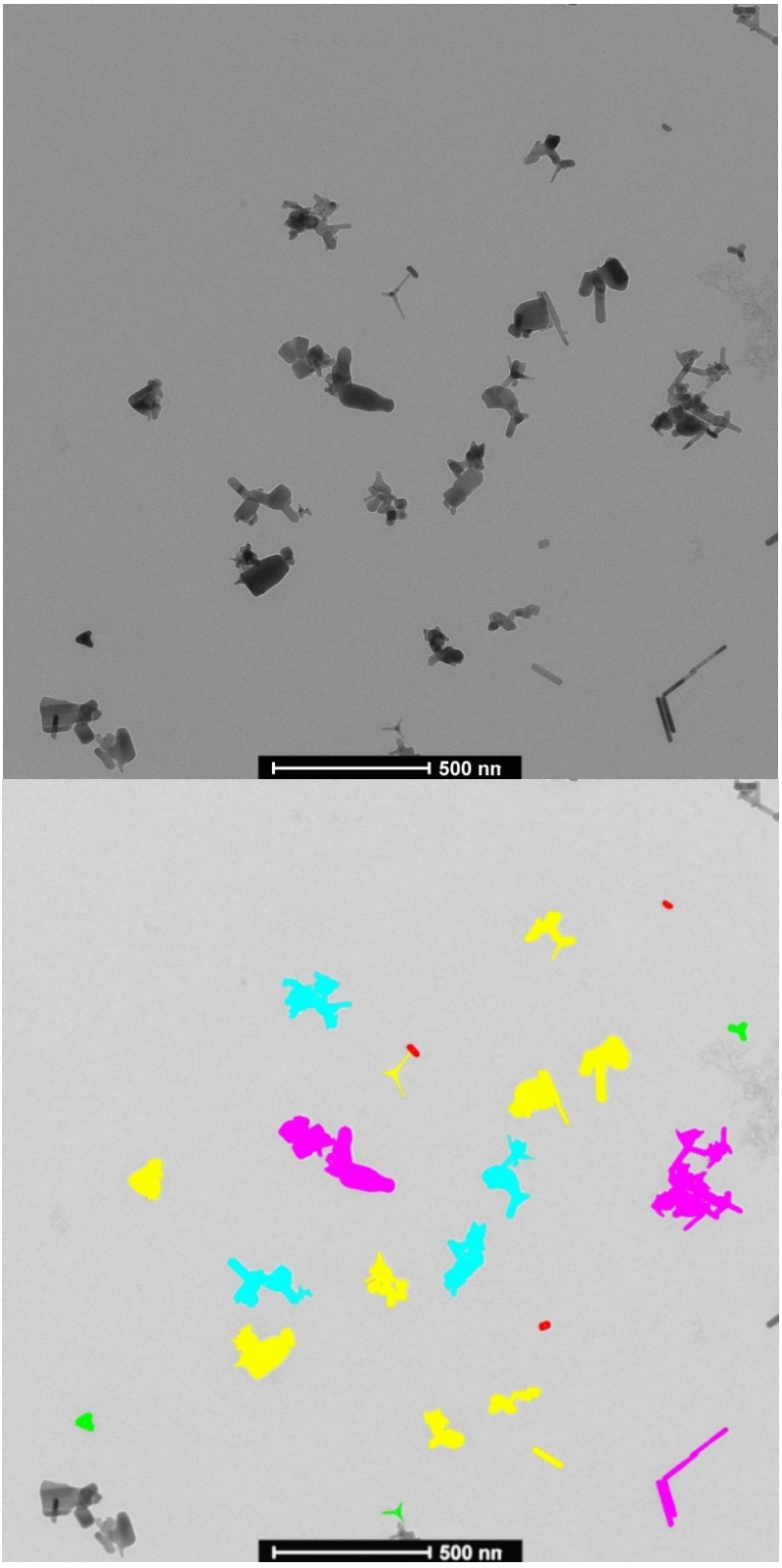


**Figure 28: Illustration of the detection of ZnO NM-111 based on electron density using iTEM. The annotated bottom panel shows the particles in color that are detected in the original micrograph (top panel). Particles at the borders of detection region are colored in grey and excluded from analysis.**

The descriptive statistics of 26 parameters of ZnO NM-111, measured by quantitative TEM analysis are given inTable 8.

**Table 8: Descriptive statistics of the quantitative TEM analysis of ZnO NM-111.**

| Column | Size | Mean | Std Dev | Std. Error | Max | Min | Median | 25% | 75% |
|---|---|---|---|---|---|---|---|---|---|
| Area | 226 | 12529 | 19246 | 1280 | 205131 | 218 | 6841 | 2280 | 15904 |
| Convex Area | 226 | 18688 | 37577 | 2500 | 469128 | 226 | 9049 | 2859 | 21491 |
| Hole Area | 226 | 85 | 651 | 43 | 9574 | 0 | 0 | 0 | 6 |
| Rectangle Max | 226 | 32817 | 69568 | 4628 | 889394 | 364 | 15631 | 5111 | 38912 |
| Rectangle Mean | 226 | 29369 | 60971 | 4056 | 770479 | 328 | 13449 | 4564 | 34465 |
| Rectangle Min | 226 | 25016 | 51942 | 3455 | 657686 | 272 | 11460 | 3835 | 29322 |
| ECD | 226 | 106 | 69 | 5 | 511 | 17 | 93 | 54 | 142 |
| Feret Max | 226 | 170 | 126 | 8 | 1062 | 22 | 143 | 82 | 219 |
| Feret Mean | 226 | 141 | 103 | 7 | 889 | 18 | 119 | 68 | 189 |
| Feret Min | 226 | 101 | 76 | 5 | 638 | 10 | 89 | 49 | 138 |
| Next Neighbor Distance | 226 | 267 | 122 | 8 | 774 | 25 | 237 | 183 | 354 |
| New Radius of Inner Circle | 226 | 31 | 19 | 1 | 92 | 4 | 28 | 15 | 41 |
| Central Distance Max | 226 | 93 | 72 | 5 | 626 | 11 | 77 | 44 | 124 |
| Central Distance Mean | 226 | 57 | 38 | 3 | 305 | 8 | 50 | 30 | 77 |
| Central Distance Min | 226 | 21 | 17 | 1 | 86 | 1 | 17 | 8 | 29 |
| Diameter Max | 226 | 170 | 126 | 8 | 1062 | 22 | 143 | 81 | 219 |
| Diameter Mean | 226 | 152 | 111 | 7 | 960 | 19 | 129 | 73 | 201 |
| Diameter Min | 226 | 107 | 80 | 5 | 646 | 9 | 93 | 51 | 143 |
| Hole Count | 226 | 1 | 2 | 0 | 24 | 0 | 0 | 0 | 1 |
| Convex Perimeter | 226 | 463 | 340 | 23 | 2938 | 58 | 393 | 221 | 623 |
| Perimeter | 226 | 593 | 710 | 47 | 8564 | 57 | 444 | 241 | 739 |
| Aspect Ratio | 226 | 1,8 | 0,7 | 0,0 | 5,6 | 1,1 | 1,6 | 1,4 | 2,0 |
| Convexity | 226 | 0,8 | 0,2 | 0,0 | 1,0 | 0,3 | 0,8 | 0,7 | 0,9 |
| Elongation | 226 | 2,0 | 0,9 | 0,1 | 6,8 | 1,0 | 1,7 | 1,4 | 2,3 |
| Shape Factor | 226 | 0,5 | 0,2 | 0,0 | 1,0 | 0,0 | 0,4 | 0,3 | 0,6 |
| Sphericity | 226 | 0,4 | 0,2 | 0,0 | 0,9 | 0,0 | 0,3 | 0,2 | 0,5 |

The raw data of six selected parameters are presented as number-based histograms in Figure 29.

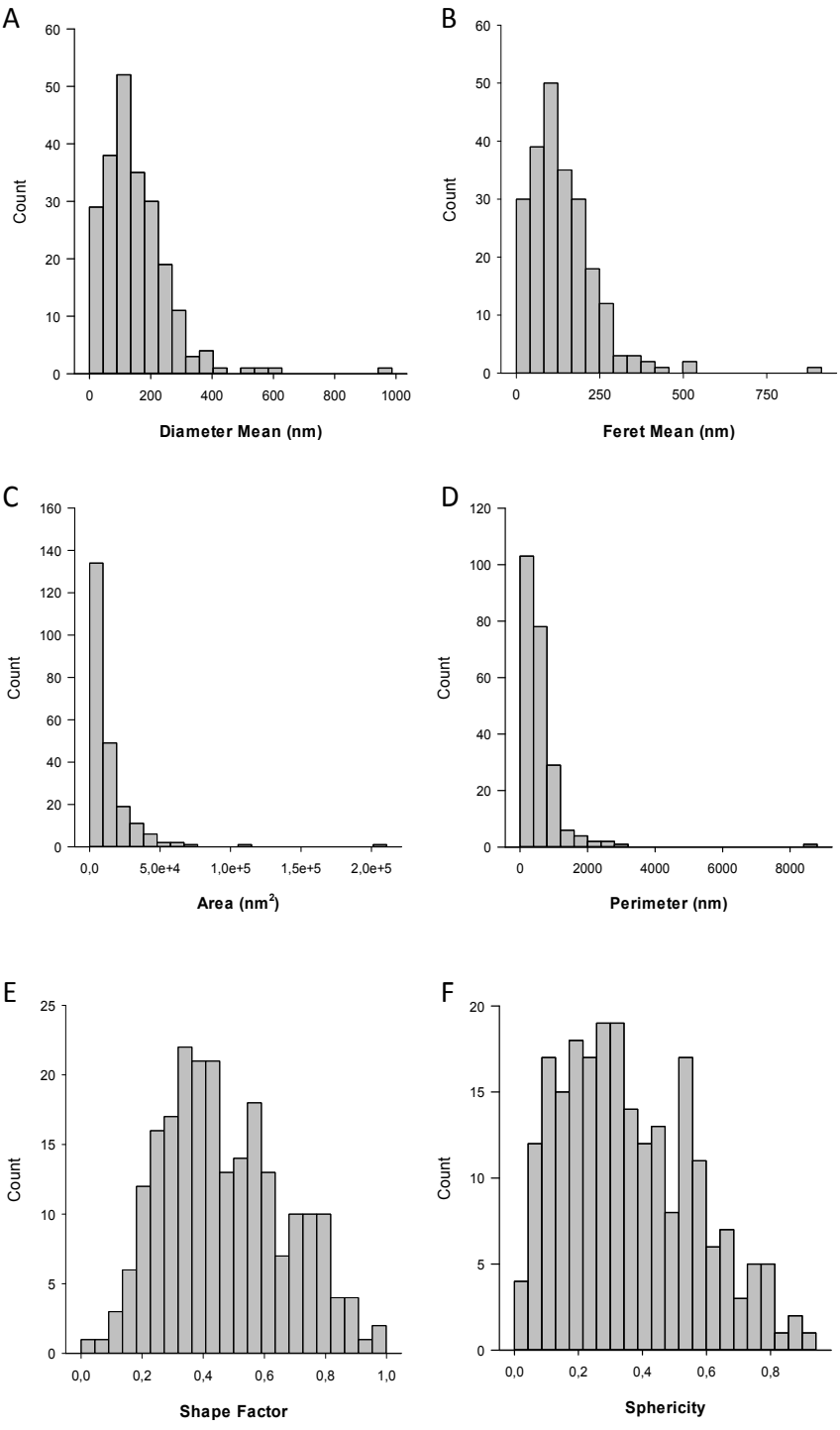


**Figure 29: Histograms showing the number-based distributions of 6 selected parameters of ZnO NM-111. The mean diameter (A) and the ferret mean (B) describe the size of the particle. The area (C) and perimeter (D) are estimates of the volume and surface area, respectively. The shape factor (E) and the sphericity (F) describe the morphology of the particles.**

#### 4.8.3.6 Qualitative TEM analysis of NM-112

The protocol optimised for dispersion of NM-11X zinc oxide (paragraph 5.8) allowed obtaining a suspension of NM-112 that was stable for at least 10 minutes. An acceptable amount of NM was coated onto the grid surface and particles were evenly distributed over the complete grid surface. The majority of particles consisted of small to large 'groups of primary particles', although some individual particles were observed also (Figure 30). The observed 'groups' of particles can be interpreted as individual or aggregated particles that form larger agglomerates. It is assumed that the fraction of the attached NM suitably represents the dispersed NM.

Figure 30 shows that these particles are BSA-coated.

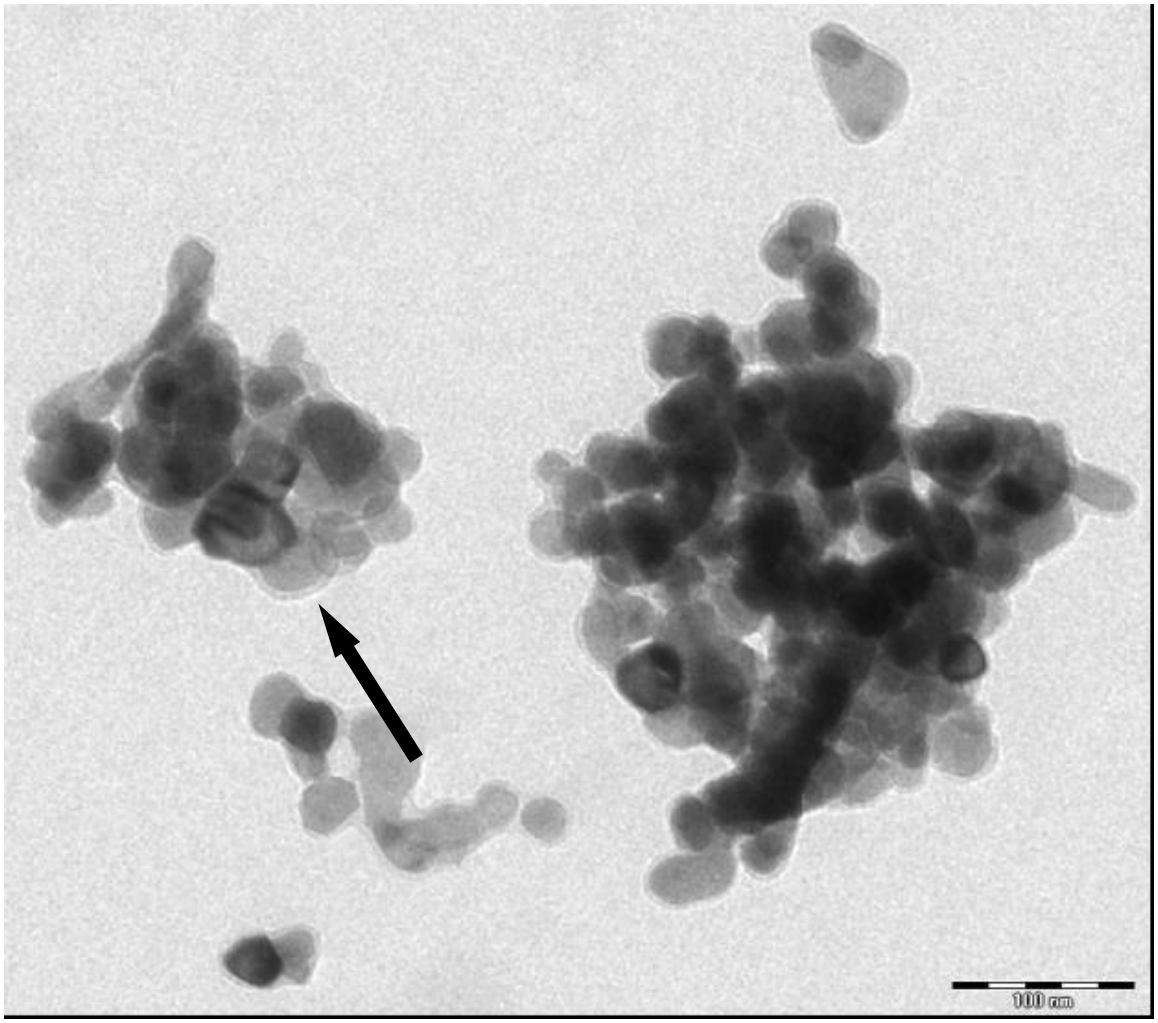


**Figure 30: Selected micrograph of ZnO nanoparticles NM-112 illustrating the aggregates/agglomerates of the well-rounded primary particles. The arrow indicates the presence of a BSA coating around the ZnO particles.**

The primary particles have a size of 20 to 60 nm and an aspect ratio of about 1 and were well-rounded (Krumbein and Sloss, 1963). No diffraction contrast was observed, suggesting an amorphous structure.

#### 4.8.3.7 Quantitative TEM analysis of NM-112

It was possible to detect and measure ZnO NM-112 semi-automatically due to the high electron density of the particles (Figure 31). In ten micrographs, 512 particles were detected. The descriptive statistics of 26 parameters of ZnO NM-112, measured by quantitative TEM analysis are given in Table 9.

**Table 9: Descriptive statistics of the quantitative TEM analysis of ZnO NM-112.**

| Column | Size | Mean | Std Dev | Std. Error | Max | Min | Median | 25% | 75% |
|---|---|---|---|---|---|---|---|---|---|
| Area | 512 | 10422 | 17815 | 787 | 180964 | 54 | 3951 | 1372 | 12176 |
| Convex Area | 512 | 14236 | 27795 | 1228 | 304452 | 72 | 4693 | 1412 | 15287 |
| Hole Area | 512 | 103 | 379 | 17 | 5560 | 0 | 0 | 0 | 28 |
| Rectangle Max | 512 | 23145 | 45094 | 1993 | 475104 | 130 | 7516 | 2078 | 25533 |
| Rectangle Mean | 512 | 21230 | 41797 | 1847 | 446917 | 116 | 6963 | 1954 | 23292 |
| Rectangle Min | 512 | 18723 | 37582 | 1661 | 408111 | 95 | 6104 | 1788 | 20186 |
| ECD | 512 | 92 | 70 | 3 | 480 | 8 | 71 | 42 | 125 |
| Feret Max | 512 | 133 | 114 | 5 | 815 | 12 | 100 | 51 | 178 |
| Feret Mean | 512 | 113 | 95 | 4 | 675 | 11 | 84 | 44 | 153 |
| Feret Min | 512 | 87 | 73 | 3 | 523 | 7 | 63 | 35 | 116 |
| Next Neighbor Distance | 512 | 194 | 89 | 4 | 511 | 16 | 184 | 129 | 247 |
| New Radius of Inner Circle | 512 | 26 | 15 | 1 | 136 | 2 | 22 | 16 | 34 |
| Central Distance Max | 512 | 71 | 63 | 3 | 476 | 6 | 53 | 26 | 96 |
| Central Distance Mean | 512 | 47 | 36 | 2 | 240 | 4 | 36 | 21 | 63 |
| Central Distance Min | 512 | 19 | 15 | 1 | 94 | 0 | 15 | 10 | 24 |
| Diameter Max | 512 | 133 | 114 | 5 | 814 | 11 | 100 | 51 | 178 |
| Diameter Mean | 512 | 119 | 101 | 4 | 709 | 11 | 90 | 46 | 161 |
| Diameter Min | 512 | 90 | 77 | 3 | 526 | 6 | 65 | 35 | 124 |
| Hole Count | 512 | 1 | 3 | 0 | 24 | 0 | 0 | 0 | 1 |
| Convex Perimeter | 512 | 371 | 314 | 14 | 2218 | 33 | 277 | 145 | 506 |
| Perimeter | 512 | 486 | 562 | 25 | 4965 | 34 | 289 | 142 | 629 |
| Aspect Ratio | 512 | 1,5 | 0,4 | 0,0 | 3,3 | 1,0 | 1,5 | 1,3 | 1,7 |
| Convexity | 512 | 0,8 | 0,1 | 0,0 | 1,0 | 0,5 | 0,9 | 0,8 | 1,0 |
| Elongation | 512 | 1,7 | 0,5 | 0,0 | 4,2 | 1,0 | 1,5 | 1,3 | 1,9 |
| Shape Factor | 512 | 0,6 | 0,3 | 0,0 | 1,0 | 0,1 | 0,6 | 0,4 | 0,8 |
| Sphericity | 512 | 0,4 | 0,2 | 0,0 | 1,0 | 0,1 | 0,4 | 0,3 | 0,6 |

The raw data of six selected parameters are presented as number-based histograms in Figure 32.

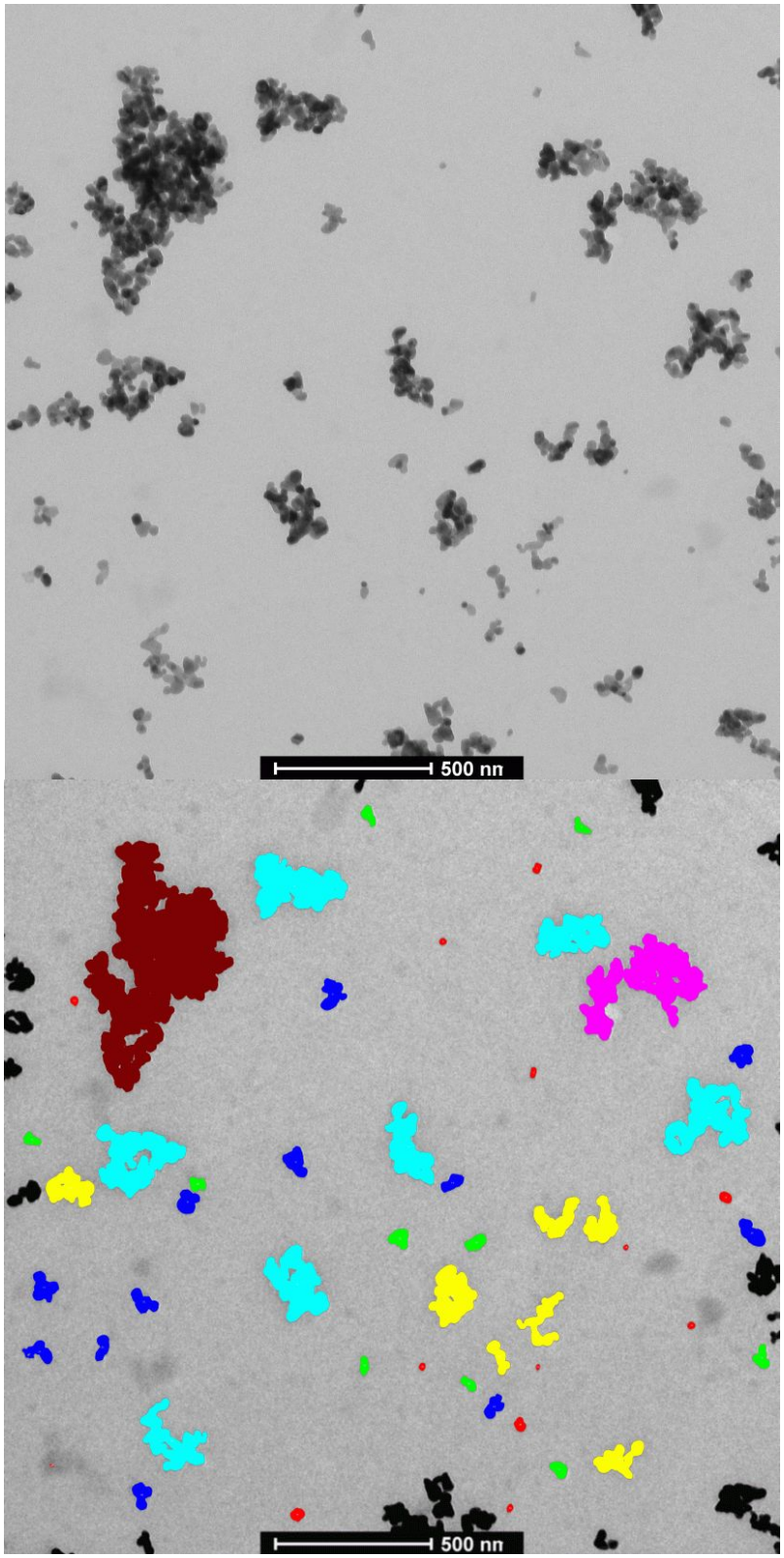


**Figure 31: Illustration of the detection of ZnO NM-112 based on electron density. The annotated bottom panel shows the particles that are detected in the original micrograph in color (top panel). Particles at the borders of detection region are colored in grey and excluded from analysis.**

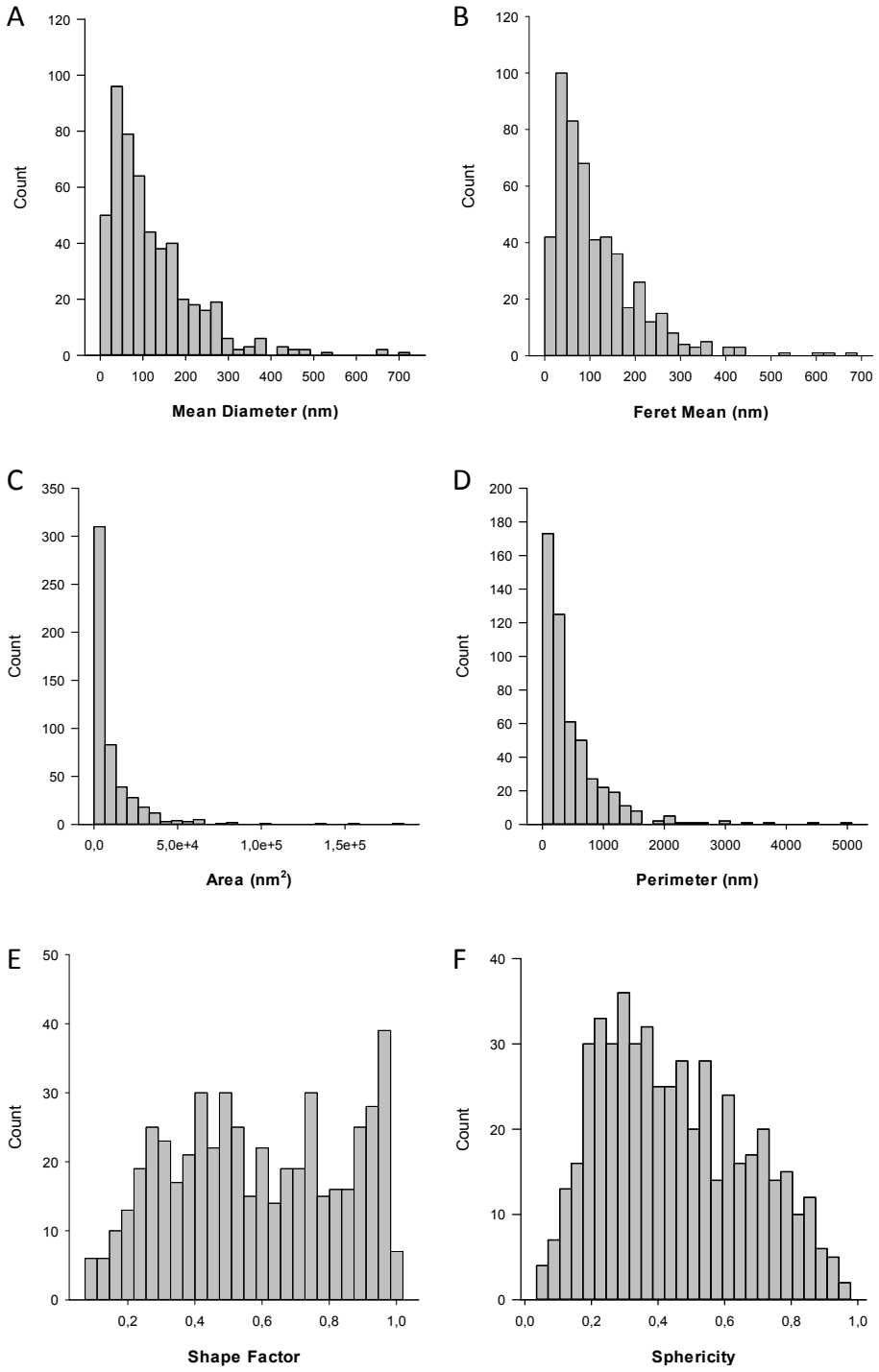


**Figure 32: Histograms showing the number-based distributions of 6 selected parameters of ZnO NM-112. The mean diameter (A) and the ferret mean (B) describe the size of the particle. The area (C) and perimeter (D) are estimates of the volume and surface area, respectively. The shape factor (E) and the sphericity (F) describe the morphology of the particles.**

#### 4.8.3.8 Qualitative TEM analysis of NM-113

The protocol optimised for dispersion of NM-11X zinc oxide (paragraph 5.8) allowed obtaining a suspension of NM-113 that was stable for at least 10 minutes. Particles were evenly distributed over the complete grid surface and their amount was sufficient to allow quantitative analysis. The majority of particles consisted of small to large agglomerates of primary particles, although some individual particles were observed also (Figure 33). It is assumed that the fraction of the attached NM suitably represents the dispersed NM.
Figure 33 also shows that these particles are BSA-coated.

Particle projections appeared very heterogeneous in size, shape and agglomeration/aggregation state. The primary particles have a size of 40 to 500 nm and an aspect ratio of about 1-2 and were angular (Krumbein and Sloss, 1963). This angular morphology and the observed diffraction contrast suggest a crystalline organization of the NM.

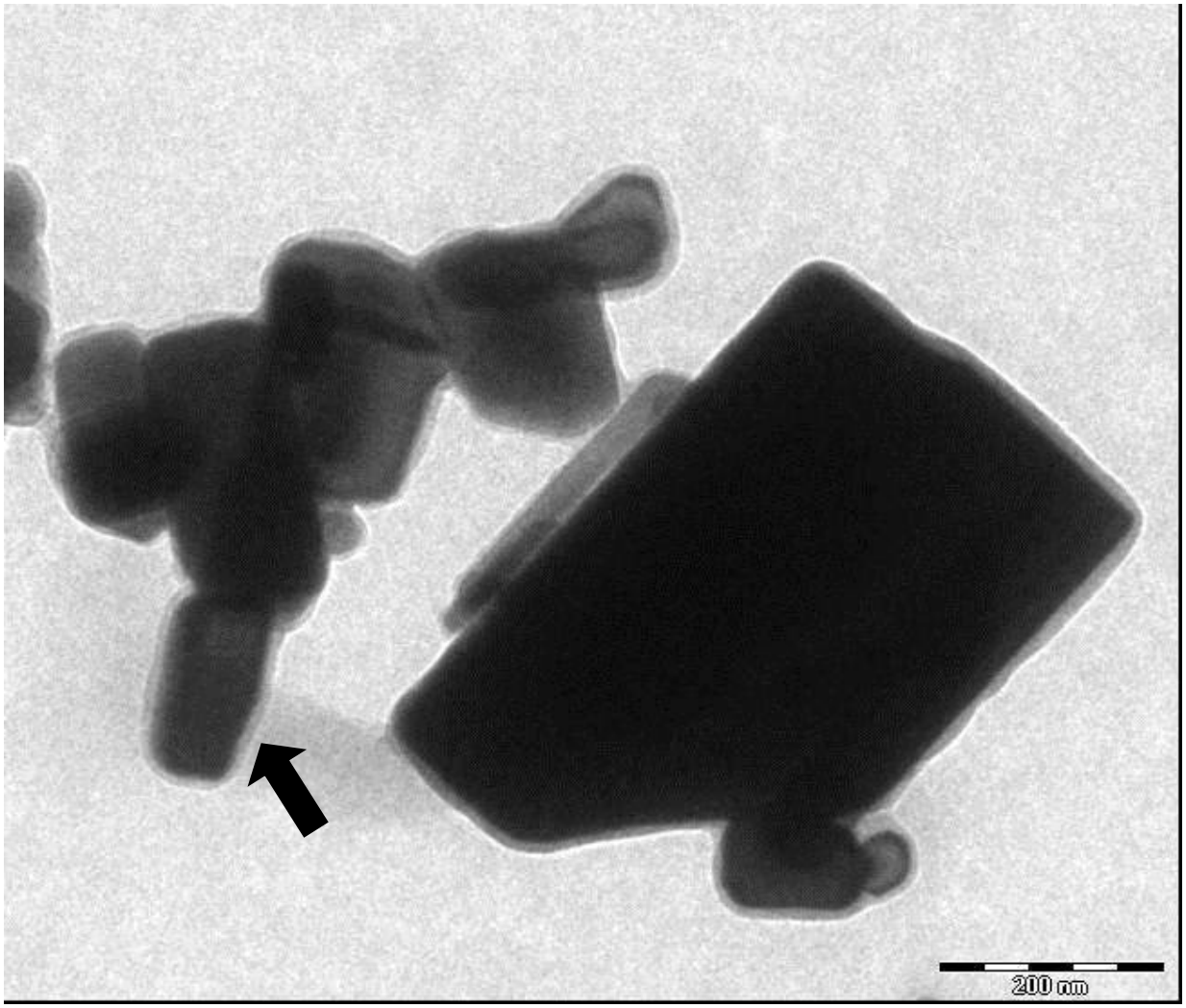


**Figure 33: Selected micrograph of ZnO nanoparticles NM-113. The arrow indicates the presence of a BSA coating around the ZnO particles.**

#### 4.8.3.9 Quantitative TEM analysis of NM-113

It was possible to detect and measure ZnO NM-113 semi-automatically due to the high electron density of the particles (Figure 34). In ten micrographs, 109 particles were detected.

The descriptive statistics of 26 parameters of ZnO NM-113, measured by quantitative TEM analysis are given in Table 10.

The raw data of six selected parameters are presented as number-based histograms in Figure 35.

**Table 10: Descriptive statistics of the quantitative TEM analysis of ZnO NM-113.**

| Column | Size | Mean | Std Dev | Std. Error | Max | Min | Median | 25% | 75% |
|---|---|---|---|---|---|---|---|---|---|
| Area | 109 | 271149 | 396265 | 37955 | 2747943 | 457 | 153851 | 31300 | 318703 |
| Convex Area | 109 | 378383 | 633098 | 60640 | 4502315 | 465 | 180282 | 36192 | 411526 |
| Hole Area | 109 | 5996 | 50846 | 4870 | 530404 | 0 | 0 | 0 | 4 |
| Rectangle Max | 109 | 647018 | 1107685 | 106097 | 7059173 | 642 | 304703 | 57871 | 696663 |
| Rectangle Mean | 109 | 586214 | 989733 | 94799 | 6308863 | 630 | 280863 | 55105 | 610703 |
| Rectangle Min | 109 | 508195 | 854506 | 81847 | 5451469 | 579 | 248296 | 50826 | 531125 |
| ECD | 109 | 472 | 352 | 34 | 1871 | 24 | 443 | 200 | 637 |
| Feret Max | 109 | 724 | 609 | 58 | 3112 | 27 | 616 | 286 | 959 |
| Feret Mean | 109 | 602 | 491 | 47 | 2516 | 25 | 530 | 237 | 793 |
| Feret Min | 109 | 449 | 363 | 35 | 2188 | 22 | 408 | 174 | 623 |
| Next Neighbor Distance | 109 | 1017 | 523 | 50 | 2732 | 210 | 929 | 609 | 1339 |
| New Radius of Inner Circle | 109 | 135 | 85 | 8 | 356 | 9 | 123 | 71 | 195 |
| Central Distance Max | 109 | 390 | 325 | 31 | 1591 | 13 | 335 | 156 | 527 |
| Central Distance Mean | 109 | 246 | 188 | 18 | 1025 | 11 | 224 | 101 | 332 |
| Central Distance Min | 109 | 94 | 74 | 7 | 366 | 5 | 84 | 33 | 127 |
| Diameter Max | 109 | 724 | 609 | 58 | 3111 | 27 | 616 | 287 | 958 |
| Diameter Mean | 109 | 643 | 532 | 51 | 2625 | 25 | 552 | 249 | 857 |
| Diameter Min | 109 | 469 | 385 | 37 | 2198 | 20 | 423 | 178 | 657 |
| Hole Count | 109 | 1 | 2 | 0 | 18 | 0 | 0 | 0 | 1 |
| Convex Perimeter | 109 | 1990 | 1629 | 156 | 8307 | 75 | 1753 | 788 | 2628 |
| Perimeter | 109 | 2659 | 3269 | 313 | 23683 | 75 | 2019 | 809 | 3153 |
| Aspect Ratio | 109 | 1,6 | 0,4 | 0,0 | 2,8 | 1,1 | 1,5 | 1,3 | 1,8 |
| Convexity | 109 | 0,8 | 0,1 | 0,0 | 1,0 | 0,5 | 0,8 | 0,8 | 0,9 |
| Elongation | 109 | 1,7 | 0,5 | 0,0 | 3,8 | 1,1 | 1,6 | 0,2 | 0,1 |
| Shape Factor | 109 | 0,5 | 0,2 | 0,0 | 1,0 | 0,1 | 0,5 | 0,4 | 0,7 |
| Sphericity | 109 | 0,4 | 0,2 | 0,0 | 0,9 | 0,1 | 0,4 | 0,4 | 0,7 |

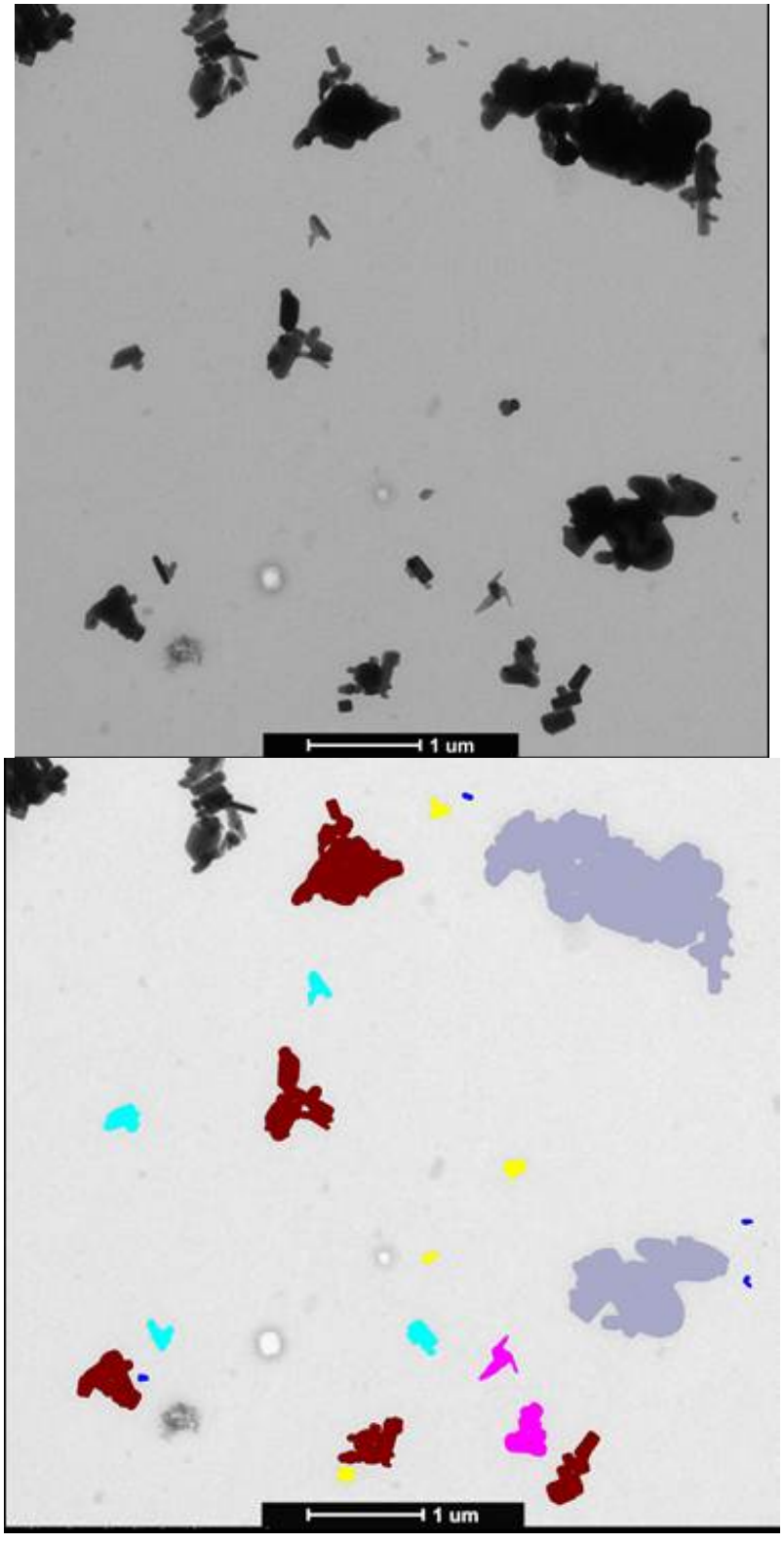


**Figure 34: Illustration of the detection of ZnO NM-113 based on electron density. The annotated bottom panel shows the particles that are detected in the original micrograph in color (top panel). Particles at the borders of detection region are colored in grey andexcluded from analysis.**

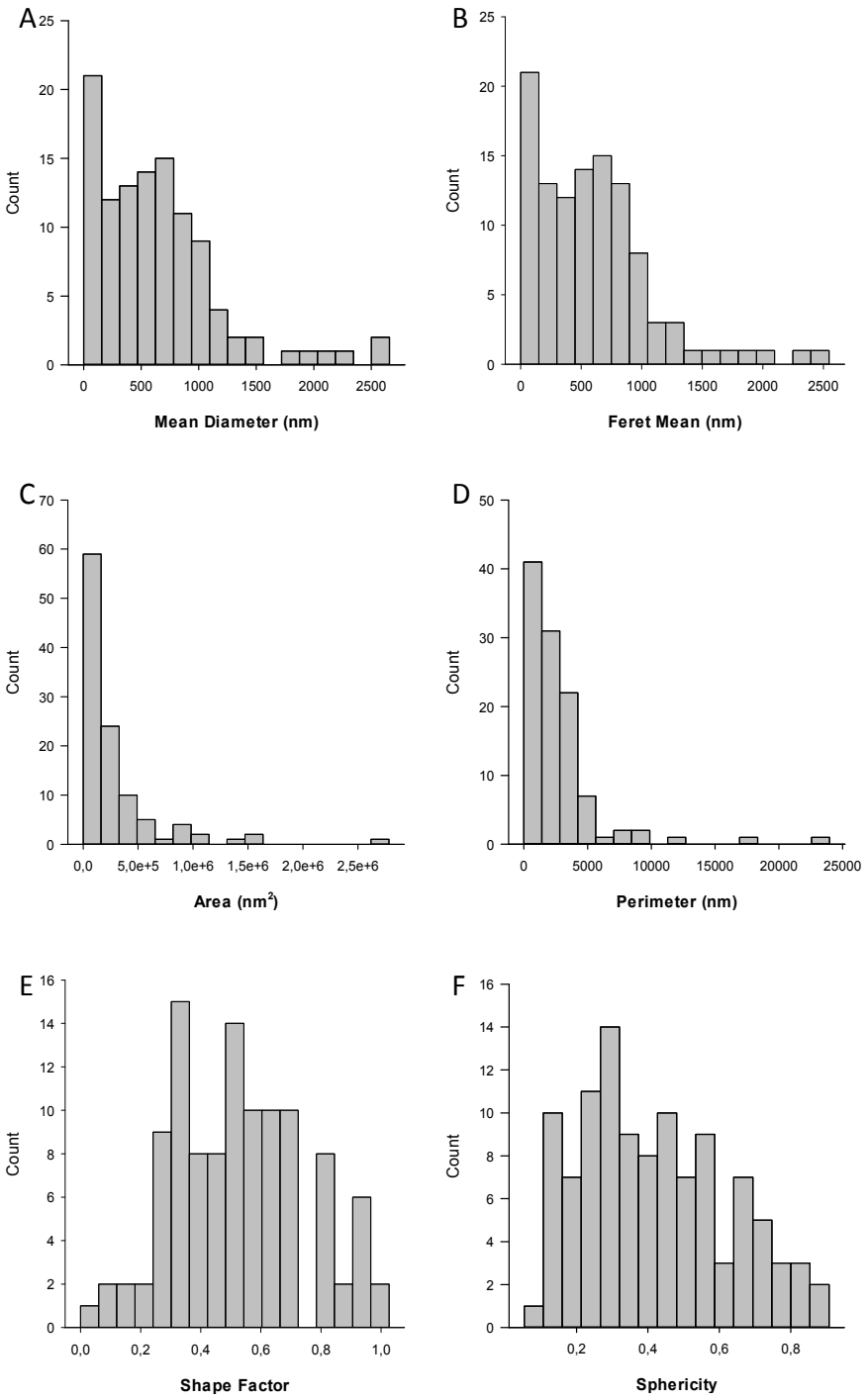


**Figure 35: Histograms showing the number-based distributions of 6 selected parameters of ZnO NM-113. The mean diameter (A) and the ferret mean (B) describe the size of the particle. The area (C) and perimeter (D) are estimates of the volume and surface area, respectively. The shape factor (E) and the sphericity (F) describe the morphology of the particles.**

## 4.9 SEM Image Analysis

### 4.9.1 SEM Method

SEM micrographs were analysed manually; this was done by manually tracing contours of primary particles on to a transparency sheet. The transparency sheet was scanned for further image analysis using ImageJ software, which automatically calculated particle diameter dimensions.

### 4.9.2 SEM Results

Table 11 shows the corresponding mean Feret's diameter (of the primary particles) of the various NMs. Here, we report Feret's diameter, a parameter that is widely used in imaging of irregular shaped particles. Feret's diameter can be defined as the "maximum calliper length" *i.e.* the longest distance between any two points along the selection boundary (Chang *et al.,* 2002). Overall, results show that particle size (as reported from SEM analysis) is much larger than the corresponding reported crystallite size by XRD. This is not surprising as a particle (or grain) may be made up of several different crystallites.

**Table 11: Size of primary particles, as defined by their corresponding Feret's diameter. Mean diameter (± 1 SD) of a minimum of 50 particles measured from the SEM images. The SD here represents the broadness of the size distribution (not error).**

| Sample Name | Mean Feret's diameter/nm from SEM images |
|---|---|
| NM-110 | 151 ± 55.6 |
| NM-111 | 140.8 ± 65.8 |
| NM-112 | 42.5 ± 3.6 |
| NM-113 | 891.8 ± 800 |

Table 11 also shows the SD associated with the mean particle size; the SD value will give an indication of polydispersity *i.e.* polydispersity will increase as SD becomes large. This can be exemplified by NM-113 in which the polydispersity of the primary particle size is large (Figure 36) and reflected in their corresponding SD values.

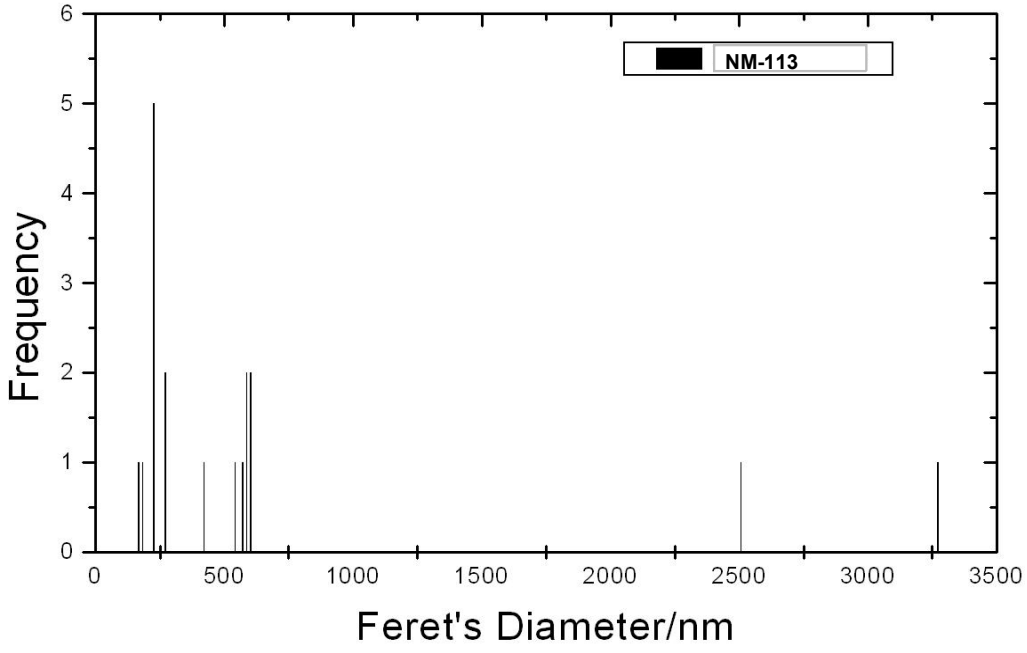


**Figure 36: Distribution of primary particle size (Feret's diameter) measured using image analysis of SEM micrographs for NM-113.**

## 4.10 Homogeneity Testing using SEM

Table 12 summarises the primary particle size (as defined by their corresponding Feret's diameter) of the JRC sub-sampled powders for NM-110 and NM-111 samples. Results presented in this table are in raw, tabular format.

**Table 12: Size of primary particles, as defined by their corresponding Feret's diameter [nm] for: a) NM-110 and b) NM-111. Replicates: 1 vial, 6 replicates per vial. Values are the mean diameter (± 1 SD) of 50 particles as measured by SEM. Note that the SD here represents the broadness of the size distribution (not error).**

**a)**

| NM-110 | | | | | | | | | | | | |
|---|---|---|---|---|---|---|---|---|---|---|---|---|
| | NM110-0305 | | NM110-4899 | | NM110-3975 | | NM110-1866 | | NM110-0286 | | NM110-2617 | |
| Rep | mean | s.d. | mean | s.d. | mean | s.d. | mean | s.d. | mean | s.d. | mean | s.d. |
| 1 | 120.9 | 55.7 | 109.2 | 56.4 | 111.2 | 72.1 | 102.1 | 66.8 | 117.4 | 61.1 | 115.9 | 60.1 |
| 2 | 120.9 | 57.6 | 113.7 | 42.2 | 115.4 | 60.2 | 112.6 | 59.7 | 111.3 | 49.2 | 116.7 | 87.0 |
| 3 | 117.6 | 58.0 | 106.5 | 62.4 | 114.7 | 48.6 | 115.2 | 58.7 | 113.1 | 53.3 | 121.8 | 58.4 |
| 4 | 117.5 | 58.1 | 106.6 | 52.3 | 123.2 | 60.2 | 109.0 | 49.5 | 120.7 | 116.9 | 119.7 | 58.7 |
| 5 | 111.7 | 64.1 | 105.1 | 47.6 | 122.0 | 61.0 | 117.6 | 72.2 | 120.8 | 71.5 | 121.6 | 126.1 |
| 6 | 104.8 | 57.1 | 105.9 | 46.6 | | | 116.2 | 42.2 | 121.6 | 130.9 | 121.8 | 89.4 |

**b)**

| NM-111 | | | | | | | | | | | | |
|---|---|---|---|---|---|---|---|---|---|---|---|---|
| | NM111-2419 | | NM111-1869 | | NM111-0486 | | NM111-1017 | | NM111-3396 | | NM111-4479 | |
| Rep | mean | s.d. | mean | s.d. | mean | s.d. | mean | s.d. | mean | s.d. | mean | s.d. |
| 1 | 113.0 | 66.5 | 107.7 | 52.6 | 114.7 | 79.6 | 120.0 | 57.2 | 125.9 | 72.3 | 127.7 | 189.9 |
| 2 | 122.2 | 107.8 | 114.1 | 48.0 | 124.1 | 76.4 | 119.0 | 118.6 | 118.1 | 84.2 | 120.1 | 53.8 |
| 3 | 127.7 | 134.1 | 102.6 | 62.6 | 112.6 | 57.6 | 125.1 | 68.1 | 126.0 | 84.2 | 118.5 | 41.8 |
| 4 | 123.1 | 42.7 | 102.2 | 54.2 | 118.3 | 73.0 | 119.8 | 118.3 | 120.1 | 82.6 | 127.9 | 65.4 |
| 5 | 113.2 | 47.0 | 110.1 | 48.7 | 113.4 | 74.3 | 124.8 | 79.0 | 127.5 | 81.7 | 127.9 | 68.8 |
| 6 | 119.6 | 67.3 | 104.1 | 47.6 | 123.0 | 89.7 | 110.7 | 57.0 | 117.3 | 63.6 | | |

For the homogeneity study, 6 vials of 1000 of NM-110 and NM-111 were chosen using a random stratified sample picking scheme and analysed for their Feret's diameters by SEM.

Data were checked for single and double outliers by applying the Grubbs test at a confidence level of 95% and 99%. No outliers were found. Regression analysis was performed to detect possible trends regarding the filling sequence or analytical sequence. No significant slopes were found at 95 % or 99 % level. In conclusion, the materials can be regarded as homogeneous for their Feret's diameter. Furthermore it was checked whether the data followed a normal or

unimodal distribution using normal probability plots and histograms, respectively. Data showed a unimodal distribution for NM-110 and a slight bi-modal distribution of Feret's diameters in NM-111, respectively. Finally, the uncertainty contribution from possible heterogeneity was estimated by a one-way analysis of variance (ANOVA) as described by Van der Veen *et al.,* (Van der Veen *et al.,* 2001):

Method repeatability ($s_{wb}$) expressed as a relative standard deviation is given as follows:

**Equation 1:**

$$s_{wb} = \frac{\sqrt{MS_{within}}}{\bar{y}}$$

$MS_{within}$: mean square within a bottle from an ANOVA
$\bar{y}$: average of all results of the homogeneity study

Between-unit variability ($s_{bb}$) expressed as a relative standard deviation is given by the following equation:

**Equation 2:**

$$s_{bb} = \frac{\sqrt{\frac{MS_{between} - MS_{within}}{n}}}{\bar{y}}$$

$MS_{between}$: mean square among bottles from an ANOVA
$n$: average number of replicates per bottle

The heterogeneity that can be hidden by method repeatability is defined as follows:

**Equation 3:**

$$u_{bb}^{*} = \frac{s_{wb}}{\sqrt{n}} \sqrt[4]{\frac{2}{\nu_{MSwithin}}}$$

$\nu_{MSwithin}$: degrees of freedom of $MS_{within}$

The larger value of $s_{bb}$ or $u^*_{bb}$ was used as uncertainty contribution for homogeneity, $u_{bb}$ (see Table 13 for a summary of results, values were converted into relative uncertainties).

**Table 13: Homogeneity study results for NM-110 and NM-111.**

| | **NM-110** | **NM-111** |
|---|---|---|
| $s_{wb}$ [%] | 4.1 | 18.5 |
| $s_{bb}$ [%] | 3.4 | n.c. |
| $u^*_{bb}$ [%] | 0.9 | 3.8 |
| **$u_{bb}$ [%]** | **3.9** | **3.8** |

n.c. = not calculable because $MS_{between} < MS_{within}$

## 4.11 Particle Size Distribution of Aerosolised NMs

### 4.11.1 Particle Size Distribution Method

TSI Fluidised Bed Aerosol Generator (FBAG) was used to produce an aerosol from the dry powder sample. After introduction of the NM into the FBAG, the aerosol generated was allowed to stabilise for a day prior to sending the aerosol to an SMPS. A Scanning Mobility Particle Sizer (TSI 3080 SMPS), consisting of a DMA and CPC system, was used to determine the particle size distribution. The Differential Mobility Analyser (DMA) within the SMPS was calibrated using reference material polystyrene latex beads from NIST. The Condensation Particle Counters (CPC) within the SMPS setup were calibrated according to NPL's UKAS accredited (ISO 17025) procedure, using an internally calibrated Faraday Cup Electrometer and soot generator (model CAST 2). The SMPS was set to record at 3-minute intervals; an extended stable segment of data was used for analysis (50-hours in the first instance). The data was processed using TSI Aerosol Instrument Management (AIM) software, in which the mean size distribution from the stable time segment was estimated. The size distribution was also analysed using an in-house curve fitting program (as implemented in a recent SMPS intercomparison at METAS).

### 4.11.2 Particle Size Distribution Results

Figure 37 shows the aerosol particle size distribution for NM-110 using a SMPS; the spectrometer data are plotted using a normalised concentration. As shown in Figure 37, the full size distribution is cut off at the upper end by the range of the SMPS.

In order to estimate the effective mean, a lognormal was fitted to the distribution in Figure 37 and the geometric mean (and the corresponding geometric standard deviation) was estimated to be 278.0 nm (SD $\pm$ 1.5 nm).

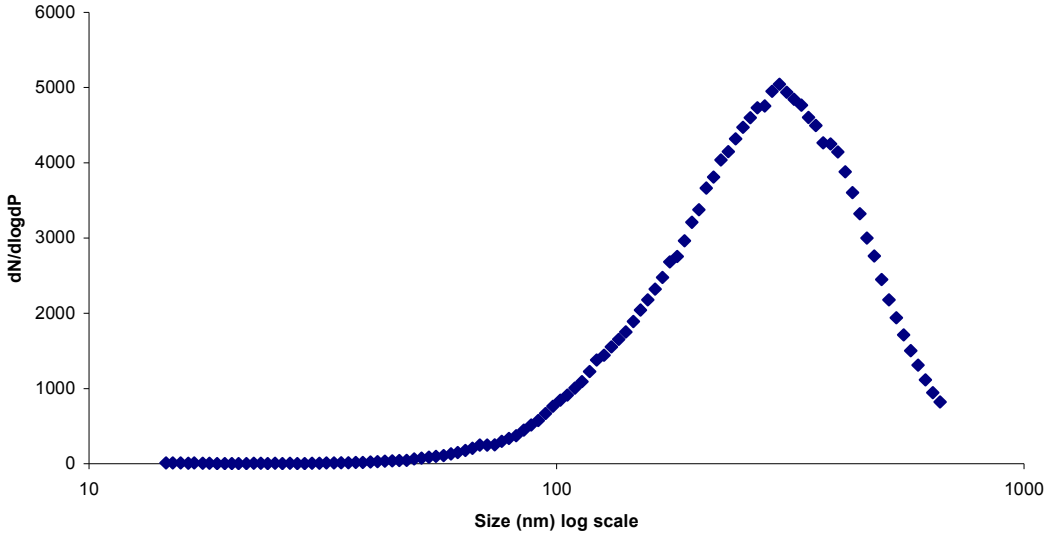


**Figure 37: SMPS spectrometer data of NM-110 (Batch No. ZC250#56#01). Normalised concentration vs. particle diameter data, taken from stable 51-hour segment of sampling time. The powder sample was aerosolised using a fluidised bed aerosol generator prior to SMPS analysis. Data were taken from a stable 51-hour segment of sampling time; this plot thus displays the mean size distribution of the aerosolised powder over this time.**

## 4.12 Specific surface area

### 4.12.1 Brunauer Emmett Teller (BET) Method

BET surface area measurements were determined using Autosorb-1 (Quantachrome Instruments). The Autosorb-1 was calibrated using a quartz rod of a known volume, which is traceable to NIST. This calibration was then further checked using two BAM certified reference materials: BAM-PM-102 (nominal specific surface area (SSA) 5.41$m^2g^{-1}$) and BAM-PM-104 (nominal SSA 79.8 $m^2g^{-1}$). These two reference materials allowed the range of SSA of the nanoparticles to be encompassed with known specific surface area materials, thus adding confidence to the measurements. Surface area measurements were acquired using an 11-point BET gas adsorption method, with nitrogen as the adsorbate. Prior to analysis, the powdered sample was transferred to a sample bulb, then sealed and subsequently de-gassed overnight at 300°C under a high vacuum and subsequently weighed on a analytical balance in order to determine the sample mass after the degassing step.

### 4.12.2 BET Results

Table 14 summarises the results of BET specific surface area measurements. Results show a wide range of the specific surface area values for various NM powders *i.e.* from 6.2 to 27.2 $m^2$/g. Results show that NM-112 has the largest surface area of 27.2 $m^2$/g and the smallest being NM-113 of 6.2 $m^2$/g. The variation in specific surface area of the zinc oxide samples (Table 14) corresponds well with their inverse proportional variations in particle and crystallite sizes as shown in Table 11.

**Table 14: Summary of the specific surface area values as obtained by the BET gas adsorption technique; the data are the means of values (± 2 SD) of two replicates acquired on different days.**

| Sample Name | Mean BET SSA ($m^2$/g) |
|---|---|
| NM-110 | 12.4 ± 0.6 |
| NM-111 | 15.1 ± 0.6 |
| NM-112 | 27.2 ± 1.2 |
| NM-113 | 6.2 ± 0.3 |

BET Surface Area measurements were repeated using a Micromeritics Tristar II 3020. Surface area measurements were acquired using an 11-point BET gas adsorption method, with nitrogen as the adsorbate. Prior to analysis, the powdered sample was transferred to a sample bulb, then sealed and subsequently de-gassed overnight at 300°C under a high vacuum and subsequently weighed on a analytical balance in order to determine the sample mass after the degassing step.

The mean BET specific surface areas of a different set of samples from the same batch to that reported Table 14 were determined predominantly using Micromeritics instrumentation except in one case (NM-111) where the BET specific surface area was measured on both Quantochrome and Micromeritics. The results are reported in table 15 below in the right-hand column (Micromeritics) and can be compared with data in the middle column (Quantochrome) taken from Table 14 and measured in a different laboratory.

**Table 15: Summary of the specific surface area values as obtained by the BET gas adsorption technique; the data are the means of values (± 2SD; SD) of replicates acquired on different days.**

| Sample Name | Mean BET SSA ($m^2$/g) (Quantochrome) | Mean BET SSA ($m^2$/g) (Micromeritics) |
|---|---|---|
| NM-110 | 12.4 ± 0.6 | 11.76 ± 0.55 |
| NM-111 | 15.1 ± 0.6 | 14.2 ± 3.5* |
| NM-112 | 27.2 ± 1.2 | 27.25 ± 0.5 |
| NM-113 | 6.2 ± 0.3 | 5.78 ± 0.05 |

* Average of data set obtained from 1 Quantochrome measurement and 1 Micromeritics measurement

Generally, there is good agreement between the two data sets obtained across different laboratories.

## 4.13 Porosity

### 4.13.1 Porosity Method

Porosity may be determined using the Barrett-Joyner-Halenda (BJH) method of analysis of adsorption and desorption isotherms to determine pore area, specific pore volume and pore size distribution independent of external area due to the particle size of the sample. The t-plot method is commonly used to determine the external surface area, pore volume and pore surface area in microporous solids.

### 4.13.2 Porosity Results

Table 16 presents the micropore surface area and volume, external surface area and a determination of the average pore width for all four samples.

**Table 16: Summary of the specific surface area values as obtained by the BET gas adsorption technique; the data are the means of values (± 2SD; SD) of replicates acquired on different days.**

| Sample Name | t-Plot Micropore Surface Area: $m^2/g$ | t-Plot External Surface Area: $m^2/g$ | t-Plot micropore volume: $cm^3/g$ | BJH Desorption average pore width (4V/A): Å |
|---|---|---|---|---|
| NM-110 | 1.79315± 0.58 | 9.97± 0.98 | 0.000805± 0.00029 | 89.7445± 4.5 |
| NM-111 | 0 | 17.4935 | 0 | 194.42* |
| NM-112 | 5.3518± 0.85 | 21.9027± 1.17 | 0.0024255± 0.0004 | 157.63± 10.3 |
| NM-113 | 1.38765± 0.66 | 4.39675± 0.11 | 0.000638± 0.11 | 107.49± 12.7 |

*Data set obtained from Micromeritics sample only

All samples have very low microporosity. The major contribution to total surface area is from external surfaces and is thus predominantly determined by particle size and shape rather than high internal porosity. NM-112 has the highest surface area and micropore volume of all the samples approximately 3-4 times greater than other samples.

## 4.14 Surface Chemistry

### 4.14.1 Surface Chemistry Method

X-ray Photoelectron Spectroscopy (XPS) measurements were obtained in ultra-high vacuum using a Kratos AXIS Ultra DLD (Kratos Analytical, UK) instrument fitted with a monochromated Al K$\alpha$ source, which was operated at 15kV and 5mA emission. Photoelectrons from the top few nanometres of the surface were detected in the normal emission direction over an analysis area of approximately 700 x 300 micrometres. Spectra in the range 1400 to –10 eV binding energy and a step size of 1 eV, using a pass energy of 160 eV, were acquired from selected areas of each sample. The peak areas were measured after removal of a Tougaard background. The manufacturer's intensity calibration and commonly employed sensitivity factors were used to determine the concentration of the elements present. High resolution narrow scans of some of the peaks of interest were acquired with a step size of 0.1 eV and 20 eV pass energy. (The manufacturer calibrated the intensity calibration over the energy range). The energy scale was calibrated according to ISO 15472 Surface chemical analysis – X-ray photoelectron spectrometers – Calibration of energy scales. However, the charge neutraliser was used when acquiring the spectra, which shifted the peaks by several eV. The C 1s hydrocarbon peak (285 eV binding energy) was used to determine the shift for identifying the peaks.

Samples were prepared using carbon adhesive tape to affix them to 1 cm copper squares. Care was taken to cover the tape with the powders as completely as possible but some samples had better coverage than others and in a lot of cases there was a signal detected from the tape as well as the powder itself. The tape contained oxygen and silicon in addition to carbon.

### 4.14.2 Surface Chemistry Results

The elemental composition of the different NM powders as measured by XPS is summarised in Table 17, in which the elemental concentrations of the elements:

carbon (C), oxygen (O), silicon (Si) and zinc (Zn) are shown. As evident from the results, there was a significant contribution of carbon and this can be largely attributed to contamination on the particles. Areas of best coverage were selected for analysis. XPS analysis of the carbon tape alone showed a composition of 74% C, 21% O and 5% Si. From the lack of any significant signal from Si on samples NM-110, NM-112 and NM-113, it was estimated that there was better than 90% coverage within these analysis areas. A different sample preparation procedure could be adopted to separate background carbon signal from that on the particles during XPS measurements. XPS results showed the presence of Si in the NM-111 sample *i.e.* Si 2s of 3.5%. This can be attributed to the fact that this sample was coated with triethoxycapryl silane and hence the silicon signal contribution. The silicon contribution with the NM-110 of 0.3 % is lower than the estimated detection limit for Si of ~ 0.5% and can be regarded as lying within the noise level.

**Table 17: XPS element atomic concentrations results; the powders were spread on to an adhesive carbon tape.**

| Sample Name | C 1s (%) | Ce 3d (%) | O 1s (%) | Si 2s (%) | Zn $2p_{3/2}$ (%) |
|---|---|---|---|---|---|
| NM-110 | 69.0 | 0.0 | 25.1 | 0.3 | 5.6 |
| NM-111 | 67.9 | 0.0 | 24.3 | 3.5 | 4.3 |
| NM-112 | 64.7 | 0.0 | 26.9 | 0.0 | 8.4 |
| NM-113 | 25.6 | 0.0 | 44.3 | 0.0 | 30.1 |

#### 4.14.2.1 Homogeneity testing using XPS

Table 18 shows the elemental compositions for sub-samples of NM-110 and NM-111. The powders are adhered on to a (adhesive) carbon tape, in which the elemental composition of the tape was shown to be (atomic %) 74.3% C, 20.9% O, 4.8% Si. It is clear from the table of results that there is significant carbon and oxygen signal for both NM-110 and NM-111, which potentially originates from the carbon tape on which the NMs were fixed. Although the area (analysis area of ~ 700 x 300 μm, with information depth of ~ 8nm) was carefully chosen to obtain maximum particle coverage, it is clear that the carbon and oxygen tape background signal is contributing towards the XPS signal.

**Table 18: XPS results for JRC sub-sampled powders for: a) NM-110 and b) NM-111. Replicates: 1 vial, 1 replicate per vial.**

**a)**

| NM-110/atomic% | | | | |
|---|---|---|---|---|
| **Sample batch** | **C 1s%** | **O 1s%** | **Si 2s%** | **Zn $2p_{3/2}$%** |
| NM-110-4899 | 57.7 | 29.8 | 1.0 | 11.5 |
| NM-110-2617 | 45.7 | 35.2 | 0.2 | 18.9 |
| NM-110-1866 | 43.8 | 36.2 | 0.0 | 19.9 |
| NM-110-3795 | 35.7 | 39.7 | 0.0 | 24.7 |
| NM-110-0286 | 38.0 | 38.8 | 0.0 | 23.1 |
| NM-110-0305 | 36.0 | 39.6 | 0.0 | 24.4 |

**b)**

| NM-111/atomic% | | | | |
|---|---|---|---|---|
| **Sample batch** | **C 1s%** | **O 1s%** | **Si 2s%** | **Zn $2p_{3/2}$%** |
| NM-111-4825 | 59.1 | 28.3 | 3.4 | 9.2 |
| NM-111-2419 | 68.6 | 23.7 | 3.9 | 3.9 |
| NM-111-1869 | 70.6 | 23.2 | 3.5 | 2.7 |
| NM-111-4779 | 67.7 | 24.3 | 3.8 | 4.1 |
| NM-111-1017 | 57.7 | 28.4 | 4.1 | 9.7 |
| NM-111-3396 | 70.2 | 23.3 | 3.4 | 3.1 |
| NM-111-0486 | 72.8 | 22.3 | 3.4 | 1.5 |

Nonetheless, we can deduce clear significant difference in the XPS results between the two sets of vials, which are as follows:-

The count rate of Zn peaks were always lower for NM-111 samples compared to NM-110 samples *i.e.* 4 to 11.5 kcps and 19 to 23 kcps, respectively. This can be attributed to the presence of a triethoxycarpryl silane coating associated with NM-111 samples.

The Si level is much higher (3.1 to 4.1 %) in NM-111 if compared to NM-110 (0 to ~1%). This is consistent with the presence of a silane coating with the former sample. The silicon signal contribution (of less than 1%) can be attributed to silicon background signal from the fixing tape.

## 4.15 Other relevant Information

### 4.15.1 Thermogravimetric Analysis (TGA)

#### 4.15.1.1 TGA Method

Thermogravimetric Analysis (TGA) was done using a Mettler Toledo TGA/SDTA 851e and an oxygen atmosphere. The heating rate was 10 K/min and the temperature range was from 25 °C to 1000 °C. The sample holders used for the TGA measurements were made of alumina and had a volume of 70 µL or 150 µL. We report the total mass-loss from TGA as Loss On Ignition (LOI).

#### 4.15.1.2 TGA Results

The TGA only showed slow mass-increase for NM-110 during heating and hence no sign of combustible material, as exhibited in Figure 38.

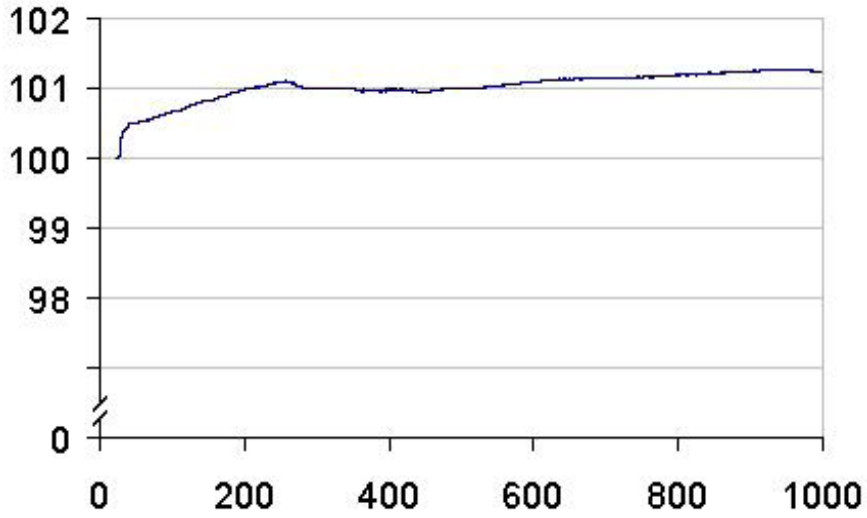


**Figure 38: TGA-curve for NM-110.**

The TGA curve of NM-111 is provided in
Figure 39; it shows that only a very small weight loss appears approximately around 400 °C, which most likely can be ascribed to the silane coating. This is approximately about 1 wt%.

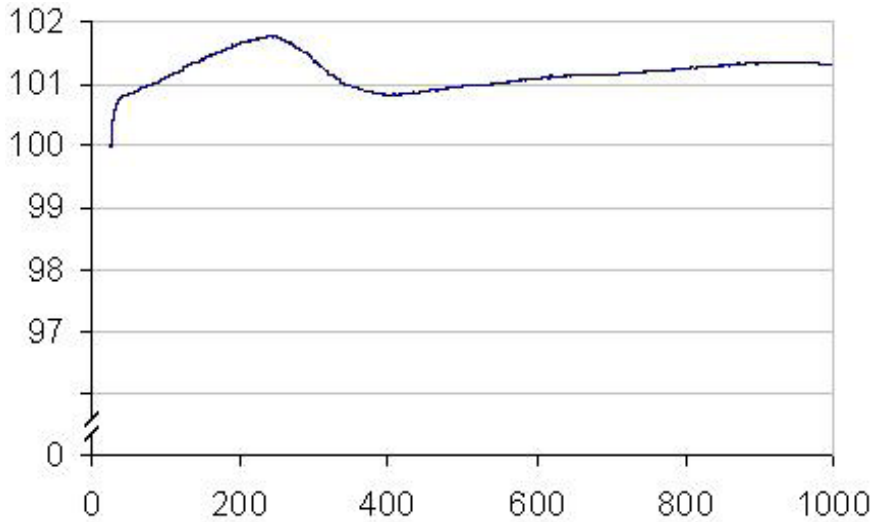


**Figure 39: TGA-curve for NM-111.**

### 4.15.2 Chemical Analysis

#### 4.15.2.1 Chemical Analysis Method

Potential inorganic impurities in the tested nanomaterial were investigated by digesting powdered nanoparticles with various oxidant mixtures (carefully optimised for each nanoparticle) in an Ehos1600 Microwave (Milestone, Bergamo, Italy). The resulting solution was then evaporated to dryness and reconstituted in 25 ml of MilliQ water, which was analyzed by Inductively Coupled Plasma-Optical Emission Spectroscopy (ICP-OES) using an Optima 5300DV ICP-OES (Perkin-Elmer, MA, USA). The reported concentrations are averaged values obtained from three sub-samples individually digested and analyzed.

All samples were prepared in duplicates using about 0.15 g for analysis. ZnO samples were digested using a concentrated $HNO_3$ acid. Resultant solutions were diluted to 100 mL, internal standard Sc was added and the resultant solutions were analysed by Varian 730 Axial Inductively Coupled Plasma-Atomic Emission Spectroscopy (ICP-AES). Certified multi-element solutions were also used to check the accuracy of the method.

#### 4.15.2.2 Chemical Analysis Results

Very low inorganic trace element impurities were detected by ICP-OES for NM-110 as shown in Table 19. No individual impurity particles or crystal structures of the identified elements were identified by TEM.

**Table 19: Trace elements impurities detected in NM-110.**

| Element | µg/g (ICP-OES) |
|---|---|
| Ni | 9 |
| Pb | 8 |
| Co | 3 |

Very low inorganic impurities were detected by ICP-OES for NM-111 as shown in Table 20.

**Table 20: Trace elements impurities detected in NM-111.**

| Element | µg/g (ICP-OES) |
|---|---|
| Ni | 9 |
| Pb | 8 |
| Co | 3 |

In general all samples were found to have little or no secondary elements present (Table 21). NM-112 had substantially higher levels of detectable alkali metals (Ca, Na) as well as Al than all the other samples whilst NM-113 appeared to have a significantly higher level of detectable Cu than all other samples.

**Table 21: All results are expressed in units of mass fraction [ppm] or relative mass fraction [%].**

| Sample Reference | NM-110 | NM-111 | NM-112 | NM-113 |
|---|---|---|---|---|
| Al 396.152 | 24 ppm | 27 ppm | 130 ppm | 7.9 ppm |
| Ca 422.673 | 44 ppm | 74 ppm | 680 ppm | 38 ppm |
| Ce 446.021 | <10ppm | <10ppm | <10ppm | <10ppm |
| Co 238.892 | <2.5ppm | <2.5ppm | <2.5ppm | <2.5ppm |
| Cr 267.716 | <1.5ppm | 1.9 ppm | 0.63 ppm | <1.5ppm |
| Cu 324.754 | 15 ppm | 4.8 ppm | 2.7 ppm | 120 ppm |
| Fe 259.940 | <5ppm | <5ppm | <5ppm | <5ppm |
| K 769.897 | <15 ppm | <15 ppm | <15 ppm | <15 ppm |
| Mg 285.213 | <2ppm | <2ppm | <2ppm | <2ppm |
| Mn 257.610 | <0.3ppm | <0.3ppm | 0.9 ppm | <0.3ppm |
| Na 589.592 | 3 ppm | 17 ppm | 176 ppm | 4.2 ppm |
| Ni 231.604 | <20ppm | <20ppm | <20ppm | <20ppm |
| P 213.618 | <90ppm | <90ppm | <90ppm | <90ppm |
| Pb 283.305 | <40ppm | <40ppm | <40ppm | <40ppm |
| S 181.972 | <200ppm | <200ppm | <200ppm | <200ppm |
| Si 251.611 | 195 ppm | 265 ppm | 210 ppm | 236 ppm |
| Sn 283.998 | <1ppm | <1ppm | <1ppm | <1ppm |
| Ti 336.122 | 6.4 ppm | 7.7 ppm | 8.2 ppm | 6.4 ppm |
| V 311.070 | <0.02ppm | <0.02ppm | <0.02ppm | <0.02ppm |
| Zn 213.857 | **89.80%** | **87.39%** | **90.40%** | **87.63%** |
| Zr 339.198 | <3ppm | <3ppm | <3ppm | <3ppm |

# 5 NM Characterisation: As prepared test item in vehicle/media

This section describes the characteristics of the NM materials for nano-ZnO for the NM as prepared test items (*cf*. *Section 3.3: Scenarios for characterisation of NM-Series RMNs*). By definition, the characteristics depend on the test system used and the requirements of the specific test systems and applied standard operating procedures including selection of the vehicle/media. The results regarding the selected properties depend on the choice of vehicle or media and the conditioning protocol. The term “vehicle” is used in Good Laboratory Practice (GLP) and generally used in studies regarding effects on human health. The term “media” is widely used in studies regarding environmental toxicology and fate. “Vehicle” and “media” thereby both describe the matrix, in which the test material is presented to the test system. The endpoints for hazard and fate are described in the Guidance Manual for sponsors. For typical *in vitro* tests, SOPs for test item preparation are presented together with the corresponding properties for ZnO-NMs. Stability of the dispersion should be addressed.

***SCENARIO 2: NM as prepared Test Item***[‡‡]

Dispersion in air/ aqueous media; physico-chemical properties (matrix dependent):

(1) Size and size distribution, shape-
(2) Agglomeration/ aggregation
(3) Zeta-Potential (aqueous media)
(4) Dispersibility, solubility
(5) Composition, purity
(6) Redox potential
(7) Photocatalytic Radical Formation Potential

[‡‡] cf. Section 3.3: Scenarios for characterisation of NM-Series RMNs.

## 5.1 Agglomeration/Aggregation (Matrix dependent)

### 5.1.1 Dynamic Light Scattering

A number of caveats have been made regarding the suitability of the method with regard to this measurand, such as mentioned in Chapter 5.11. Klein *et al.,* stated in a report on nanomaterials (Klein *et al.,* 2011): *"If measurands are addressed, which are different from the measurand and property to be determined, but which may give a hint to a certain property or under ideal conditions may be brought into context and calibrated to provide a meaningful result, the results have to be carefully interpreted, when being taken into account as additional data."* In January 2011, the attendants of the expert meeting of Steering Group 7 of the OECD WPMN issued a recommendation, which reads: *"After thorough discussions, the participants of the SG7 ECM recommended that the results of DLS measurements alone on mixtures of nanomaterials or polydisperse size distributions of a specific NM (typical for the NMs used in the sponsorship programme and relevant for industry) may be of limited value since multimodal particle size distribution may not be accurately analysed by DLS only".* It is therefore strongly recommended to use a second method with an established traceability chain.

#### 5.1.1.1 Method

Hydrodynamic size (z-average mean) measurements were obtained using a Zetasizer Nano ZS (Malvern Instruments, UK) equipped with a 633 nm laser. A reference standard (polystyrene, latex bead, nominal size of 100 nm) was used to qualify the performance of the instrument. Sample analysis involved filling of a disposable capillary cell (DTS1060, Malvern). The advantage of using this cell is that zeta-potential measurements can be taken immediately after acquiring the DLS measurement. Prior to their use, these cells were thoroughly cleaned with ethanol and de-ionised water, as recommended by the instrument vendor. Individual cell was then filled with the appropriate sample and flushed before re-filling; measurement was carried out on the second filling. Malvern Instrument's Dispersion Technology software (Version 4.0) was used for data analysis. For

particle size it is the z-average diameter (the mean hydrodynamic diameter) that is reported and measurements were done in DI water.

#### 5.1.1.2 Results

Figure 40 shows the DLS measurement data of NM-110. The mean particle size based on three measurements was approximately 275 nm with a standard deviation of 4 nm. The polydispersity index (PDI) was approximately 0.145 with a standard deviation of 0.008 indicating that the particles were polydisperse. As a rule of thumb, PI values smaller than about 0.04 are considered monodisperse (NIST, 2007).

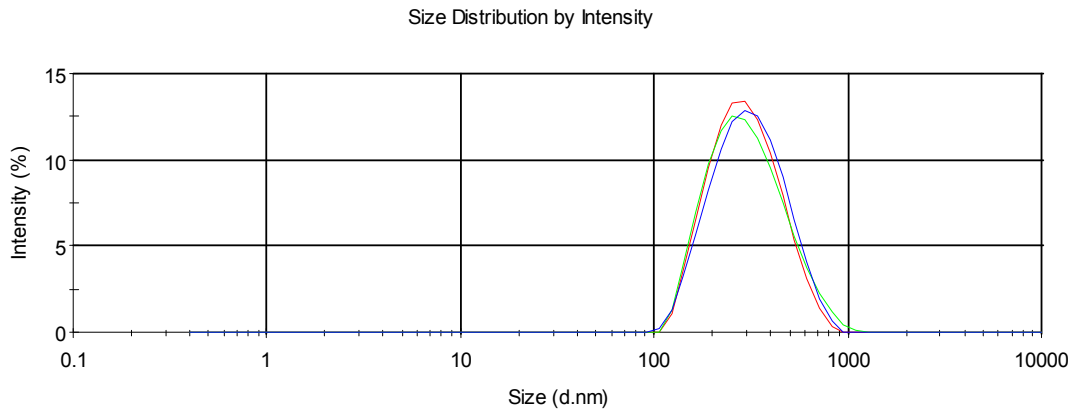


**Figure 40: DLS measurement data for NM-110.**

Figure 41 shows the DLS measurements of NM-111. The mean particle size based on three measurements was approximately 253 nm with a standard deviation of 1 nm. The polydispersity index (PDI) was approximately 0.401 with a standard deviation of 0.009 indicating that the particles were polydisperse.

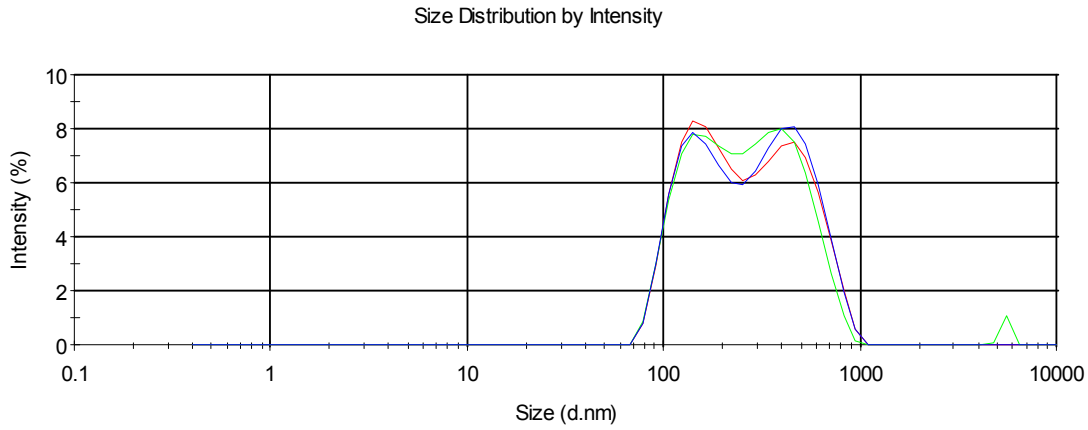


**Figure 41. DLS measurement data for NM-111.**

Figure 42 shows the DLS measurements of NM-113. The mean particle size based on three measurements was approximately 508 nm with a standard deviation of 2 nm. The polydispersity index (PDI) was approximately 0.15 with a standard deviation of 0.015 indicating that the particles were polydisperse.


**Figure 42: DLS measurement data for NM-113.**

### 5.1.2 CPS Disc Centrifuge

#### 5.1.2.1 Method

Particle size distribution by centrifugal sedimentation was acquired using CPS Disc Centrifuge Model DC 20000 instrument (Analytik Ltd, UK). At the start of the method, the centrifuge was brought up to speed by partially filling the disc with a sucrose gradient fluid and dodecane cap fluid. The purpose of the gradient fluid was to stabilise the sedimentation; the purpose of the cap fluid was to maintain the gradient inside the disc. The disc centrifuge was then allowed to equilibrate at 6000 rpm for 1 hour; this gradient will be stable and used within the next 6 hours. 0.2 ml of the nanoparticle sample (50 mg/L) was injected into the disc; a calibration standard was injected after every three samples. Analysis was run against a calibration standard, PVC 0.377 µm. The Disc Centrifuge Control System software (CPS Instruments Inc.) was used to acquire and process the data.

#### 5.1.2.2 Results

Table 22 and Table 23 show the CPS disc centrifugal sedimentation results, with Table 22 showing the equivalent spherical mean particle diameter and Table 23 showing the corresponding $D_{10}$, $D_{50}$, $D_{90}$ values (oversize percentiles). $D_{10}$, $D_{50}$, $D_{90}$ values are often used to describe the particle size distribution of the sample.

**Table 22: Particle size measurements by CPS disc centrifuge. The equivalent spherical particle diameter as measured by CPS centrifugal sedimentation; the mean and ± SD of 3 replicates are shown. NM-111 is hydrophobic and hence difficult to disperse and was not measured.**

| Sample Name | DI water (nm) | Fish medium (nm) | Seawater (nm) | Daphnia medium (nm) |
|---|---|---|---|---|
| NM-110 | 193±3 | 290±20 | 309±10 | 296±16 |
| NM-111 | - | - | - | - |
| NM-112 | 277±7 | 390±70 | 510±40 | 500±200 |
| NM-113 | 590±30 | 620±20 | 660±20 | 631±5 |

If $D_{10}$ = 1225 nm, then this means that 10 mass % of the particles will have particle diameter of 1225 nm or larger. Results show that the largest mean

particle size exists when the NMs are dispersed in seawater; this is reflected on the particle mean size as well as the corresponding $D_{90}$ values. Results also show that the smallest particle size exists when the NMs are dispersed in DI water. This suggests that larger agglomerates exist in the ecotoxicology media, with the largest agglomerates found in seawater.

**Table 23: Particle size measurement by CPS disc centrifuge. The corresponding $D_{10}$, $D_{50}$, $D_{90}$ values (oversize percentiles) from the averaged CPS measurements. NM-111 is hydrophobic and hence difficult to disperse and was not measured.**

| Sample Name | DI water (nm) | Fish medium (nm) | Seawater (nm) | Daphnia (nm) |
|---|---|---|---|---|
| NM-110 | $D_{10}$ 286±2<br>$D_{50}$ 82.8±1.9<br>$D_{90}$ 107.3±1.7 | $D_{10}$ 400±30<br>$D_{50}$ 270±20<br>$D_{90}$ 130±30 | $D_{10}$ 417±12<br>$D_{50}$ 301±8<br>$D_{90}$ 193±7 | $D_{10}$ 410±20<br>$D_{50}$ 285±16<br>$D_{90}$ 140±30 |
| NM-111 | - | - | - | - |
| NM-112 | $D_{10}$ 720±30<br>$D_{50}$ 40.1±0.7<br>$D_{90}$ 64.6±0.6 | $D_{10}$ 1000±200<br>$D_{50}$ 190±17<br>$D_{90}$ 93 ±4 | $D_{10}$ 1180±20<br>$D_{50}$ 330±70<br>$D_{90}$ 130±50 | $D_{10}$ 100±200<br>$D_{50}$ 400±200<br>$D_{90}$ 100±50 |
| NM-113 | $D_{10}$ 870±60<br>$D_{50}$ 572±19<br>$D_{90}$ 306±7 | $D_{10}$ 890±40<br>$D_{50}$ 606±12<br>$D_{90}$ 336±8 | $D_{10}$ 930±50<br>$D_{50}$ 639±15<br>$D_{90}$ 399±14 | $D_{10}$ 930±20<br>$D_{50}$ 612±3<br>$D_{90}$ 332±6 |

### 5.1.3 Turbidity Measurements

#### 5.1.3.1 Turbidity Method

Turbidity was measured using HF Scientific – Micro100 RI turbidity meter (Cole-Palmer, UK); this meter has an infrared light source that meets the international standard ISO 7027 for turbidity measurements. The meter was calibrated on standards, which are based on AMCO-AEPA-1 microspheres. Standard values of 1000, 10 and 0.02 NTU were used to calibrate the meter. Prior to use, the meter was allowed to warm up for 30 minutes. Sample cuvettes (HF Scientific (USA)) were used to hold the sample. Note that glass thickness may vary from cuvette to cuvette and within the same cuvette. Hence, individual vials were indexed; indexing of the cuvette entails finding the point of the cuvette that light passes through that gives the lowest reading; once indexed the holder can be marked accordingly. Prior to their use, cuvettes were cleaned, in accordance to manufacturer's instructions. This involved washing the interior and exterior of

the cuvette with a detergent (2% Hellmanex in DI water); it was then rinsed several times in distilled water before finally rinsing in DI water. The cuvette was further rinsed with the sample two times before filling (30ml) and analysed. The cuvette was placed into the meter and signal allowed to settle before taking readings.

#### 5.1.3.2 Turbidity Results

Table 24 shows the corresponding "half-lives" of the NM powders when dispersed in the various media. The concept of "half lives" has been put forward in the OECD guidelines on NM testing and this value is an indication of dispersion stability through time *i.e.* the larger the half life value the longer it takes for the concentration to reduce by half and thus the more stable the dispersion.

Results show that overall NMs are most stable when dispersed in DI water and least stable when in an ecotoxicology media.

**Table 24: Dispersion stability as measured by turbidity measurements. NM-111 is hydrophobic and hence difficult to disperse and was not measured.**

| Sample Name | DI water (min) | Fish media (min) | Seawater (min) | Daphnia media (min) |
|---|---|---|---|---|
| NM-110 | 4038 | 816 | 738 | 768 |
| NM-111 | - | - | - | - |
| NM-112 | 2526 | 498 | 402 | 444 |
| NM-113 | 966 | 216 | 228 | 324 |

## 5.2 Zeta potential (Surface Charge) – Matrix dependent

### 5.2.1 Zeta-Potential Method

Electrophoretic measurements were obtained using a Zetasizer Nano ZS (Malvern Instruments, UK) equipped with a 633 nm laser. The reference standard (DTS1230, zeta-potential standard from Malvern) was used to assess the performance of the instrument. Sample preparation involved filling of a disposable capillary cell (DTS1060, Malvern). Prior to their use, these cells were

thoroughly cleaned with ethanol and de-ionised water, as recommended by the instrument vendor. For analysis, the individual cell was filled with the appropriate sample and flushed before re-filling; measurement was carried out on the second filling. Malvern Instrument's Dispersion Technology software (Version 4.0) was used for data analysis and zeta-potential values were estimated from the measured electrophoretic mobility data using the Smoluchowski equation.

### 5.2.2 Zeta-Potential Results

The measured zeta-potential values for the NMs (50 mg/L) are summarised in Table 25.

**Table 25: The mean values of zeta-potential (of six replicates) for different nanomaterials dispersed in various media at a concentration of 50 mg/L.; * DI water + 5 mM NaCl - this medium was employed to compare with the DI results when in the presence of inert background electrolyte. Values are the mean and ± 1 SD of six replicates.**

| Sample Name | DI water (mV) | DI water + 5mM NaCl* (mV) | Fish medium (mV) | Seawater (mV) | Daphnia medium (mV) |
|---|---|---|---|---|---|
| NM-110 | 24.3±0.4 | 20.8±0.8 | 10.8±0.1 | N/A | 1.3± 0.2 |
| NM-112 | 24.6 ±0.4 | 25.2±0.6 | 12.4±0.3 | N/A | 4.9± 0.2 |
| NM-113 | 20.2±0.4 | 13.9±0.6 | 4.4±0.4 | N/A | -4.6± 0.4 |

Results show that zeta-potential values of NMs when dispersed in seawater cannot be successfully measured (due to high conductivity) and thus displayed as N/A on the table; such unsuccessful measurements were reported in the corresponding "quality report" at the end of the measurement. In general, results indicate high zeta-potential values for NMs that are dispersed either in DI water (or DI water + 5 mM NaCl), and thus confer stability in such media. Results show values of zeta-potential measured were lower when the NMs were dispersed in an ecotoxicology media indicating much poorer dispersion stability in such media.

## 5.3 Redox Potential

### 5.3.1 Redox Potential Method

Redox potential were measured using an ORP Oakton® Waterproof ORP Testr®, purchased from Cole Palmer UK; this in effect measures the potential difference across two electrodes *i.e.* a Pt electrode against a double junction Ag/AgCl reference electrode. The electrode was used in accordance to the manufacturer's instructions. Prior to use the electrode was pre-condition in clean tap water for 30 minutes before rinsing in distilled water. When making measurements, the electrode was carefully placed in a vial containing the sample; there must be sufficient liquid sample to cover the sensing element. The electrode was carefully stirred a little and then placed in a fixed position, slightly above the bottom of the container. The signal output was allowed to settle for 5 minutes before a reading *i.e.* the "field potential" was noted. After measurement, the electrode was cleaned with tap water and final rinse was with distilled water, after which further measurements can be made. When not in use, the electrode was stored in a solution of Oakton® electrode storage solution, as recommended by the manufacturer.

The redox potential ORP electrode was calibrated against YSI® Zobell ORP Calibration Solution (purchased from Cole Palmer); this reagent was made available in dry form and was reconstituted with 125 mL of DI water prior to use, after which the solution has ~ 6 months expiry date. This standard solution was also used to verify the performance of the electrode in the beginning and end of the study.

For Ag/AgCl reference, the redox potential value for Zobell solution was 231 ±10 mV (depending on temperature); at ~ 20 °C, this value was ~ 237 mV. Redox potential was carried out on freshly dispersed NM in various media; the media was DI water and the three ecotoxicology media (fish, daphnia, water flea and seawater).

All field potential values recorded were subjected to an additive correction factor of +206 mV; this was necessary so that the final value was reported as if the reference electrode was a standard hydrogen reference electrode instead of the Ag/AgCl.

Dispersion of the individual nanomaterial in the appropriate liquid media was carried out in accordance to the protocol recommended under PROSPECT.

### 5.3.2 Redox Potential Results

There is still some ambiguity concerning the measurement of the redox potential (*i.e.* as to what and how to measure), particularly when in a nanoecotoxicological context. The study investigates the redox potential measurements, using ORP probe electrode, of various ZnO dispersions, in various liquid media. Although the redox potential values acquired from ORP electrode may be indicative of the redox state of the entire system it is difficult to quantify the reliability of such measurements.

**Table 26: Redox potential of liquid media blanks only.**

| Media Blanks Only | Redox potential (mV) | pH |
|---|---|---|
| DI water | 405 | N/A |
| Fish media | 418 | 7.34 |
| Daphnia media | 425 | 7.94 |
| Seawater | 384 | 8.75 |

**Table 27: Redox potential of NM dispersion in various liquid media, the value quoted is relative to the standard hydrogen reference electrode; values quoted in mV. NM-111 was not measured as it was difficult to disperse.**

| Media | NM-110 | NM-112 | NM-113 |
|---|---|---|---|
| DI water | 396 | 398 | 398 |
| Fish media | 427 | 424 | 430 |
| Daphnia media | 422 | 415 | 415 |
| Seawater | 379 | 380 | 374 |

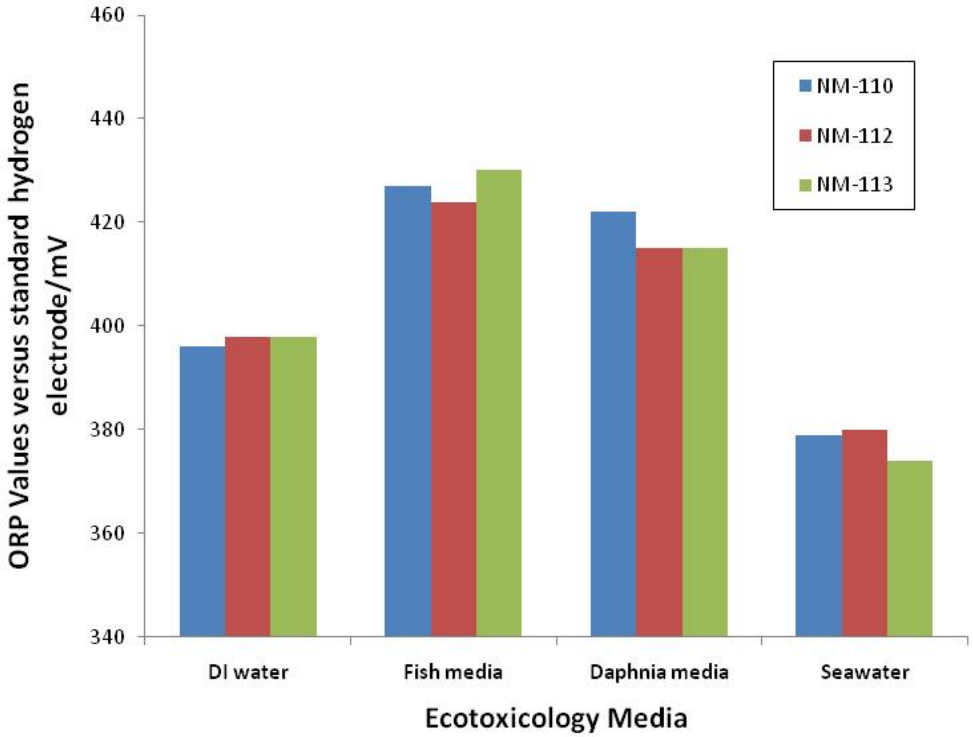


**Figure 43: Graphs of results summarised in Table 17.**

## 5.4 Photocatalytic Radical Formation Potential - Matrix dependent

### 5.4.1 Method

A 5 M KI (Sigma, St. Louis, MO) solution in ultra-pure water was freshly prepared; shaking and vortexing was preferred to sonication to dissolve KI. KI solution was added to the samples of NMs as received after dispersion (50mg/L), to obtain a typically 1 mL volume sample, with 0.1M KI. 6 x 3 samples were prepared for each NM/media combination. Additionally, 6 x 3 samples containing 0.1 M KI only and 50mg/L Anatase NMs (Anatase Nanopowder ($TiO_2$), Sigma) for each media were prepared as negative and positive controls respectively; 6 NM samples plus controls were prepared and assessed in total. All samples were contained in individual 2mL microcentrifuge tubes. Samples were irradiated under a 1kW Solar Simulator (Newport Corporation, Stratford, CT). The instrument possesses a Personal wavelength correction$^{TM}$ Certificate by Newport. The irradiance of the Solar Simulator was measured to be 1000 $Wm^{-2}$ using an optical power/energy meter (Newport, model 842-PE). Irradiation was performed on groups of 40 microcentrifuge tubes. The tubes were placed vertically under the centre of the lamp of the solar simulator, on an in-house made polystyrene holder, their cups having been removed. The samples were subjected to 10min periods of irradiation, followed by 5min period of non-irradiation to reduce sample overheating. After each 10 min period, 1x3 samples for each NM/media combination and controls were removed from the irradiations. Samples irradiated for 0 min, 10 min, 20 min, 30 min, 40 min and 60 min were collected for each NM/media combination and controls. The samples containing NMs were centrifuged at 20800 rcf for 15 min and 800 μL of supernatant was collected in a new micro-centrifuge tube and then analysed using UV-visible spectroscopy.

The UV-visible spectrum (absorbance scans from 300 nm to 500 nm) was acquired for samples that were irradiated for 60 minutes. Optical absorbance at 352 nm was acquired for all samples. Absorption spectra were acquired with a Lambda 850 UV-Vis spectrometer supported by UV Winlab software [Version

5.1.5] (Perkin Elmer, Waltham, MA). The instrument wavelength calibration was checked using Holmium glass standards (Serial # 9393, Starna Scientific, Hainault, UK). For the reference channel of the spectrophotometer a matched cell containing the corresponding dispersing media (with no nanoparticles) was used. Absorption spectra were acquired on samples that have been irradiated for 60 minutes. Absorbance scans from 300 nm to 500 nm were performed, using a slit width of 2 nm and a scan rate of 50 nm/min. After each sample, the cuvette was cleaned with a 2% solution of Hellmanex detergent, rinsed with pure water and ethanol and then blow-dried. Optical absorbance at 352nm was performed using a plate-reader Victor$^3$ 1420 multilabel counter (Perkin Elmer), supported by Wallac 1420 software (Perkin Elmer). 300$\mu$L of each sample (supernatant after centrifugation) was placed in the wells of a 96-well plate. Only the wells of rows 2 to 6 and columns 1 to 10 were used, as they had the same level of noise. The absorption at 352nm was measured using a 0.1s measurement time. Measured absorption values were displayed on a 0 arbitrary unit (a.u.) to 2 a.u. scale.

### 5.4.2 Results

Figure 44 shows the UV-visible spectra of tri-iodide ions, as produced when Anatase nanopowder particles are dispersed in four different media, in the presence of KI. The dispersions were exposed for 60 minutes, under 1000 W/m$^2$ white light irradiation. Results show that the spectra exhibit typical maxima at 352 nm (see Figure 44). The absorbance values at 352 nm can be used to quantify tri-iodide concentrations ($\varepsilon$ = 26000 Lmol$^{-1}$cm$^{-1}$).

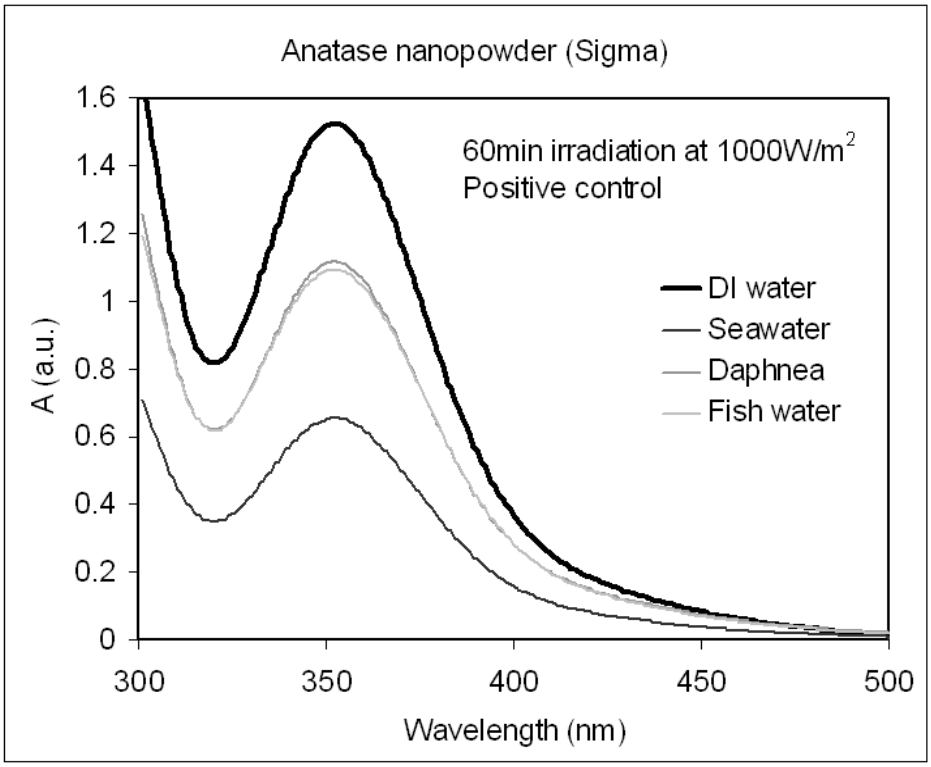


**Figure 44: UV-Visible absorption spectra of Anatase NM (positive control) in 4 different media (DI water, seawater, daphnia and fish media) after being irradiated with solar simulator at 1000 W/m$^2$, for 60 minutes.**

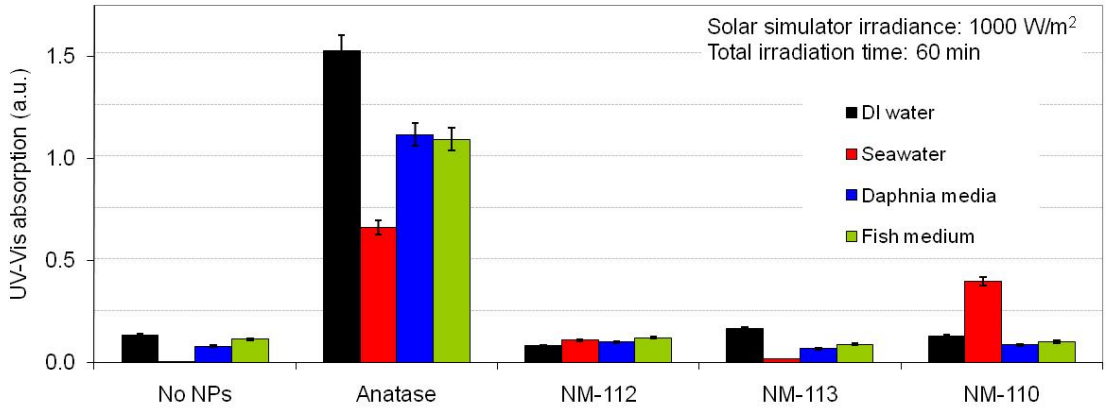


**Figure 45: Absorbance readings at 352 nm, of NMs in 4 different media (DI water, seawater, daphnia and fish media) after being irradiated with solar simulator at 1000 W/m$^2$, for 60 minutes. Anatase NM dispersed in the four different media was used as positive control; media with no NMs were used as a negative control. The values are normalised to the absorption measured for the negative control in DI water.**

Figure 45 compares the absorption measured at 352 nm for all the NM samples in four different media after 60 min of total irradiation; the corresponding negative control (*i.e.* media with no NMs) are also shown. Results show that

there was a certain level of tri-iodide ($I_3^-$) measured in the irradiated sample containing media only. Interestingly, tri-iodide was suppressed in seawater and may be attributed to a higher concentration of ions (potentially with some scavenging capacity either to ROS species or to electron (or holes) at the NM surface) in this media. As expected, results for Anatase ($TiO_2$), being the most active photocatalytic material, show a much higher rate of tri-iodide formation than the corresponding NMs. In particular, the absorbance signal was highest in DI water, with the lack of ionic species in the media. Again, when in seawater, the absorbance signal was reduced (as in the corresponding blank *i.e.* seawater with no Anatase). There are several possible explanations for this:

1. Presence of scavengers in solution, as previously described.
2. Enhanced aggregation/sedimentation of the NMs in seawater media compared to other media.

NM-110 is interesting, in that it does not follow a similar pattern observed with Anatase. With NM-110, the absorbance signal is much higher in seawater than when dispersed in the other three media. At present we offer no explanation for this observation. With the other NMs, the absorbance signals were within a similar range to that of the corresponding irradiated blank. Samples that were kept in the dark exhibited no absorption peak at 352 nm.

Lastly, a UV-visible plate reader was used to follow the cumulative production of $I_3^-$ with varying irradiation time; this was quantified by measuring absorption at 352 nm. In summary, results show that absorbance signal generally increases with irradiation time and this can be attributed to the increase in the amount of ROS being generated. Again, the results are consistent with previous observations, in that:

1. Anatase gave the highest absorbance reading.
2. NM-110 gave a higher absorbance reading in seawater compared when in other media.

## 5.5 Handling Procedure for Weighing and Sample Introduction

A handling procedure has been established in cooperation with scientists at the different research institutions, which used the NM-Series for zinc oxide. The NM vial contains an Argon atmosphere. The vial should be kept upright and stored under appropriate conditions at room temperature and in the dark until use. Dedicated sample and test item preparation protocols need to be used depending on the specific requirements of the measurement procedure or the test method.

The suggested handling protocol for NM-110, NM-111, NM-112 and NM-113 zinc oxide reads:

*BE FAST, once the vial is open! If possible, work in a glove box under inert dry atmosphere. The vial containing the NM material is filled with argon. Keep the vial upright. Record the individual sample ID number as indicated on the NM label. If working outside glove box, please wear gloves.*

1. *record laboratory conditions including relative humidity of the laboratory air for QA*
2. *weigh NM material vial still closed with cap and with the funnel (to be used in step 5)*
3. *remove cap from vial*
4. *open sample dilution vessel*
5. *transfer immediately sample into the sample dilution vessel using a clean and dry plastic funnel*
6. *handle gently and avoid air dispersion and losing material*
7. *close sample dilution vessel*
8. *close vial with cap*
9. *immediately weigh the empty vial together with the cap and the plastic funnel*

10. c*alculate mass difference. The mass difference corresponds to the total mass of material, which you have transferred into the sample dilution vessel.*

***General remarks:***

*The NM material maybe hygroscopic therefore fast and correct operation is of paramount importance. This is especially valid for the weighing procedure; i.e. one has to avoid any kind of water uptake by the sample material.*

## 5.6 Dispersion protocol for NM-110, NM-112 and NM-113 – the PROSPECT dispersion protocol

The method below is written for the preparation of nanoparticles dispersion (in particular Zinc Oxide and Cerium Oxide) in DI water (concentration of 15 mg/L, but can be adapted (at some other concentration)) and aqueous based liquid media. This method is not particularly suited for the dispersion of NM-111 (coated Zinc Oxide nanoparticles) and the researcher is advised to use the method described under Section 5.7. There is also a dispersion protocol training video[§§] available. The user is advised to view this video before using the dispersion protocol.

### 5.6.1 Materials

1. 1 large glass beaker (1 L)
2. Volumetric (glass) flask (1 L)
3. DI water (resistivity of ~ 18 MΩ)
4. Ultrasonic probe[***] (Cole-Parmer® 130-Watt Ultrasonic Processors (50/60 Hz, VAC 220); product number EW-04714-51); the probe is a 6 mm (1/4") titanium and is tuned to resonate at 20 kHz, ±50 Hz)
5. Mini Lab Jack
6. Stainless steel spatula
7. Disposable pipette (preferably standard glass Pasteur pipette, 150 mm length)
8. Vial 2 (as detailed above in Section 5.1) containing NM-110 (or NM-112, NM-113) (~15 mg)
9. Vial 3 (pre-cleaned, with no specific dimensions) to contain a suitable volume of DI water (or ecotoxicology media), such that you will end up with 1 mg/ml nanoparticle concentration in Vial 2

[§§] The PROSPECT dispersion protocol can be viewed using the following link, http://www.nanotechia-prospect.org/publications/basic.

[***] Although exposure of the nanoparticles to a high intensity ultrasonic probe appears to be more effective than other de-agglomeration tools, its limitations have not been fully investigated. For example, probe tip disintegration/erosion through time can potentially contaminate samples. Probes can also have highly variable performance, particularly at the lower end of the market. In addition, the high amount of shear provided by the ultrasonic probe can alter nanoparticle architecture and also increase the temperature of the dispersion.

### 5.6.2 Method

**Step 1**: Add a few drops of DI water (or liquid media) taken from Vial 3, using a glass pipette to the nanoparticle powder in Vial 2, in order to create a thick paste. Do this whilst mixing using a pre-cleaned spatula and apply sufficient energy to remove visible aggregates in the paste. The purpose of this wetting step is to sufficiently substitute solid-air interface with solid-liquid interface, as recommended by guidelines in BS ISO 14887 (2000) ["Sample Preparation – dispersing procedures for powders in liquids].

**Step 2**: Add the rest of DI water from Vial 3 into Vial 2 (containing the paste of nanoparticle powder) and gently mix using a clean spatula.

**Step 3**: Place Vial 2 on to a lab jack and insert the ultrasonic probe tip half way down the small vial. De-agglomerate using an ultrasonic probe for 20 s (at 90 % amplitude; this should give a temperature rise of ~5 °C in the dispersion). The operator should determine the acceptable temperature rise during sonication in the given time period. If longer sonication time is required then the operator must provide a better control of the temperature inside the vial. One option is to immerse Vial 2 in an ice bath during the sonication. During sonication, ensure that the tip is not touching the sides of the glass vial. In addition, do not place your hands near the de-agglomerating unit whilst it is operating.

**Step 4**: Once completed, transfer the nanoparticle suspension to the desired total volume (to make the "stock") and mix gently with a glass rod. Flush the small vial with further DI Water (or liquid media) and add this to the rest of the suspension. This "washing" step is important to ensure that all of the nanoparticles are transferred from the small vial to the larger beaker, such that dosage measurement (by mass) can be interpreted accurately. Gently stir with a glass rod. For greater accuracy, make up to the desired volume using appropriate volumetric flask/ pipette.

**Step 5**: The dispersion is now ready for analysis. For the nanoparticle analysis, this will involve the sample splitting of “the stock”. From guidelines found in ISO 14488:2007 “[Particulate materials sampling and sample splitting for the determination of particulate properties”] sample splitting using a pipette is recommended as this method (relative to sample splitting using multiple capillary tubes) is simple to do and less prone to contamination. Prior to taking an aliquot out of the stock, agitate the stock dispersion; this can be achieved by gently mixing using a clean glass rod to ensure homogeneity of the sample.

## 5.7 Dispersion protocol for NM-11X Zinc Oxide in Serum

The PROSPECT protocol is unable to disperse NM-111 effectively due to the particles having a hydrophobic silane coating. In order to prepare a dispersion of NM-111 particles, the following dispersion method is recommended. It has been developed for the ENPRA[†††] project and can also be applied to NM-110.[‡‡‡] Apart from zinc oxide NMs, this protocol can also be used to disperse nanoparticles of titanium dioxide (NM-101, NM-105) ($TiO_2$), silver (NM-300, NM-300K) and multi-walled carbon nanotubes (NM-400, NM-401, NM-402). An alternative method to disperse coated zinc oxide particles has also been published by Wiench *et al.,* (Wiench *et al.,* 2009).

### 5.7.1 Method

Weigh approximately 10 to 15 mg of particles corresponding to approximately 4 to 6 ml of dispersion media. Wetting with 0.5 vol % of ethanol (EtOH) is essential before sonicating to achieve a good suspension in the dispersion media.

1. Weigh the vial for the stock suspension with the cap.
2. Remove cap from suspension vial.
3. Remove cap from material vial.
4. Transfer material to stock suspension vial (at least sufficient material for 25 ml suspension).
5. Close the material vial.
6. Close the stock suspension vial.
7. Weigh the stock suspension vial and calculate the mass difference.
8. Add calculated amount of dispersion media.

[†††] The ENPRA project is a major current European project funded by the European Commission under Framework Programme 7 to develop and implement a novel integrated approach for engineered nanoparticle risk assessment. Further details on ENPRA can be obtained from the project website, http://www.enpra.eu.

[‡‡‡] A paper, describing the protocol and performance in detail, is in preparation by Jensen et al..

Use the highest standard of de-ionised water available and filtration through a 0.45 µm filter or smaller. Add 2 vol% serum to obtain the dispersion medium. The dispersion medium can be frozen at -20 °C for long term storage.

The recommended sonifier is a Branson Sonifier S-450d (Branson Ultrasonics Corp., Danbury, CT, USA) equipped with a standard 13 mm disruptor horn (Model number: 101-147-037)[§§§]. We recommend the use of 10 ml Schott Duran glass beakers, D=2.6 cm. The sample is continuously cooled in ice during the heat build-up caused by the sonication procedure, see Figure 46. Add pre-cooled MilliQ to the insulated box with ice in order to ensure a more direct cooling of the sample.

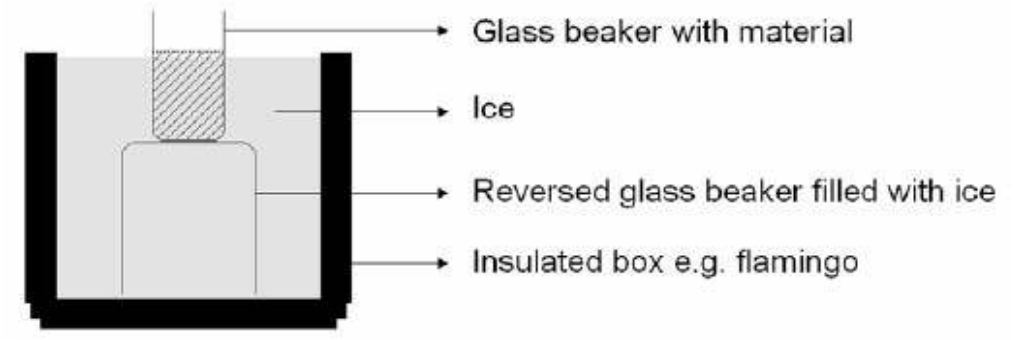


**Figure 46: Illustration of the arrangement of the vial containing stock dispersion during the sonication procedure.**

Tilt the vial so the nanoparticles are gathered in a small area. Wet the particles with 0.5% vol/vol EtOH (96%) for 1 minute. Prepare a stock suspension of 2.56 mg/ml by adding 99.5% standard dispersion media. Addition of EtOH is required to disperse the hydrophobic coating particles. It is suggested that both coated (NM-111) and uncoated zinc oxide particles (NM-110, NM-112, NM-113) be prepared this way for comparability. Sonicate continuously for 16 minutes. Make sure that the sample is continuously cooled by ice/water.

Ensure that the sonicator horn does not touch the bottom of the glass when it is switched on. Make sure that the horn is located in the top half of the liquid but

[§§§] Further details of the horn can be obtained from http://www.sonifier.com/pdf/DISRUPTO.PDF. More details of the sonicator can be obtained from http://www.sonifier.com/s450_digital.asp.

below the liquid surface. Do not start the sonicator before the probe has penetrated the liquid. Use approximately 4 to 6 ml of MilliQ.

For *in vivo*: The stock suspension will be used as is or diluted with dispersion medium (MilliQ with 2% mouse serum) to the lower concentrations (1-64 µg/ml).

For *in vitro*: The stock solution 2.56 mg/ml (particles in MilliQ with 2% serum of choice) should be diluted at least 10 times with full normal cell media. Highest test concentration will thus be 256 µg/ml. Add MilliQ containing 2% serum to the cell media to determine if the dilution has any effect on your cells/assay.

The dispersion should be stable within the hour but it is recommended that it is used immediately.

## 5.8 Dispersion protocol for NM-11X Zinc Oxide in Bovine Serum Albumin (BSA)

In some cases, it may be more appropriate to disperse the NMs in BSA rather than Serum depending on the standard operating procedure for the chosen test method and the corresponding test item preparation protocol. The following protocol has been developed for the Nanogenotox project[****] and can also be applied to Zinc Oxide NMs.[††††] This protocol can also be used to disperse nanoparticles of titanium dioxide NM-100, NM-101, NM-102, NM-103, NM-104, NM-105 ($TiO_2$), silicon dioxide NM-200, NM-201, NM-202, NM-203, NM-204 and multi-walled carbon nanotubes NM-400, NM-401, NM-402, NM-403. A 2.56 mg/ml stock dispersion is prepared by pre-wetting the nanomaterial in 0.5 vol % ethanol (≥ 96 % purity) followed by dispersion in 0.05 wt% BSA-water during 16 minutes of probe sonication. For harmonization, it is recommended to produce 6-8 ml dispersions in 20 ml tall glass scintillation vials. The resulting dispersion can be administered directly or diluted directly into the different test mediums. The dispersion agents (Ethanol and BSA) are considered to be acceptable for most *in vitro* and *in vivo* bioassays for toxicological testing. The 2.56 mg/ml concentration was chosen for easy dilution in the concentration series 1, 2, 4, 8, 16… 256 mg/ml.

### 5.8.1 Materials

1. Pure and sterile-filtered water
2. Bovine Serum Albumin (sterile)
3. Ethanol (96 vol %)
4. 1 flask for batch dissolution of BSA
5. 1 flask for sterile-filtered 1% w/v stock BSA-water solution
6. 1 flask for 0.05% w/v BSA-dispersion medium

[****] NanoGenoTox is a Joint Action collaboration project funded by the Executive Agency for Health and Consumers (EAHC) under the Public Health Programme of the European Commission and supported by the European Commission - JRC. Further details on the Nanogenotox project can be obtained from http://www.nanogenotox.eu

[††††] A short description of the protocol can be found at the project web-page and a complete information can be found in Jensen K.A., Kembouche Y., Christiansen E., Jacobsen N.R., Wallin H., Guiot C., Spalla O., Witschger O. (2011b), *Final Protocol for producing suitable manufactured nanomaterial exposure media.* NANOGENOTOX deliverable report n°3: July 2011 34 pp, as well as a paper in preparation lead by Dr Jensen describing development criteria and performance in detail.

7. Sterile filter (0.2 mm)
8. Vials (*e.g.* 20 ml scintillation vials with caps) for NM powder dispersions
9. Steel and glass spatula
10. Pipette and pipette tips
11. Weighing boat/weighing paper
12. Electrostatic neutraliser
13. Weighing scales
14. Control or reference weights
15. Probe sonicator
16. Ice (Ice-water)

**Water**

It is recommended to use the Nanopure Diamond UV since the MilliQ-filtered water has been found to be contaminated with Fe and Zn elements at promille levels even after mounted after de-ionization units. It is also recommended to analyse the water prior to use, especially in case that analysis and experiments may be influenced by trace-elements at low concentrations. For general sampling and validation, collection of water in acid cleaned chemically stable bottles suitable for element chemical analysis is recommended. Control the water quality (*e.g.* particles by DLS, elemental concentration, CFU and endotoxin) prior to use. If the water sample passes the quality test, the water may be evaluated pure and used for the experiment.

**Bovine Serum Albumin (BSA)**

Several types of albumin may be selected to fit specific toxicological test protocols. It is important that the selected albumin has passed tests for purity and sterility. It is recommended to use Bovine Serum Albumin (Fraction V), Sigma (catalogue number: A-9418).

**Production of sterile-filtered BSA water**

The production of the 0.05% w/v BSA-water (the dispersion medium) is done in two steps:

1. Preparing a sterile-filtered 1% w/v BSA stock solution and
2. Dilution to reach a 0.05% w/v BSA dispersion medium.

**Procedure for making a 1% w/v BSA stock solution:**

1. Add from pipette 50 ml water Nanopure to a 100 ml mixing flask.
2. Weigh out 1 g BSA (powder) in a weighing boat and pour it into the flask with 50 ml water, rinse the weighing boat into the mixing bottle with Nanopure water to retrieve as much BSA as possible into the mixing flask.
3. Pour Nanopure water into the mixing flask up to100 ml to reach a 1 % w/v BSA water solution.
4. Gently stir or swirl the BSA-solution for a few minutes (be careful to avoid foam formation by not using agitated stirring) and leave the mixing flask in the refrigerator over-night for complete dissolution of the BSA.
5. Sterile filter the solution into a new flask through a 0.2 µm sterile disposable filter ware with collection flasks after complete dissolution of BSA in the mixing flask. A subsequent step of sterile filtration of the volume to be used for each toxicity test is recommended to ensure no bacterial contamination in the tests. Sterile filtration causes about 28% loss of BSA resulting in a true BSA concentration of 0.036% w/v in the stock dispersion as determined by a Pierce BCA protein Assay Kit for microplate reading.

**Procedure for making a 0.05% w/v BSA solution for nanomaterial dispersion**

The 0.05% w/v BSA solution to be used for test item preparation is achieved by simple dilution of the 1% w/v batch solution. For example: 2 ml 1 % w/v BSA is diluted with 38 ml Nanopure water (Dilution factor = 20x) to reach a batch solution of 0.05 w/v%.

**Weighing nanomaterial powder**

Weighing should be done in a ventilated weighing box, a glove box or a fume hood designated for sensitive weighing with an accuracy of at least 0.1 mg or better.

**Materials**

- Weighing scales with an accuracy of 0.1 mg or better
- Reference or control weights with masses within the scale of the weighing project
- Wet and dry wipes for cleaning
- Weighing boat
- Steel and glass spatulas
- Vials: 20ml Scint-Burk glass pp-lock + Alu-foil (WHEA986581; Wheaton Industries Inc.)
- Vials with nanomaterials
- Tray for storage of vials

**Preparation of weighing area**

1. Turn on the weighing box, glove box, fume-hood 15-30 minutes before use.
2. Ensure wearing appropriate personal protection equipment (two- or three layer of gloves[‡‡‡‡], lab-coat, laboratory shoes etc.) and that personal respiratory protection equipment is easily accessible in case of an accident.
3. Ensure all material to be used for weighing and storage is present (nanomaterials, bottles/vials for weighing material in, cleaning tissue (both wet and dry wipes) before commencing the work.
4. Calibrate the weighing scales with traceable reference weight and log the data. Check that accuracy is within acceptance.

[‡‡‡‡] It is recommended to use two- or three layers of gloves for dermal protection. 1) Inner glove in textile, 2) and/or inner glove using long powder-free nitrile or latex rubber glove, 3) powder-free nitrile glove.

**Weighing out the nanomaterial**

1. Open a clean empty vial for preparation of the stock dispersion and place it on the weighing scales. Tare the weighing scales.
2. Carefully open the vial without shaking it (NM-materials are packed in argon atmosphere).
3. Remove the electrostatic charge on the vial using a neutraliser (*e.g.* ionization blower) and carefully weigh out the required mass with a spatula in steel or glass.
4. Close the lid on both vials.
5. When the weighing is completed, clean the weighing scales and work area for potential spills using wet and dry wipes.
6. Pack waste in a suitable waste bag and discard according to local or institutional directions.
7. Ventilate the work-area (ventilated weighing station, fume hood, glove box etc.) for 15 minutes after weighing and cleaning has been completed.

**Calculation of EtOH and BSA-water volume for preparing the 2.56 mg/ml stock dispersion**

For preparing a 2.56 mg/ml stock dispersion in a 6 ml EtOH and BSA-water, each vial must contain at least 15.36 mg nanomaterial. For harmonization of the dispersion energy it is recommended to stay as close as possible to 6 ml EtOH and BSA-water.

Calculation of the correct volume is done simply using the following equation:

$$V = m/c$$

where:

m = mass of nanomaterial (mg)

c = concentration (normally 2.56 mg/ml)

V = volume of dispersion medium (ml)

### 5.8.2 Particle dispersion

**EtOH Pre-wetting and addition of BSA water**

Particles are pre-wetted using ethanol (EtOH).

*Pre-wetting procedure (mentioned volumes for 15.36 mg powder)*

1. Carefully open the glass scintillation vial with pre-weighed NM powder (ideally 15.36 mg).
2. Tilt the scintillation vial ca. 45° and add 30 ml EtOH drop-by-drop onto the particles in the vial by pipette.
3. Screw on the lid and gently mix the EtOH and powder by simultaneous gently tapping the vial on the table-top while rotating the tilted 45° vial from side to side between your fingers for approximately one minute.
4. Add 5,970 µl 0.05 % BSA water by pipette while slowly rotating and swirling the 45° tilted scintillation glass. Be careful to avoid foaming of BSA. The last ml BSA-water or so is added along the top of the inner wall of the vial to collect the NM powder in the fluid at the vial bottom.

**Probe Sonication**

The protocol was developed using a 400 Watt Branson Sonifier S-450D (Branson Ultrasonics Corp., Danbury, CT, USA) equipped with a standard 13 mm disruptor horn (Model number: 101- 147-037). The particle dispersions are continuously cooled in an ice-water bath to minimise heat development during sonication as shown previously in Figure 46.

**Sonication procedure**

1. Fill a 250 ml glass beaker with ice and place it upside-down in an insulation box (flamingo)
2. Add ca. 85-90 vol% ice into the insulation box
3. Add ca. 10-15 vol% cold water into the insulation box
4. Carefully place the glass scintillation vial with powder on top of the upside-down glass beaker and pack the ice-water around the vial to keep the dispersion cooled.
5. Insert the sonication probe between the upper quarter and upper half of the BSA-water volume in the scintillation beaker (*e.g.* find the correct height using a vial with BSA-water alone).
6. Start sonication and run it for 16 min at 400 W and 10% amplitude while controlling that the sonication probe does not touch the walls of the scintillation vial.
7. Remove the scintillation vial and add the lid.
8. Clean the sonication probe by sonication for 5 minutes (similar sonication settings) with the probe fully immersed in a 50:50 water-EtOH (>96%) mixture followed by rinsing in EtOH using a dispenser and a collection bottle underneath. The probe is allowed to air-dry in the fume-hood.

## 5.9 Dispersion protocol for NM-110 and NM-111 in cell culture medium for *in vitro* toxicity testing

This section describes the dispersion of NM-110 and NM-111 in F-12K biological cell culture media containing 10% foetal bovine serum using a sonicating water bath and measurement of their toxicity using the A549 cell line. All laboratory consumables should be sterile to avoid contamination with adventitious organisms and sample preparation and administration should be performed in class-II environment.

### 5.9.1 Materials

1. 50mL tube
2. Plastic spatula
3. 50ml sterile tube
4. P200 sterile pipette tips
5. 10ml sterile serological pipettes
6. 4-figure bench top weigh-balance
7. Sonicating water bath[§§§§] with upright rack set at 37°C
8. Standard temperature controlled water-bath
9. Bench Vortex Mixer
10. F-12K cell culture medium
11. Hyclone foetal bovine serum (FBS)
12. A549 Cell line (LGC standards UK, CCL-185)
13. T-75 vented cell culture flasks
14. Trypsin-EDTA solution
15. 96-well sterile micro-titre plates
16. Microscope
17. Plate shaker
18. Class-II microbiological safety cabinet
19. 37$^{o}$C, 5% $CO_2$ humidified incubator
20. Colorometric spectrophotometer

[§§§§] a probe tip was not used to prevent the contamination of the sample following either disintegration of the probe tip, or other reactive metals and, additionally, to avoid damaging the proteins in the cell media.

### 5.9.2 Preparation of 500 μg/ml stock solutions

The procedure for weighing and dispersing NM-110 or NM-111 to create a stock solution of 500 μg/ml is as follows:

1. Weigh the 50 ml tube for the stock suspension with the cap in a sterile Class-II microbiological safety cabinet.
2. Remove the cap from the 50ml tube. And carefully transfer 10-15 mg of NM-110 or NM-111.
3. Replace the cap on the 50 ml tube, re-weigh and calculate the mass difference.
4. Remove the lid from the 50 ml tube and add 25 μL of cell culture media containing 10% FBS to wet the powder.
5. Agitate with a glass pipette to disperse visible aggregates and to make a paste.
6. Add 5 mL of cell culture media containing 10% FBS to the paste.
7. Replace the lid and then vortex mix for 15 seconds.
8. Place the 50 ml tube containing the particle suspension into a sonicating water bath and sonicate for 10 minutes[*****].
9. Remove the tube from the sonicator and vortex mix for 15 seconds.
10. Return the tube to the sonicating water bath and sonicate for a further 10 minutes.
11. Using cell culture media containing 10% FBS, adjust the volume of the nanoparticle suspension to create a 500 μg/ml stock solution.
12. Vortex mix the stock solution for 15 seconds.
13. Immediately use this stock solution to create an appropriate dilution series of the nanomaterials in cell culture media containing 10% FBS, for example, 100, 75, 50, 25 μg/ml.

[*****] It is important to establish that sonication occurs evenly throughout the bath prior to commencing sonication of the NM materials.

### 5.9.3 Cell Culture

Cell culture was performed using the A549 cell line which is an adenocarcinoma human alveolar basal epithelial cell line from a 58-year-old Caucasian male. A549 is a hypotriploid human cell line with the modal chromosome number of 66, and is commonly used as an *in vitro* model for examining lung toxicity. Cell culture was performed as follows:

1. Pre-warm cell culture media containing 10% FBS to 37$^{o}$C in a standard temperature controlled water bath
2. Dilture approximately 3 million A549 cells into 10 ml of the pre-warmed cell culture media.
3. Transfer the 10 ml of cell culture media containing the A549 cells into a T75 vented cell culture flask and incubate at 37$^{o}$C in a 5% $CO_2$ humidified environment
4. Observe the cells every 24 hours until they have reached approximately 80% confluency replacing the cell culture media every 48 hours.
5. Detach the cells from the T75 culture flask using 0.25%Trypsin-Edta solution and place into a 50ml tube
6. Add an equal volume of cell culture media containing 10% FBS to the cells to neutralise the Trypsin-EDTA solution.
7. Perform a cell count
8. Adjust the concentration of the cells to 160,000 cells/ml using cell culture media containing 10% FBS

### 5.9.4 *In vitro* toxicity of NM-110 and NM-111

The *in vitro* toxicity of the NM-110 and NM-111 materials was established using three standard colorimetric cytotoxicity assays (MTT, WST-1 and the Neutral Red uptake assay (NR)). The MTT and WST-1 assays measure cell viability based on the reduction of tetrazolium salts to a coloured formazan product and are linked to mitochondrial metabolism (MTT) and metabolism at the cell surface (WST-1). The NR assay measures viability based on cell membrane integrity. Assays were performed in 96-well micro-titre plates on confluent cell

monolayers[†††††] according to manufacturer's instructions. Brief details of the procedures are given here.

**Preparation of cells for *in vitro* assay**

1. Pipette 100 μl of the cells suspension prepared at a concentration of 160,000 cell/ml into the wells of a 96-well micro-titre plate. Allow at least triplicate sampling for each nanoparticle test concentration
2. Incubate the cells for 24 hours at 37$^{o}$C, 5% $CO_2$ in a humidified environment to allow the cells to reach confluency
3. Carefully remove the culture medium from the cells
4. Add 100 μl of the test nanomaterial dilution series to each well and incubate for a further 24 hours at 37$^{o}$C, 5% $CO_2$ in a humidified environment
5. Carefully remove the nanomaterials suspensions and wash the cells 3 times in pre-warmed PBS at 37$^{o}$C.
6. Perform cell viability assay as set-out below:

**MTT assay**

1. Remove the PBS wash solution and add 100 μl of 0.5 mg/ml MTT solution dissolved in cell culture media containing 10% FBS to each well.
2. Incubate at 37$^{o}$C, 5% $CO_2$ in a humidified environment for 4 hours
3. After 4 hours remove the MTT solution taking care not to disturb the purple formazan crystals.
4. Solubilise the formazan by adding 100 μl of DMSO to each well and mix using a plate shaker for 45 seconds.
5. Read the optical density using a spectrophotometer at 570 nm and 690 nm.

[†††††] Prior to commencing *in vitro* toxicity measurements it is important to ensure continuity in the growth phase of the cells between assays. Before undertaking measurements using A549 cells in 96-well plates it was established that seeding the cells at a concentration of 16,000 cells per well leads to the formation of a confluent monolayer after 24 hours incubation. Concentrations for other cell lines will vary and should be examined independently.

**WST-1 Assay**

1. Remove the PBS wash solution and add 100 μl of 10% WST-1 solution dissolved in cell culture media containing 10% FBS to each well.
2. Incubate at 37$^{o}$C, 5% $CO_2$ in a humidified environment for 1 hour.
3. After 1 hour mix the samples using a plate shaker for 45 seconds.
4. Read the optical density using a spectrophotometer at 420 nm and 690 nm.

**NR assay**

1. Remove the PBS wash solution and add 250 μl of 25 μg/ml neutral red solution dissolved in cell culture media containing 10% FBS to each well.
2. Incubate at 37$^{o}$C, 5% $CO_2$ in a humidified environment for 3 hours
3. After 3 hours remove the neutral red solution and wash twice in pre-warmed PBS at 37$^{o}$C.
4. Solubilise the neutral red by adding 100 μl of desorption solution composed of 49% EtOH, 50% $H_2O$ and 1% glacial acetic acid to each well.
5. Mix the samples using a plate shaker for 45 seconds.
6. Read the optical density using a spectrophotometer at 540 nm ± 10 nm.

***In vitro* toxicity measurements**

The percentage viability of the A549 cells following 24 hours exposure to either NM-110 or NM-111 at a concentration of 0, 25, 50, 75 or 100 μg/ml and assayed using the MTT, WST-1 and NR assays are shown below in Table 28 and Table 29. Also shown for comparison are the relevant $IC_{50}$ values (where obtainable).

**Table 28: Percentage viability of A549 cells following exposure to NM-110 for 24 hours at 0, 25, 50, 75 or 100 μg/ml.**

| | MTT | | NR | | WST-1 | |
|---|---|---|---|---|---|---|
| NM-110 μg/mL | % Viability | StDev | % Viability | StDev | % Viability | StDev |
| 0 | 100.0% | 6.9% | 100.0% | 22.7% | 100.0% | 11.4% |
| 25 | 81.0% | 3.4% | 109.1% | 27.3% | 83.9% | 19.6% |
| 50 | 43.1% | 6.9% | 50.0% | 9.1% | 45.9% | 13.3% |
| 75 | 12.1% | 1.7% | 27.3% | 0.0% | 10.2% | 3.5% |
| 100 | 10.3% | 3.4% | 27.3% | 0.0% | 6.3% | 0.4% |
| $IC_{50}$ (μg/mL) | 43 | | 46 | | 48 | |

**Table 29: Percentage viability of A549 cells following exposure to NM-111 for 24 hours at 0, 25, 50, 75 or 100 μg/ml.**

| | MTT | | NR | | WST-1 | |
|---|---|---|---|---|---|---|
| NM-110 μg/mL | % Viability | StDev | % Viability | StDev | % Viability | StDev |
| 0 | 100.0% | 6.9% | 100.0% | 22.7% | 100.0% | 11.4% |
| 25 | 100.0% | 5.2% | 104.5% | 22.7% | 101.2% | 13.7% |
| 50 | 100.0% | 3.4% | 104.5% | 22.7% | 98.0% | 17.6% |
| 75 | 98.3% | 5.2% | 109.1% | 13.6% | 86.3% | 20.8% |
| 100 | 86.2% | 5.2% | 90.9% | 18.2% | 95.3% | 10.6% |
| $IC_{50}$ (μg/mL) | N/A | | N/A | | N/A | |

## 5.10 Dispersion Stability Testing

In accordance to BS ISO 14488, successful (liquid) sample splitting can only be conducted if a homogeneous dispersion has been achieved – otherwise this will result in a much higher sampling error. Prior to sample splitting, the operator should check that dispersion is sufficiently stable during the time that is required to perform sample splitting and subsequent reliable characterisation of the nanoparticle dispersion using a predetermined tool. For example, if the nanoparticle dispersion is to be characterised by Dynamic Light Scattering (DLS), then a suitable aliquot should be pipetted out from stock and the mean particle size acquired. Six replicates should be acquired to ensure that the sample is sufficiently stable within a reasonable amount of time.

If there is evidence of aggregation/sedimentation in the sample, then the dispersion is not stable enough to allow subsampling to be carried out without

incurring sub-sampling error. In addition to errors incurred from sub-sampling steps, stability testing of the dispersion is important for nanoparticle characterisation. For example, one of the pre-requisites for reliable and accurate DLS measurement is to have a sample that is stable with no signs of sedimentation, as DLS is applicable only to particles that remain fully suspended undergoing Brownian diffusional motion, throughout the measurement.

## 5.11 Dispersion Characterisation Tools

Whatever the choice of characterisation tools chosen, operators must be aware of the limitations posed by the various techniques. It is beyond the scope of this dispersion protocol to give detailed description of limitations of various techniques and so it is left for the operator to ensure that the technique chosen is suitable for a given nanoparticle dispersion under analysis. For example, in the case of DLS, this tool is not suitable to resolve a broad particle size distribution, as potentially larger particles can mask the signal of the smaller nanoparticles. In order to resolve multi-modal particle distribution, techniques that have a separation mechanism element integrated in the analytical tool will be more suitable *e.g.* CPS disc centrifuge.

# 6 Conclusions

An international public-private-partnership, scientifically supported by the JRC, has introduced the NM-Series of representative nanomaterials (NM) for testing in support of the Organisation of Economical Cooperation and Development (OECD) Working Party on Manufactured Nanomaterials (WPMN), as well as European and Member States' projects. The NMs are already being studied in international scientific co-operations, and a large number of individual test samples were distributed internationally to national authorities, research institutions, industrial laboratories and other scientific stakeholders.

The NM-110, NM-111, NM-112 and NM-113 zinc oxide are among the key materials of the programme, for which the current report presents information on characteristics, stability and homogeneity with special regard to its use and appropriateness for use as representative nanomaterial, performance standard and reference matrix for testing.

The properties of NM-110, NM-111, NM-112 and NM-113 studied and described in this report demonstrate the NM-Series' relevance for use in measurement and testing studies, such as for hazard identification and related to the safety of nanomaterials. They serve the need as representative nanomaterial, performance standard and reference matrix for harmonisation and standardisation, method development, optimisation and validation.

## 6.1 Characterisation

Most of the OECD endpoints on physical-chemical testing have been completed in this report. The remaining endpoints will be completed by the end of Phase 1 of the OECD Sponsorship Programme. For some endpoints, analysis was not completed for NM-111, as this material had a surface coating, rendering it difficult to disperse.

SEM analysis indicates that the zinc oxide NMs are highly agglomerated and aggregated. DLS indicates that in all cases the NMs consist of polydisperse distributions of particles. CPS disc centrifuge results indicate that NMs are largest in seawater and smallest in DI water indicating that larger agglomerates exist in ecotoxicology media.

Turbidity measurements show that overall NMs are most stable when dispersed in DI water and least stable when in an ecotoxicology media.

Dissolution rates were fastest when the zinc oxide NMs were dispersed in DI water, with NM-110 dissolving the fastest and NM-112 dissolving the slowest. DI water yielded the most stable dispersions and this increase in stability will mean less aggregation/agglomeration (and subsequent sedimentation) in the dispersion. Hence, the total surface area is greater when the particles are dispersed in DI water compared to corresponding ecotoxicology media; an increase in surface area means that the ion dissolution rate will also increase.

The XRD patterns for all the samples, NM-110, NM-111, NM-112 and NM-113 indicate clearly the hexagonal zincite structure. The crystallite sizes determined by XRD were in the range of 24 nm (NM-112) to 42 nm. Both NM-110 and NM-113 have the same crystallite size of 42 nm. The average crystallite size determined by Rietveld refinement yielded larger crystallite sizes compared to those measured using Scherrer's equation.

Dustiness results show a significant difference in the inhalable dustiness levels between coated (NM-111) and uncoated (NM-110) zinc oxide particles. The respirable dustiness index, however, was quite comparable and possibly influenced by larger variation than the inhalable dust fraction.

TEM analysis indicates that the primary ZnO crystals were polyhedral with quite variable morphology. Two main types of morphology could be distinguished for both NM-110 and NM-111. For NM-112, primary particles appeared to be near

spherical rather than polyhedral with regular morphology and a relatively homogenous size distribution. Particle size distribution using SEM image analysis shows that the Feret's diameter is smallest for NM-112 (42.5 nm) and largest for NM-113 (891.8 nm). Homogeneity Testing (NM-110 and NM-111) using SEM was also conducted. Results were presented in raw, tabular format and further processing of the data will be the responsibility of the reference material developer.

Specific surface area measurements using BET show a wide range of the specific surface area values for various NM powders (*i.e.* from 5.78 to 27.25 $m^2/g$. Results show that NM-112 has the largest surface area of 27.25 $m^2/g$ and the smallest being NM-113 of ~ 5.78 $m^2/g$). The measurements were repeated and results indicate that there is good agreement between the two data sets obtained across different laboratories. The variation in specific surface area of the zinc oxide samples corresponds well with their inverse proportional variations in particle and crystallite sizes.

All samples have very low microporosity. The major contribution to total surface area is from external surfaces and is thus predominantly determined by particle size and shape rather than high internal porosity. NM-112 has the highest surface area and micropore volume of all the samples approximately 3-4 times greater than other samples.

In general, results indicate high zeta-potential values for NMs that are dispersed either in DI water (or DI water + 5 mM NaCl), and thus confer stability in such media. Results show values of zeta-potential measured were lower when the NMs were dispersed in an ecotoxicology media indicating much poorer dispersion stability in such media.

XPS showed the presence of Si and this was mainly associated with NM-111 sample (particles coated with silane). XPS detected a significant contribution of carbon and this was largely attributed to contamination on the particles and/or

background signal from the tape used to fix the particles in place. Homogeneity testing using XPS was able to deduce a clear difference in the two sets of vials (NM-110 and NM-111). The count rate of Zn peaks were always lower for NM-111 samples compared to NM-110 samples. This can be attributed to the presence of a triethoxycarpryl silane coating associated with the NM-111 samples. The Si level is much higher (3.1 to 4.1 %) in NM-111 if compared to NM-110 (0 to ~1%). This is consistent with the presence of a silane coating with the former sample. The silicon signal contribution (of less than 1%) can be attributed to silicon background signal from the fixing tape.

There is still some ambiguity concerning redox potential measurements: the redox potential measurements were done using ORP probe electrode, of various ZnO dispersions, in various liquid media. Although the redox potential values acquired from ORP electrode may be indicative of the redox state of the entire system it is difficult to quantify the reliability of such measurements.

TGA shows slight increase in weight for NM-110 when heated, while a very small weight loss for NM-111 appears at 400 °C which is likely due to the silane coating. Chemical analysis by ICP-OES indicates very low inorganic trace element impurities were detected for NM-110. Very low inorganic impurities were detected for NM-111. In general all samples were found to have little or no secondary elements present. NM-112 had substantially higher levels of detectable alkali metals (Ca, Na) as well as Al than all the other samples whilst NM-113 appeared to have a significantly higher level of detectable Cu than all other samples.

## 6.2 Test Item Preparation

A handling procedure for weighing and sample introduction has been established in cooperation with scientists at the different research institutions, which used the NM-Series for zinc oxide. The procedure is generic and should also be applicable for other NMs. It is recommended that this procedure is

performed quickly as some NMs have the ability to absorb moisture from the atmosphere either due to surface coatings or very high surface area.

Several dispersion protocols were also described in this report. In all of these protocols, the NMs are dispersed into the media using sonication. These protocols have been applied for several other nanomaterials as well apart from zinc oxide. The PROSPECT protocol works extremely well to disperse uncoated nanoparticles of zinc oxide and cerium oxide. In order to disperse NM-111 (coated zinc oxide), the use of protocols described in Section 5.7, 5.8 and 5.9 (depending on the dispersion media) is recommended.

Once the dispersion of the test item has been prepared, analysis should always be performed to ensure dispersion stability. This is because successful (liquid) sample splitting can only be conducted if a homogeneous dispersion has been achieved, otherwise a much higher sampling error will be introduced. Dispersion can be assessed using a predetermined tool, for example light scattering techniques such as Dynamic Light Scattering (DLS) or even optical microscopy. Whatever the choice of characterisation tools, operators must be aware of the limitations posed by the various techniques. For example, DLS is not suitable to resolve a broad particle size distribution, as potentially larger particles can mask the signal of the smaller nanoparticles. In order to resolve multi-modal particle distribution, techniques that have a separation mechanism element integrated in the analytical tool will be more suitable, such as a CPS disc centrifuge. In addition to errors incurred from sub-sampling steps, stability testing of the dispersion is important for nanoparticle characterisation.

# References


Cayrol C., *et al.,* A mineral sunscreen affords genomic protection against ultraviolet (UV)B and UVA radiation: *In vitro* and in situ assays. Br J Dermatol 141, 1999, p. 250–258.

Chandra Ray, P., *et al.,* Toxicity and Environmental Risks of Nanomaterials: Challenges and Future Needs. J Environ Sci Health C Environ Carcinog Ecotoxicol Rev., 27(1), 2009, pp. 1-35.

Chang, H.W. and Okuyama, K., Optical properties of dense and porous spheroids consisting of primary silica nanoparticles. Journal of Aerosol Science, 2002, 33(12): p. 1701-1720.

ENPRA, Interim report, *Primary physico-chemical characteristics of engineered nanoparticles used in the ENPRA project*, 2010.

ISO/IEC 17025:1999, General requirements for the competence of testing and calibration laboratories, 1999.

ISO 9276-6:2008 Representation of results of particle size analysis - Part 6: Descriptive and quantitative representation of particle shape and morphology. 2008.

Jensen, K.A., *et al.,* Dustiness behaviour of loose and compacted Bentonite and organoclay powders: What is the difference in exposure risk?, Journal of Nanoparticle Research 11.1, 2009, P. 133-46.

Johnson, S.B., *et al.,* Adsorption of organic matter at mineral/water interfaces. 2. Outer-sphere adsorption of maleate and implications for dissolution processes. Langmuir, 2004, 20(12): p. 4996-5006.

Ju-Nam, Y., *et al.,* Manufactured nanoparticles: an overview of their chemistry, interactions and potential environmental implications. Sci Total Environ., 2008, 400(1-3): p. 396-414.

Klein C.L., *et al.,* NM 300 Silver Characterisation, Stability, Homogeneity, European Union, Luxembourg, 2011. ISBN 978-92-79-19068-1.

Krumbein, W.C. and Sloss, L.L., Stratigraphy and Sedimentation, Second Edition, W.H. Freeman and Company, San Francisco, 1963, p. 660.

Mast J. and Demeestere L., Electron tomography of negatively stained complex viruses: application in their diagnosis. Diagnostic Pathol. 2009, 4:5 doi:10.1186/1746-1596-4-5.

Morris J., *et al.,* Science policy considerations for responsible nanotechnology decisions. Nature Nanotechnology 2011, 6, 73–77.

NIST, NCL Joint Assay Protocol PCC-1 (Version 1), Measuring the Size of Nanoparticles in Aqueous Media Using Batch-Mode Dynamic Light Scattering, 2007.

Nowack, B., *et al.,* Occurrence, behavior and effects of nanoparticles in the environment. Environmental Pollution, Vol 150, Issue 1, 2007, Pg 5-22.

OECD WPMN; ENV-JM-MONO(2009)20-REV-ENG- Guidance Manual for Sponsors, OECD, Paris, 2010. Available at: http://www.olis.oecd.org/olis/2009doc.nsf/linkto/env-jm-mono%282009%2920.

OECD WPMN; ENV/JM/MONO(2010)46- List of Manufactured Nanomaterials and List of Endpoints for Phase One of the Sponsorship Programme for the Testing of Manufactured Nanomaterials: Revision, OECD, Paris, 2010. Available at: http://www.olis.oecd.org/olis/2009doc.nsf/linkto/env-jm-mono%282009%2920.

Osmond, M.J., *et al.,* Zinc oxide nanoparticles in modern sunscreens: An analysis of potential exposure and hazard. Nanotoxicology, March 2010; 4(1): 15–41.

Pinnell S.R., *et al.,* Microfine zinc oxide is a superior sunscreen ingredient to microfine titanium dioxide. Dermatol Surg, 2000, 26:309–314.

Popov A.P., *et al.,* $TiO_2$ nanoparticles as an effective UV-B radiation skin protective compound in sunscreens. J Phys D: Appl Phys 2005, 38:2564–2570.

Pourbaix, M., Atlas of Electrochemical Equilibria in Aqueous Solutions, Marcel Pourbaix, National Association of Corrosion Engineers, Houston, Texas. 1974. Available at: http://www.olis.oecd.org/olis/2009doc.nsf/linkto/env-jm-mono%282009%2920.

SCCP, Scientific Committee on Consumer Products, Statement on Zinc Oxide used in Sunscreens, 2005, Available at: SCCP/0932/05. www.ec.europa.eu/health/ph_risk/committees/04_sccp/docs/sccp_o_00 m.pdf

SCENIHR, Scientific Committee on Emerging and Newly Identified Health Risks (SCENIHR), Opinion on “Risk Assessment of Products of Nanotechnologies”, Brussels, 2009.

Schneider, T. and Jensen, K.A., "Combined Single-Drop and Rotating Drum Dustiness Test of Fine to Nanosize Powders Using a Small Drum." Annals of Occupational Hygiene 52.1, 2008: 23-34.

Thompson M., *et al.,* Harmonized guidelines for single-laboratory validation of methods of analysis (IUPAC Technical Report). *Pure and Applied Chemistry*, 2002, Vol. 75, No. 5, 835-855.

Van der Veen, A.M.H., *et al.,* Uncertainty calculations in the certification of reference materials, 2. Homogeneity study. Accred. Qual. Assur. 6, 2001, 26.

Wiench, K., *et al.,* Acute and chronic effects of nano-and non-nano-scale $TiO_2$ and ZnO particles on mobility and reproduction of the freshwater invertebrate Daphnia magna, Chemosphere 76, 2009, 1356–1365.

Wolf, R., *et al.,* Sunscreens. Clin Dermatol, 2001, 19:452–459.

# ANNEX A1: List of Tables

# ANNEX A2: List of Figures

European Commission

**EUR 25066 EN– Joint Research Centre – Institute for Reference Materials and Measurements**
Title: NM-Series of Representative Manufactured Nanomaterials – Zinc Oxide NM-110, NM-111, NM-112, NM-113 Characterisation and Test Item Preparation

Authors: C. Singh, S. Friedrichs, M. Levin, R. Birkedal, K.A. Jensen, G. Pojana, W. Wohlleben, S. Schulte, K. Wiench, T. Turney, O. Koulaeva, D. Marshall, K. Hund-Rinke, W. Kördel, E. Van Doren, P-J. De Temmerman, M. Abi Daoud Francisco, J. Mast, N. Gibson, R. Koeber, T. Linsinger, C.L. Klein

Luxembourg: Publications Office of the European Union
2011 – 141 pp. – 21.0 x 29.7 cm
EUR – Scientific and Technical Research series – ISSN 1831-9424 (online), ISSN 1018-5593 (print)
ISBN 978-92-79-22215-3
doi:10.2787/55008

**Abstract**
The European Commission's Joint Research Centre (JRC) provides scientific support to European Union policy also regarding nanotechnology. Over the last three years, the JRC, in collaboration with international public and private partners, focused part of its work on establishing and applying a priority list (NM-Series) of Representative Manufactured Nanomaterials (RMNs) in support of one of the most comprehensive nanomaterial research programmes that is currently being carried out: the Organisation for Economic Co-operation and Development's (OECD) Working Party on Manufactured Nanomaterials (WPMN) Sponsorship Programme. This collaborative programme enables the development and collection of data on characterisation, toxicological and eco-toxicological testing, as well as risk assessment and safety evaluation of nanomaterials (NMs). It is of utmost timely importance to make representative nanomaterials available to the international scientific community, in order to enable innovation and development of safe materials and products.
The present report describes the characterisation of NM-110, NM-111, NM-112, and NM-113, RMN Zinc Oxide substances, originating from defined batches of commercially manufactured material. The NM-Series materials were subsampled in collaboration with the Fraunhofer Institute for Molecular and Applied Ecology (Fh IME), in order to be made available for measurement and testing for hazard identification, risk and exposure assessment studies. The results for more than 15 endpoints are addressed in the present report, including physical-chemical properties, such as size and size distribution, crystallite size and electron microscopy images. Sample and test item preparation procedures are addressed. The RMNs are studied by a number of international laboratories.
The properties of the Zinc Oxide RMNs NM-110, NM-111, NM-112, and NM-113 described in this report demonstrate their relevance for use in measurement and testing studies of nanomaterials. The studies were performed in close collaboration between the PROSPECT consortium partners, the JRC, the Fraunhofer Institute for Molecular and Applied Ecology (Fh-IME), BASF AG Ludwigshafen, LGC standards, the National Physical Laboratory (NPL), the National Research Centre for the Working Environment, Denmark, CSIRO and the National Measurement Institute of Australia.

The mission of the JRC is to provide customer-driven scientific and technical support for the conception, development, implementation and monitoring of EU policies. As a service of the European Commission, the JRC functions as a reference centre of science and technology for the Union. Close to the policy-making process, it serves the common interest of the Member States, while being independent of special interests, whether private or national.

JRC
EUROPEAN COMMISSION

LA-NA-25066-EN-N

Publications Office

ISBN 978-92-79-22215-3